

*Paddy soil C turnover affected by
fertilization and water management*

DISSERTATION

submitted to obtain the degree of Doctor of Natural Sciences

(Dr. rer. nat.)

at the Faculty of Biology, Chemistry and Earth Sciences
of the University of Bayreuth

Qiong Liu

from *Changsha, China*

Bayreuth, 2022

The present study was prepared between February 2018 and January 2022 under the direction of Prof. Dr. Johanna Pausch at the Department of Agroecology, University of Bayreuth. The work was financially supported by the Chinese Scholarship Council (CSC).

This is a full reprint of the dissertation submitted to attain the academic degree of Doctor of Natural Sciences (Dr. rer. nat.) and approved by the Faculty of Biology, Chemistry and Earth Science of the University of Bayreuth.

Date of submission: January 19, 2022

Date of defense (disputation): June 02, 2022

Dean: Prof. Dr. Benedikt Westermann

Doctoral Committee:

Prof. Dr. Johanna Pausch, Dept. of Agroecology, University of Bayreuth (1st reviewer)

Prof. Dr. Eva Lehndorf, Dept. of Soil Ecology, University of Bayreuth (2nd reviewer)

Prof. Dr. Martin Obst, Dept. of Experimental Biogeochemistry, University of Bayreuth (Chairman)

Dr. Sven Frei, Dept. of Hydrology, University of Bayreuth

Summary

Rice feeds more than half of the world's population; in addition, artificial rice paddies are an important contributor to global carbon emissions. Carbon turnover (production and oxidation) primarily comprises microbially mediated processes, and microorganisms (abundances and communities) are strongly affected by anthropogenic activities in paddy soils, such as fertilization and water management. In turn, microbial abundance and community shifts can strongly influence soil C turnover by affecting soil organic matter (SOM) decomposition through priming effects (PEs).

This thesis aimed to gain a more comprehensive understanding of C turnover (CO_2 and CH_4) in paddy soils by determining the temporal dynamics of CO_2 and CH_4 and disentangling the underlying mechanisms.

Uncertainty still exists about the contributions of the two main pathways (acetoclastic methanogenesis and hydrogenotrophic methanogenesis) to CH_4 production throughout the rice growing season, especially under field conditions. To fill this knowledge gap, in Study 1 and 2, we took soil gas samples using passive diffusion gas samplers to determine the temporal dynamics of CO_2 and CH_4 . Since labile C input affects microbial processes in soil, the C allocation from above- to belowground pools was quantified by $^{13}\text{CO}_2$ pulse labelling of rice plants.

Of particular interest was the result of the natural abundance ^{13}C enrichment of CO_2 over time under flooded conditions, indicating that hydrogenotrophic methanogenesis continuously contributed to CH_4 production. Alternating wet-dry cycles (AWD) resulted in a significant decrease in CH_4 concentrations, along with conspicuous isotopic signals indicative of CH_4 oxidation. However, the time and magnitude of AWD should be carefully considered as it can reduce rice yield. Sulfate fertilizer had positive effects on rice plant biomass and grain yield, though it showed no effect on lowering CH_4 concentrations. Especially under AWD conditions, sulfate fertilizer increased shoot biomass and stabilized grain production. Additionally, based on $^{13}\text{CO}_2$ pulse labelling results, more than 50% of newly assimilated C was retained aboveground at grain-filling stage (14 days after pulse labelling), which is likely explained by a high C demand for fruit production. We did not detect any effect of sulfate addition and AWD on ^{13}C allocation in the plant-soil system.

In addition to these short-term effects of fertilizer addition, in Study 3, soil samples were collected from a long-term experimental trial and analyzed for microbial biomass and community composition. Both mineral and organic fertilization can prevent microbial biomass from decreasing vertically. In addition, Gram-positive (G+) bacteria benefited the most from mineral fertilizers, and the partial replacement of mineral fertilizer with manure primarily enhanced the abundance of G+ bacteria at 0–30 cm soil depth. In contrast, replacement with straw particularly enhanced the abundances of fungi at 10–20 cm soil depth, which is explained by the key role of fungi in straw decomposition.

Study 4 was designed to investigate how the changes of microbial activity and communities, shown in Study 3, affect SOM decomposition through PE. ^{13}C -glucose was added to incubated soils to mimic C input by rhizodeposition. Following glucose addition, SOM-derived microbial biomass C decreased at 0–10 cm in all soils (apparent PE). It was suggested that in upper soil depths with frequent C input through

rhizodeposition and organic fertilizers, microorganisms focused on renewing their C rather than investing in growth after substrate addition.

N mining mechanism suggests that primed CO_2 is higher under nutrient-limited conditions as microorganisms produce extracellular enzymes to mine SOM for limiting nutrients. Our results fit well with this mechanism, as lower percentage primed CO_2 (PE_{CO_2}) was observed in soil with balanced nutrient conditions (NPK). In contrast, in low nutrient (unfertilized) or extra C (organic fertilized) conditions, PE_{CO_2} was higher because of the demand for nutrients. However, the higher positive primed-DOC together with weak PE_{CO_2} in topsoil than subsoil cannot be explained by N mining. Therefore, we proposed a mineral-related mechanism: glucose addition increased DOC by release of mineral-bound C biotically and/or abiotically. Apart from accelerating SOM decomposition, positive PE_{CO_2} can also be achieved by direct utilization of those released C. However, after 20 days of incubation, the organic C concentration was reduced by rebinding or co-precipitating to mineral surfaces, which can explain the negative PE at later incubation phases commonly observed in paddy soils.

In summary, this thesis extends our understanding of plant-microbe interactions on CO_2 and CH_4 turnover in paddy soils. In addition, we drew attention to complex mechanisms of C turnover in submerged paddy soils: 1) apparent PE, 2) biotic and/or abiotic release of mineral-bound OC, 3) negative PE at later incubation phases. Considering the mineral-associated mechanisms (substrate desorption and resorption with soil matrix) in further investigations is crucial, as they alter substrate availability to microorganisms and thus affect soil C stocks. Moreover, the studied mechanisms are vital for maintaining food security and mitigating global warming through adaptations in management practices in rice cropping systems.

Zusammenfassung

Reis ernährt mehr als die Hälfte der Weltbevölkerung. Darüber hinaus tragen künstlich angelegte Reisfelder erheblich zu den globalen Kohlenstoffemissionen (C) bei. Der C-Umsatz umfasst mikrobiell vermittelte Prozesse (Produktion und Oxidation). Mikroorganismen (Häufigkeit und Gemeinschaften) werden stark durch anthropogene Aktivitäten in Reisböden wie Düngung und Wassermanagement beeinflusst. Die Abundanz der Mikroorganismen und die Zusammensetzung der mikrobiellen Gemeinschaft können wiederum den C-Umsatz im Boden stark verändern, indem sie den Abbau der organischen Bodensubstanz (OBS) durch Priming Effekte (PEs) beeinflussen.

Das Ziel dieser Arbeit war es, ein umfassenderes Verständnis des C-Umsatzes (CO_2 und CH_4) in Reisböden zu erlangen, indem die zeitliche Dynamik von CO_2 und CH_4 und die zugrunde liegenden Mechanismen untersucht wurden.

Nach wie vor besteht Unklarheit über den Beitrag der beiden Hauptwege zur CH_4 -Produktion (acetoklastische Methanogenese und hydrogenotrophe Methanogenese) während der Reisanbausaison, insbesondere unter Feldbedingungen. Um diese Wissenslücke zu schließen, haben wir in den Studien 1 und 2 Bodengasproben mit passiven Diffusionsgassammlern entnommen, um die zeitliche Dynamik der CO_2 - und CH_4 -Produktion zu bestimmen. Da der Eintrag von labilem C mikrobielle Prozesse im Boden beeinflusst, wurde die C-Verlagerung von oberirdischen zu unterirdischen Pools durch $^{13}\text{CO}_2$ -Pulsmarkierung von Reispflanzen quantifiziert.

Von besonderem Interesse war das Ergebnis der natürlichen ^{13}C -Anreicherung von CO_2 im zeitlichen Verlauf unter überstauten Bedingungen. Die ^{13}C -Anreicherung deutete darauf hin, dass die hydrogenotrophe Methanogenese kontinuierlich zur CH_4 -Produktion beiträgt. Ein Wechsel zwischen Entwässerung und erneuter Überstauung (alternating wet-dry cycles, AWD) führte zu einer deutlichen Reduktion der CH_4 -Konzentration im Boden, zusammen mit auffälligen Isotopensignalen, die auf eine CH_4 -Oxidation hinweisen. Der Zeitpunkt und das Ausmaß der Entwässerung sollten jedoch sorgfältig abgewogen werden, da dies den Reisertrag verringern kann.

Sulfatdüngung wirkte sich sowohl auf die Biomasse der Reispflanzen als auch auf den Kornertrag positiv aus, zeigte jedoch keine Wirkung auf die CH_4 -Konzentration. Insbesondere unter AWD-Bedingungen erhöhte Sulfatdünger die Sprossbiomasse und stabilisierte die Getreideproduktion. Darüber hinaus wurde anhand der Ergebnisse der $^{13}\text{CO}_2$ -Pulsmarkierung gezeigt, dass im Stadium der Kornfüllung (14 Tage nach der Pulsmarkierung) mehr als 50 % des kürzlich assimilierten C in den oberirdischen Pflanzenteilen verblieb, was sich unter anderem durch einen hohen C-Bedarf für die Fruchtproduktion erklärt. Zudem konnten wir keinen Einfluss von Sulfatzugabe und AWD auf die ^{13}C -Allokation im Pflanze-Boden-System feststellen.

Im Gegensatz zu diesen kurzfristigen Wirkungen der Düngerzugabe wurden in Studie 3 Bodenproben aus einem Langzeitexperiment gesammelt und auf mikrobielle Biomasse und Zusammensetzung der mikrobiellen Gemeinschaft analysiert. Sowohl die mineralische als auch die organische Düngung können verhindern, dass die mikrobielle Biomasse vertikal abnimmt. Darüber hinaus profitierten gram-positiv (G+) Bakterien am meisten von Mineraldüngern, wobei der teilweise Ersatz von Mineraldüngern durch Gülle in erster Linie die Abundanz von G+ Bakterien in 0–30 cm Bodentiefe erhöhte. Dagegen steigerte der Ersatz von Mineraldüngern

durch Stroh die Pilzhäufigkeit in 10–20 cm Bodentiefe, was sich durch die wichtige Rolle der Pilze beim Strohabbau erklären lässt.

In Studie 4 wurde untersucht, wie sich die in Studie 3 gezeigten Veränderungen der mikrobiellen Aktivität und Gemeinschaften auf den OBS-Abbau durch Priming-Effekte auswirken. ^{13}C -Glukose wurde inkubierten Böden zugesetzt, um den C-Eintrag durch Rhizodeposition nachzuahmen. Kurz nach der Zugabe von Glukose wurde in bestimmten Bodentiefen ein Verlust der ursprünglichen mikrobiellen Biomasse (MBC) zusammen mit einem geringen mikrobiellen Wachstum beobachtet. Es wird vermutet, dass sich Mikroorganismen in den oberen Bodenschichten mit häufigem C-Eintrag aufgrund von Rhizodeposition nach Substratzugabe eher auf die Erneuerung ihres C (apparent PE) statt auf das Wachstum konzentrieren. Der N-Mining-Mechanismus legt nahe, dass das CO_2 aus Priming (PE_{CO_2}) unter nährstofflimitierten Bedingungen höher ist, da Mikroorganismen extrazelluläre Enzyme produzieren, um durch den OBS-Abbau an die limitierten Nährstoffe zu gelangen. Unsere Ergebnisse bestätigen diesen Mechanismus, da in Böden mit ausgewogenem Nährstoffbedingungen (NPK) ein geringerer PE_{CO_2} beobachtet wurde. Im Gegensatz dazu war PE_{CO_2} unter nährstoffarmen (ungedüngten) Bedingungen oder nach zusätzlicher C-Zugabe (organisch gedüngte Böden) aufgrund des Nährstoffbedarfs höher. Ein höherer „geprimter“ Gehalt an gelösten organischen C im Oberboden als im Unterboden kann jedoch dadurch nicht erklärt werden. Daher schlagen wir einen neuen mineralinduzierten Mechanismus vor: Glukosezugabe setzt mineralgebundenen organischen C (OC) biotisch und/oder abiotisch frei. Neben der Beschleunigung des OBS-Abbaus kann durch die direkte Nutzung dieses freigesetzten OC auch ein positiver PE_{CO_2} -Wert erreicht werden. Darüber hinaus kann sich OC im Verlauf der Inkubation wieder an Mineralien binden, was die Bioverfügbarkeit des Substrats verringert und einen negativen PE verursacht, wie es häufig in Reisböden zu beobachten ist.

Die vorliegende Arbeit erweitert unser Verständnis über die Auswirkungen von Pflanzen-Mikroben-Interaktionen auf die CO_2 - und CH_4 -Umsätze in Reisböden. Des Weiteren konnten wir die Aufmerksamkeit auf komplexe Mechanismen des C-Umsatzes in Reisböden lenken. Die Berücksichtigung neuer mineralassoziierter Mechanismen (Substratdesorption und -resorption an die Bodenmatrix) in weiteren Untersuchungen ist von entscheidender Bedeutung, da diese die Bioverfügbarkeit des Substrats für die Mikroorganismen und damit die C-Vorräte im Boden verändern können. Darüber hinaus sind die untersuchten Mechanismen des C-Umsatzes von entscheidender Bedeutung für die Aufrechterhaltung der Nahrungsmittelsicherheit und die Abschwächung der globalen Erwärmung durch Anpassungen der Bewirtschaftungspraktiken in Reisanbausystemen.

Table of Contents

Summary	I
Zusammenfassung	III
Table of Contents	V
List of Tables	VIII
List of Figures	X
Abbreviations	XIII
I Extended Summary	1
1. Introduction	1
1.1 Organic carbon stocks of paddy soils	1
1.2 Fertilizer and water management effects on C turnover in paddy soils.....	2
1.3 Mechanisms of CO ₂ and CH ₄ turnover in soils	2
1.4 Objectives	5
2. Materials and methods.....	6
2.1 Characteristics of the soils used in the studies.....	6
2.2 Isotope approaches to disentangle CO ₂ and CH ₄ fluxes in soil	6
2.3 Gas and soil sampling	7
2.4 Analysis.....	8
3. Results and discussion.....	9
3.1 CH ₄ turnover, photosynthesized C allocation and rice yield affected by AWD and sulfate fertilizer (Study 1 & 2)	9
3.2 Microbial communities across the soil profile altered by long-term fertilization (Study 3).....	10
3.3 Soil priming effect patterns in top- and subsoil altered by fertilization (Study 4)	11
4 Conclusions and outlook	14
5 Contributions to the included manuscripts	15
Acknowledgments	17
References	18
II Manuscript	23
II.1 Alternating wet-dry cycles rather than sulfate fertilization control pathways of methanogenesis and methane turnover in rice straw-amended paddy soil ...	23
Abstract	24
1. Introduction	25
2. Materials and methods.....	27
2.1 Experimental set-up	27

2.2 Soil gas and pore water sampling	27
2.3 Soil and plant sampling.....	28
2.4 Analyses and data processing.....	28
2.5 Statistical evaluation	29
3. Results	29
3.1. Plant properties and pore water DOC	29
3.2. CO ₂ and CH ₄ concentrations in soil air and their isotope ratios under wet-drying and sulfate fertilization treatments	30
3.3. Relationship between δ ¹³ C-CO ₂ and δ ¹³ C-CH ₄	32
4. Discussion	33
4.1. Effect of wet-dry cycles and sulfate fertilization on CH ₄ and CO ₂ production	33
4.2. Rice growth effects on methanogenesis pathways.....	35
Acknowledgments	36
References	37
Supplementary materials	40
II.2 Effect of alternating wet-dry cycles and sulfate fertilization on plant-soil C allocation and rice yield.....	45
Abstract	46
1. Introduction	47
2. Materials and methods.....	47
2.1 Experimental set-up	47
2.2 Pulse labelling and sampling	48
2.3 Analyses and data processing.....	48
2.4 Statistical evaluation	49
3. Results	49
3.1 Plant biomass and yield	49
3.2 Total ¹³ C amount in the plant-soil system.....	49
4. Discussion	51
4.1. Photosynthetic C allocation	51
4.2. Effect of AWD and sulfate fertilizer on plant properties	51
Acknowledgments	52
References	53
II.3 Vertical and horizontal shifts in the microbial community structure of paddy soil under long-term fertilization regimes	55
Abstract	56
1. Introduction	57
2. Results	58

3. Discussion	61
3.1 Microbial abundance along the soil depth gradient	61
3.2 Dependence of microbial community structure on fertilization strategies	61
4. Conclusions	62
Acknowledgments	63
References	64
Supplementary methods	67
1.1 Site description and fertilization strategies	67
1.2 Soil sampling and chemical analysis	67
1.3 Extraction of phospholipid fatty acids (PLFA)	68
1.4 Measurement of soil respiration.....	68
1.5 Statistical analysis	68
References	69
II.4. Mineral bound organic carbon explains the negative priming effect in paddy soils	73
Abstract	74
1. Introduction	75
2. Materials and methods.....	76
2.1 Soil sampling and incubation.....	76
2.2 Gas and soil sampling	77
2.3 Gas and soil analyses	77
2.4 Statistical evaluation	77
3. Results	78
3.1. CO ₂ efflux	78
3.2. Percentage PE _{CO₂}	78
3.3. Soil C and Fe (II) contents and Percentage PE _{MBC}	79
4. Discussion	85
4.1. Apparent vs. real PE mechanisms shortly after glucose addition	85
4.2. Possible mechanism for explaining negative PE _{CO₂}	85
5. Conclusions	86
Acknowledgments	86
References	87
Supplementary materials	90
(Eidesstattliche) Versicherungen und Erklärungen	100

List of Tables

Table I-1 Biomass productions after harvest in 2018 (mean \pm SE, n=3). Root biomass was estimated using the equation: root biomass = straw biomass * root to shoot ratio (mean values in Fig II.2-1).	10
Table II.1-1 Total straw production after harvest in 2017 and 2018 (mean \pm SE, n=3).	33
TableII.1-S1 Fertilization information of the field experiment in 2017 and 2018.	40
TableII.1-S2 Summary results from a two-way ANOVA with repeated measures of CO ₂ and CH ₄ concentrations and their isotope composition, plant height and pore water DOC contents at different rice growth stages. Basis of results for Figures 2-4.	41
TableII.1-S3 Redox potential values (Eh) in pore water (mV) in 2017 and 2018 (mean \pm SD, n=3). noS+FL: continuous flooding; S+FL: sulfate fertilizer + continuous flooding; noS+AWD: wet-dry cycles, and S+AWD: sulfate fertilizer + wet-dry cycles.	41
Table II.2-1 Biomass productions after harvest in 2018 (mean \pm SE, n=3).....	50
TableII.3-S1 Total phospholipid fatty acids (PLFAs) (mg C kg ⁻¹) in paddy soil under fertilization regimes at different soil depths (mean \pm SE, n=3).....	70
TableII.3-S2 Basic physicochemical properties of paddy soil under fertilization regimes at different soil depths (mean \pm SE, n=3). MBC, microbial biomass carbon; MBN, microbial biomass nitrogen; DOC, dissolved organic carbon.	71
TableII.3-S3 Adonis analysis of the effects of treatments and soil depths and their interaction on the specific microbial PLFAs (permutation=999).....	72
Table II.4-S1 Basic physicochemical properties of paddy soil under fertilization regimes at different soil depths before incubation (mean \pm SE, n=3).....	94
Table II.4-S2 Glucose-derived CO ₂ emission rates (% of total glucose input per day) at three soil samplings, and the absolute amount of primed MBC, DOC and cumulative primed CO ₂ (mg kg ⁻¹) at day 2 in 60-days incubated paddy soil under long-term fertilization regimes at different soil depths (mean \pm SE, n=3).	95
Table II.4-S3 Adonis analysis of the effects of treatments and soil depths and their interaction on glucose-derived CO ₂ emission rates and total Fe (II) contents (permutation=999). Basis of results for Table II.4-S2 and Figure II.4-5.	96
Table II.4-S4 Percentage priming effect (% of basal respiration per day) and the absolute amount of SOM-derived CO ₂ (mg kg ⁻¹) at three sampling times in 60-days incubated paddy soil under long-term fertilization regimes at different soil depths (mean \pm SE, n=3).	97
Table II.4-S5 C pool changes from day 2 to day 20 (mg kg ⁻¹) in 60-days incubated paddy soil under long-term fertilization regimes at different soil depths (mean \pm SE, n=3). X _{Glu} and X _{SOM} represented the glucose-derived C and SOM-derived C in X pool, respectively. The data was calculated using the equation: X ₂₀ -X ₂ . X ₂₀ and X ₂ represented the different C pools at day 20 and day 2, respectively. Positive	

values indicate a pool increase, whereas negative values indicate a pool decrease. Basis of results for Figure 3 & S3.....	98
Table II.4-S6 C pool changes from day 20 to day 60 (mg kg^{-1}) in 60-days incubated paddy soil under long-term fertilization regimes at different soil depths (mean \pm SE, n=3). X_{Glu} and X_{SOM} represented the glucose-derived C and SOM-derived C in X pool, respectively. The data was calculated using the equation: $X_{60}-X_{20}$. X_{60} and X_{20} represented the different C pools at day 60 and day 20, respectively. Basis of results for Figure 3 & S3.....	99

List of Figures

- Figure I-1 Conceptual framework of the main processes causing CH₄ production in paddy soils. Arrows in different colours and respective Latin numbers represent different C processes in paddy soil: (I) acetoclastic methanogenesis; (II) hydrogenotrophic methanogenesis; (III) CH₄ oxidation; (IV) SRB using acetyl-CoA/carbon monoxide dehydrogenase pathway; (V) SRB using tricarboxylic acid cycle; (VI) H₂-utilizing sulfate reducing bacteria. 4
- Figure I-2 Experimental set-up of pulse labelling approach..... 7
- Figure I-3 Cross plot of $\delta^{13}\text{C-CO}_2$ and $\delta^{13}\text{C-CH}_4$ at three rice growth stages under two fertilization treatments and water regimes (mean \pm SE). Circles demonstrate data under flood conditions without S fertilization, down triangles – flood with S, squares – wet-dry regime without S, diamonds – wet-dry regime with S. Dashed arrows show the direction of cross-plot parameters in paddy soil: (I) acetoclastic methanogenesis caused $\delta^{13}\text{C-CH}_4$ depletion; (II) hydrogenotrophic methanogenesis caused $\delta^{13}\text{C-CH}_4$ depletion and $\delta^{13}\text{C-CO}_2$ enrichment; (III) $\delta^{13}\text{C-CH}_4$ enrichment and $\delta^{13}\text{C-CO}_2$ depletion by CH₄ oxidation pathway; (IV) $\delta^{13}\text{C-CO}_2$ depletion caused by sulfate reduction pathway plus soil respiration (SR) including root- and microbial respiration; and sulfate-induced $\delta^{13}\text{C-CH}_4$ depletion. For the stem elongation stage, n=6 as there were similar water-logged conditions. For booting and flowering stages, n=3. 9
- Figure I-4 Changes to the microbial community in paddy soil at different soil depths and under different fertilization regimes based on: (a) ratio of fungal to bacterial phospholipid fatty acids (PLFAs); (b) ratio of G+ to G- bacterial PLFAs; and (c) ratio of G+ bacteria to actinomycete PLFAs (n = 3)..... 11
- Figure I-5 Percentage priming effect (% of basal respiration per day) in 60-days incubated paddy soil under long-term fertilization regimes at different soil depths (mean \pm SE, n=3). Numbers under each bar represented the days after incubation. 13
- Figure II.1-1 Conceptual framework of the main processes causing ¹³C-isotope fractionation in CO₂ and CH₄ in paddy soils. Arrows in different color and respective Latin numbers represent different C processes in paddy soil. Upward and downward arrows in the table represent the ¹³C-enrichment and depletion during different C processes, respectively. 26
- Figure II.1-2 Rice plant height over rice growth season (n=6) (a), plant biomass and root to shoot ratio at flowering stage (n=3) (b) (mean \pm SE). The two wet-dry periods were at 56-63 DAT and 70-77 DAT, respectively. 30
- Figure II.1-3 Pore water dissolved organic C concentrations over rice growth season (mean \pm SE, n=3). 30
- Figure II.1-4 Concentrations of CO₂ (a), CH₄ (b) and delta values of CO₂ (c) and CH₄ (d) in gas bottles in soil depth from 0-20 cm (mean \pm SE, n=3)..... 31
- Figure II.1-5 Cross plot of $\delta^{13}\text{C-CO}_2$ and $\delta^{13}\text{C-CH}_4$ at three rice growth stages under two fertilization treatments and water regimes (mean \pm SE). Dashed arrows show

- the direction of cross-plot parameters in paddy soil: (green) hydrogenotrophic methanogenesis caused $\delta^{13}\text{C}\text{-CH}_4$ depletion and $\delta^{13}\text{C}\text{-CO}_2$ enrichment (pathway II); (brown) $\delta^{13}\text{C}\text{-CH}_4$ enrichment and $\delta^{13}\text{C}\text{-CO}_2$ depletion by CH_4 oxidation pathway III; (black) $\delta^{13}\text{C}\text{-CO}_2$ depletion caused by sulfate reduction pathway IV plus soil respiration (SR) including root- and microbial respiration; and sulfate induced $\delta^{13}\text{C}\text{-CH}_4$ depletion. For the stem elongation stage, data of wet-drying treatments were combined with flooding of respective S treatments (grey circle and triangle, $n=6$) as there were similar water-logged conditions at this stage. For booting and flowering stages, $n=3$ 32
- Figure II.1-S1 Fertilization, rice growth stages and sampling time schedules of the field experiment in 2018. For details, please refer to the text in Materials and methods. 42
- Figure II.1-S2 Mean concentration of CO_2 , CH_4 and their mean delta values (a) CO_2 , (b) CH_4 concentrations and mean delta values of CO_2 (c) and CH_4 (d) before drying conducted (stem elongation stage 54DAT), and mean concentration of CO_2 (e, i), CH_4 (f, j) and mean delta values of CO_2 (g, k) and CH_4 (h, l) after wet-drying conducted at booting and flowering stages, respectively, in gas bottles at 0–10 cm and 10–20 cm soil depth (mean \pm SE, $n=6$). 43
- Figure II.1-S3 Pore water total dissolved sulfur concentrations over rice growth season in 2017 (a) and 2018 (b) (mean \pm SE, $n=3$). 44
- Figure II.2-1 Plant biomass and the root to shoot ratio at flowering stage (mean \pm SE, $n=21$, 3 replicates * 7 sampling times). The two wet-dry periods were at 56-63 DAT and 70-77 DAT, respectively. Small letters indicate significant differences at $P < 0.05$ based on Duncan's test within treatments. 50
- Figure II.2- 2 The assimilated ^{13}C allocation in rice plants (a) ^{13}C in shoot; (b) ^{13}C in root; (c) ^{13}C -root to ^{13}C -shoot ratio after ^{13}C pulse labelling under different treatments (mean \pm SE, $n=3$). 50
- Figure II.3-1 Changes to the microbial community in paddy soil at different soil depths and under different fertilization regimes based on: (a) ratio of fungal to bacterial phospholipid fatty acids (PLFAs); (b) ratio of gram-positive (G+) to gram-negative (G-) bacterial PLFAs; and (c) ratio of gram-positive to actinomycete PLFAs ($n=3$). 59
- Figure II.3-2 Redundancy analysis of phospholipid fatty acid content from soil samples: (a) 0–40 cm, (b) 0–20 cm, and (c) 20–40 cm. SOC: soil organic carbon. Data for depths of 0–10 cm (black), 10–20 cm (red), 20–30 cm (yellow), and 30–40 cm (orange) are shown. 60
- Figure II.3-S1 (a) Soil respiration rate and (b) soil metabolic quotient ($q\text{CO}_2$) in paddy soil under fertilization regimes at different soil depths ($n=3$). 72
- Figure II.4-1 Glucose-derived CO_2 efflux (% of total glucose input per day) in 60-days incubated paddy soil (a) CK+Glu; (b) NPK+Glu; (c) ST+Glu; (d) OM+Glu under long-term fertilization regimes at different soil depths (mean \pm SE, $n=3$). Statistical analysis was presented in supplementary Table II.4-S2. 79
- Figure II.4-2 Percentage priming effect (% of basal respiration per day) in 60-days

incubated paddy soil under long-term fertilization regimes at different soil depths (mean \pm SE, n=3). Numbers under each bar represented the days after incubation.	80
Figure II.4-3 Absolute amount of DOC and MBC derived from soil organic matter (SOM-C) and glucose (Glu-C) (mg kg^{-1}) at day 2 (a, d), day 20 (b, e) and day 60 (c, f) in incubated paddy soil under long-term fertilization regimes at different soil depths (mean \pm SE, n=3). Control-C represent the DOC, and MBC contents in the incubated soil without glucose addition at the same sampling day.	82
Figure II.4-4 Percentage primed MBC (a, Percentage PEMBC) and the relationship between Percentage PEMBC and glucose-induced MBC change (b) at day 2 in incubated paddy soil under long-term fertilization regimes at different soil depths (mean \pm SE, n=3).	83
Figure II.4-5 total Fe (II) contents (mg kg^{-1}) at sampling time day 2 (a), day 20 (b), and day 60 (c) in 60-days incubated paddy soil with (Glu+) and without (Control) glucose addition under long-term fertilization regimes at different soil depths (mean \pm SE, n=3).	84
Figure II.4-S1 Absolute amount of CO ₂ emission rates (mg C kg^{-1} dry soil per day, basal respiration rate) in 60-days incubated paddy soil without glucose addition under fertilization regimes at different soil depths (mean \pm SE, n=3). CK, no fertilizer; NPK, chemical fertilizers; ST, rice straw combined with chemical fertilizers; OM, 70% NPK + 30% chicken manure.	90
Figure II.4-S2 Absolute amount of cumulative CO ₂ emission at day 60 (mg C kg^{-1} dry soil, basal respiration) in 60-days incubated paddy soil without glucose addition under fertilization regimes at different soil depths (mean \pm SE, n=3). CK, no fertilizer; NPK, chemical fertilizers; ST, rice straw combined with chemical fertilizers; OM, 70% NPK + 30% chicken manure.	91
Figure II.4-S3 Absolute amount of CO ₂ efflux derived from soil organic matter and glucose (mg C kg^{-1} dry soil per day) in 60-days incubated paddy soil under fertilization regimes at different soil depths (mean \pm SE, n=3).	92
Figure II.4-S4 C retention in soil system (including glucose-derived soil organic C and glucose-derived dissolved organic C in the supernatant) and C loss through cumulative primed CO ₂ at day 20 (a) and day 60 (b) in incubated paddy soil under long-term fertilization regimes at different soil depths (mean \pm SE, n=3). SOC: soil organic C; DOC: dissolved organic C. Numbers above the bar represent the total C retention as a percentage of added glucose at the corresponding soil and depth. .	93

Abbreviations

ANOVA	analysis of variance
AWD	alternating wet-dry cycles
C	carbon
CO ₂	carbon dioxide
CH ₄	methane
GHGs	greenhouse gases
SOM	soil organic matter
noS+AWD	wet-dry cycles without sulfate fertilizer
noS+FL	continuous flooding without sulfate fertilizer
S+AWD	sulfate fertilizer + wet-dry cycles
S+FL	sulfate fertilizer + continuous flooding
ID	inner diameter
OD	outer diameter
SE	standard error
PDB	Pee Dee Belemnite
DOC	dissolved organic carbon
SRB	sulfate-reducing bacteria;
MA	methanogenic archaea
DAT	days after transplanting
MBC	microbial biomass carbon
MBN	microbial biomass nitrogen
G ⁻	gram-negative bacteria
G ⁺	gram-positive bacteria
PLFA	phospholipid fatty acid
CK	control soil
NPK	mineral fertilizers
NPK + ST	rice straw combined mineral fertilizers
NPK + OM	70% NPK + 30% chicken manure
CK + Glu	control soil with glucose addition

Abbreviations

NPK+ Glu	mineral fertilizers with glucose addition
ST+ Glu	rice straw combined mineral fertilizers with glucose addition
OM+ Glu	70% NPK + 30% chicken manure with glucose addition
PE	priming effect
PE _{CO2}	percentage primed CO ₂
PE _{MBC}	percentage primed MBC

I Extended Summary

1. Introduction

1.1 Organic carbon stocks of paddy soils

Soil, as the largest carbon (C) pool in terrestrial ecosystems, was estimated to globally contain 1550 Gt of organic carbon in the upper 100 cm depths, which doubles the amount of the atmospheric pool (Batjes, 1996; Lal, 2008). Artificial paddy soils, in which rice is grown, cover more than 163 million ha contributing to ~9% of the world's cropland area (Oertel et al., 2016), and contains ~10% higher C than the global mean stock for all soils (Liu et al., 2021).

Atmospheric carbon dioxide (CO₂) is rapidly increased since the Industrial Revolution, and the emissions from land use and land cover change (LULCC) are the second largest anthropogenic source of C into the atmosphere (2.0 Gt year⁻¹) and the most uncertain component of the global C cycle (Houghton, 1999; Scharlemann et al., 2014). The flux of carbon from the atmosphere to soil is primarily mediated by plants. Green plants assimilate CO₂ through the Calvin cycle (Calvin, 1962) for food and energy to maintain respiration and biomass growth. In addition, part of the assimilated C is transferred to the soil via dead biomass of the plants and exudates of living roots (i.e. rhizodeposition) (Hütsch et al., 2002). Globally, the annual rate of photosynthesis is 120 Gt C, most of which is returned to the atmosphere in the form of CO₂ through plant and soil respiration (Lal, 2008).

The issue of paddy soil is more complex. Except ~11% photosynthesis C transported to soil through rhizodeposition, ~17% photosynthesis C is directly left in soil after the harvest. The remaining ~72% in shoot is harvest, of which the non-edible parts, i.e., straw, need further disposal (Liu et al., 2019). The amount of crop residue produced in the world is estimated at 2.8 Gt year⁻¹ for cereal crops (rice, maize, and wheat) (Lal, 2005), and their C contents are around 37–49% of dry biomass (Velthof et al., 2002; Pan et al., 2017; Huang et al., 2018). Straw burning causes air pollution, and greenhouse gases (GHGs) emissions mainly in the form of CO₂ (Miura and Kanno, 1997). Whereas straw returning into flooded paddy fields favors the emissions of methane (CH₄) (Chidthaisong et al., 1996; Feng et al., 2013). Globally, around 97% of rice is grown under flooded conditions (Oertel et al., 2016).

Both CO₂ and CH₄ are defined as GHGs due to their capability to cause global warming, which is a matter of great concern (Linguist et al., 2012b). Rice feeds half of the world's population, and flooded paddy fields are a critical contributor to global CH₄ emissions due to the demand for food production (Fairhurst and Dobermann, 2002). Rice systems were estimated to emit 100 kg CH₄-C ha⁻¹ season⁻¹ (Linguist et al., 2012a). Global CH₄ emissions from paddy soils are estimated to be 0.03 Gt CH₄ yr⁻¹ in 2008–2017, accounting for ~8% of total global anthropogenic emissions of CH₄ (Saunio et al., 2020).

To keep food security and mitigate global warming, understanding the mechanisms of C turnover (both CO₂ and CH₄) is vital. However, in paddy fields where human disturbances are inevitable and frequent, C turnover is more complex than natural soil systems, being highly variable in time and space.

Thus, the present thesis focuses on the CO₂ and CH₄ turnover in paddy soils with special emphasis on the impact of agricultural practices such as fertilization and water management.

1.2 Fertilizer and water management effects on C turnover in paddy soils

Fertilization is a crucial factor for ensuring sustainable food demand to feed the ever-growing world population. There are commonly two types of fertilizers and their combination for arable soils: mineral fertilizers, and organic fertilizers including the straw return and manure amendment. Notably, for paddy soils, combined mineral and organic fertilizers with equal nitrogen (N) was even more efficient in enhancing rice yield than additional organic amendment on the basis of mineral fertilization (Zhou et al., 2016). Carbon sequestration can also be achieved through fertilization. Over the long-term, mineral fertilizers, straw return, and manure were estimated to enhance soil organic C in paddy fields at the rate of 0.10, 0.30, and 0.34 g kg⁻¹ year⁻¹, respectively (Tian et al., 2015).

Sulfate fertilization was an efficient method to suppress CH₄ emission in paddy soils (Cai et al., 1997; Ro et al., 2011; Linquist et al., 2012b). For example, ammonium sulfate reduced CH₄ emissions over the years and seasons by 25% to 56% compared with urea applied at the same rate (Corton et al., 2000). The underlying mechanism is the competition for substrates (both acetate and H₂) between sulfate-reducing bacteria (SRB) and methanogenic archaea (MA) (Fig I-1, pathways IV-VI) (Schonheit et al., 1982; Whiticar et al., 1986; Ro et al., 2011).

Water management is another important factor for sustainable food production, especially for crops grown in semi-aquatic conditions, such as paddy rice. However, a fully flooded water supply favors the performance of anaerobic microorganisms, e.g. methanogens, and causes CH₄ emissions (Hussain et al., 2015). Proper irrigation, such as alternating wet-dry cycles (AWD), was reported to decrease CH₄ emission by inhibiting methanogens via oxygen (O₂) supply and also increasing the rate of CH₄ oxidation (Zhang et al., 2012a). Although it is known that sulfate fertilization and water management can efficiently reduce CH₄ emission, there is a clear knowledge gap between field studies that focus on quantification of GHGs emissions and lab studies that investigate mechanisms.

To close this knowledge gap, this thesis investigated short-term sulfate fertilization effects on dynamics and mechanisms of CO₂ and CH₄ under field conditions as well as the efficiency of water management in reducing GHGs (Study 1, 2). In addition to these short-term effects, this thesis focused on the long-term effects of fertilizer application on microbial biomass and communities, which play an essential role in SOM turnover (Study 3, 4).

1.3 Mechanisms of CO₂ and CH₄ turnover in soils

Before escaping to the atmosphere, CO₂ and CH₄ undergo various biogeochemical and physical reactions within soils, including production, oxidation, transport upward (bubbles and diffusion), and further oxidation at the soil-atmosphere interface and in

the rhizosphere. CH₄ production is solely driven by MA under anaerobic conditions (Conrad, 2005; Whalen, 2005). The two most important reactions of methanogenesis in paddy soils are acetoclastic methanogenesis and hydrogenotrophic methanogenesis (Fig I-1, pathways I & II). In the former reaction, CH₄ is produced primarily from the methyl group of acetate (Smith and Mah, 1980). During hydrogenotrophic methanogenesis, CO₂ is reduced to CH₄ with H₂ as the electron donor (Whalen, 2005). CH₄ oxidation (Fig I-1, pathways III) is driven by methanotrophs under aerobic and anaerobic soil conditions (Michael and Eckhard, 1985). It was demonstrated that the CH₄ produced in the field is oxidized to a large extent by methanotrophs. In addition, 90% of CH₄ was emitted into the atmosphere via aerenchyma of rice plants (Groot et al., 2003; Zhang et al., 2012a).

Although mechanisms of the two methanogenesis pathways are well studied, due to the overlap of many processes mentioned above within soils, uncertainty still exists about the contribution of these two pathways to CH₄ production throughout the rice growing season under field conditions.

Study 1 & 2 – *Alternating wet-dry cycles and sulfate fertilizer effects on CH₄ turnover, photosynthesized C allocation, and rice yield* – aimed to understand the CO₂ and CH₄ turnover in soil gases before subjecting to various biogeochemical and physical reactions. In addition, the effect of these two soil managements and their combination on grain production was also evaluated. We hypothesized AWD and sulfate fertilizer could both efficiently suppress CH₄ production without decreasing grain production.

Two main sources contributing to soil CO₂ emissions are plant-derived and SOM-derived CO₂. Plant-derived CO₂ includes CO₂ from plant residue (shoot and root) decay, root respiration, and microbial respiration of rhizodeposits (rhizo-microbial respiration) (Kuzyakov, 2006). SOM-derived CO₂ includes basal microbial respiration, and concomitant turnover of SOM with fresh C decomposition known as priming effects (PEs) (Kuzyakov et al., 2000).

The input of fresh organic matter may strongly affect SOM stabilization through accelerating or decelerating SOM mineralization, which refers to positive or negative PEs. This part of C flux which is highly dynamic gained scientific focuses in climate change. Negative PE was mainly explained by “preferential substrate utilization” that microorganisms preferentially utilize the added labile substrate rather than decomposing SOM due to its recalcitrance (Blagodatskaya et al., 2007). In contrast, there were two opposite mechanisms to explain positive PE in previous studies: nutrients mining and stoichiometric decomposition theory (Fontaine et al., 2011; Chen et al., 2014). In the former mechanism, organic C input could reduce the availability of other nutrients (mainly N) and result in more SOM decomposition by producing enzymes to access limited nutrients (Fontaine et al., 2011). Oppositely, the later mechanism suggests that balanced substrate addition, i.e. C/N ratios close to microbial requirements, could stimulate more *r*-strategists and accelerate SOM decomposition by higher microbial activity (Chen et al., 2014).

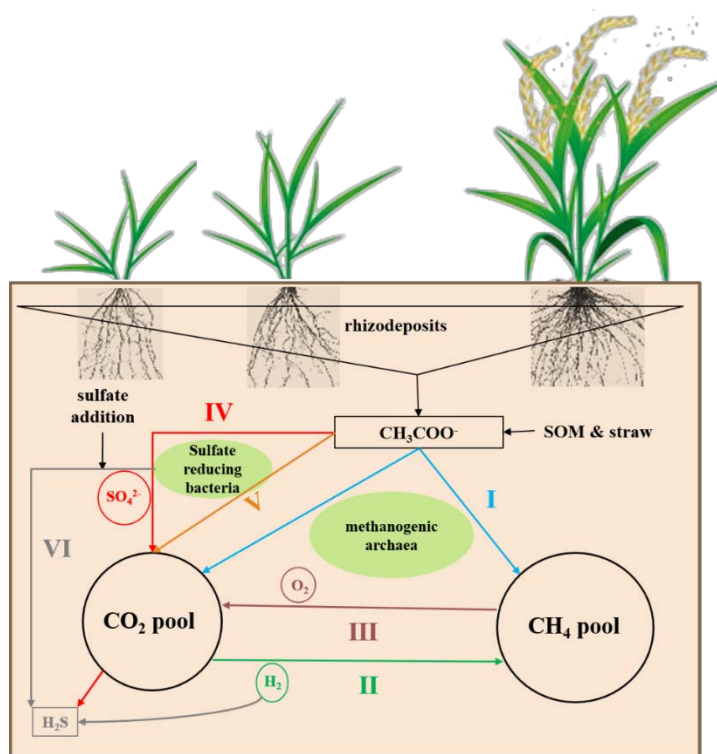


Figure I-1 Conceptual framework of the main processes causing CH₄ production in paddy soils. Arrows in different colours and respective Latin numbers represent different C processes in paddy soil: (I) acetoclastic methanogenesis; (II) hydrogenotrophic methanogenesis; (III) CH₄ oxidation; (IV) SRB using acetyl-CoA/carbon monoxide dehydrogenase pathway; (V) SRB using tricarboxylic acid cycle; (VI) H₂-utilizing sulfate reducing bacteria.

In general, PE patterns may vary depending on the soil type (Qiu et al., 2017; Cui et al., 2020), substrate type (Wei et al., 2020), the amount of added substrate (Mason-Jones et al., 2018), fertilizations (Wu et al., 2020) and temperature (Wei et al., 2021). PE may also change dynamically over time, for example, C addition triggers microbial activity and metabolism and cause “apparent priming” by pool substitution in the short-term, i.e. within a few days or weeks. In contrast to apparent priming, real priming (real SOM decomposition) needs longer-term incubation to occur when activated microorganisms start to produce extracellular enzymes to mine nutrients after the exhaustion of readily available substrate (Blagodatskaya and Kuzyakov, 2008).

It is well established that C that newly entered the soil can stimulate short-term microbial activity and thus change SOM turnover. While microorganisms play an important role in C sequestration, over the long term, how fertilizer management affects microbial communities is not fully understood.

Study 3 – Vertical and horizontal shifts in the microbial community structure of paddy soil under long-term fertilization regimes – aimed to understand how long-term fertilization managements (cumulative short-term responses) shift microbial communities, which play important roles in SOM stabilization.

Study 4 – *Mineral bound organic carbon explains the negative priming effect in paddy soils* – aimed to investigate the dynamics and patterns of PE based on the understanding of microbial community shifts after long-term fertilization. We hypothesized that long-term mineral fertilization reduces PE compared to soils without fertilizer input (control) as soil microorganisms do not need to mine SOM for nutrients. Accordingly, PE is assumed to increase if both mineral plus organic fertilizers are added (higher C/N ratios due to organic C input) due to the increasing demand for nutrients derived from SOM (nutrient mining mechanism). Consequently, we also hypothesized that lower nutrient availability in subsoil (20-40 cm) result in higher PE than in topsoil (0-20 cm), however, with apparent PE being more pronounced in topsoil due to larger microbial biomass and higher activity.

1.4 Objectives

In summary, the main objectives of the present work were:

- (1) to compare the efficiency of AWD and sulfate fertilization in decreasing CH₄ production and also to disentangle the CH₄ turnover mechanisms affected by AWD and sulfate addition in paddy soil (Study 1).
- (2) to quantify the photosynthetic C assimilation and allocation in the plant-soil system under AWD and sulfate addition managements and to evaluate these two soil managements and their combination on final yield (Study 2).
- (3) to investigate how microbial community structures respond to long-term application of organic and mineral fertilizers in paddy soil profiles (Study 3).
- (4) to explore the dynamics and patterns of PE at different depths of paddy soils that have received long-term mineral and/or organic fertilization and to disentangle the underlying mechanisms (Study 4).

2. Materials and methods

2.1 Characteristics of the soils used in the studies

The paddy soil used in Study 1 & 2 was collected at a site at Cascina Veronica, close to the town of Garlasco, Pavia, Italy (45°10'39"N, 8°53'48"E) in 2017. The soil was classified as Eutric Gleysol with 15-year rice cultivation history following corn cropping and with a $\delta^{13}\text{C}$ value of soil carbon of -21.9‰. The basic chemical properties of the soil were as follows: pH 5.6, total C 2.0%, total N 0.6%, total S 2.6 g kg⁻¹. A large batch of soil from the plough layer (0–30 cm) was collected for establishing mesocosm experiments under field conditions. Plastic containers (112 cm * 72 cm * 65 cm) were filled with 30 cm of gravel at the bottom and overlaid by 20 cm of mixed soil.

The paddy soil used in Study 3 & 4 was sampled from four soil layers (0–10, 10–20, 20–30, and 30–40 cm) at a field used for long-term fertilization experiments in Ningxiang, Hunan Province, China (111°54'–112°18'E, 28°07'–28°37'N) in 2017. The soil at the start of the experiment formed from river alluvium; the main physical and chemical properties of the soil were: pH of 5.8, 17.1 g kg⁻¹ soil organic C, 1.8 g kg⁻¹ total N, 144.0 mg kg⁻¹ available N, and 12.8 mg kg⁻¹ Olsen-P. Four fertilization regimes were established since 1986: no fertilizer (CK), mineral fertilizer (NPK) (urea, superphosphate, and potassium chloride), rice straw combined with mineral fertilizer (NPK + ST), and 70% NPK + 30% chicken manure (NPK + OM). The total amount of NPK fertilizer was identical for each fertilized soil in each season.

2.2 Isotope approaches to disentangle CO₂ and CH₄ fluxes in soil

The main challenge for investigating C turnover is dealing with the definite co-occurrence and temporal dynamics of CO₂ and CH₄ processes in soils. To gain a better understanding on C turnover in paddy soils, two main stable isotope technologies were applied in this work to achieve different objectives: 1) natural isotope fractionation and 2) pulse labelling.

Fortunately, the discrimination against ¹³C during acetoclastic methanogenesis is rather strong, resulting in ¹³C-depleted CH₄ (-50‰~-60‰ vs. Pee Dee Belemnite (PDB)) due to strong stable isotope fractionation (Whiticar, 1999). An even greater ¹³C-depletion of CH₄ was observed during hydrogenotrophic methanogenesis (down to -110‰ vs. PDB) (Krzycki et al., 1987; Whiticar, 1999). Simultaneously, there was a strong ¹³C-enrichment of residual CO₂ from hydrogenotrophic methanogenesis due to the preferred consumption of lighter ¹²C-CO₂. This gave us the chance to disentangle the CH₄ turnover mechanisms affected by specific treatments by distinguishing $\delta^{13}\text{C}$ differentiation of CO₂ and CH₄ in acetoclastic and hydrogenotrophic methanogenesis (Fig I-1, pathways I-III).

Pulse labelling can efficiently provide information on the relative allocation of recently assimilated/added C to different C pools and fluxes and allows studying the dynamics of C allocation between pools and comparing the distribution of ¹³C in rice and soil under different treatments.

For pulse labelling used in Study 2, after the second wet-dry cycle at the flowering stage, the plants were exposed to the stable isotope-tracer (¹³CO₂) for 2.5 hours (8 a.m.-1 p.m.)

in a chamber consisting of wood frames stringed with transparent low-density polyethylene (LDPE) foil with a total light transmission of ~90% (Fig. I-2). Rice straw and grains were collected and weighed after the harvest.

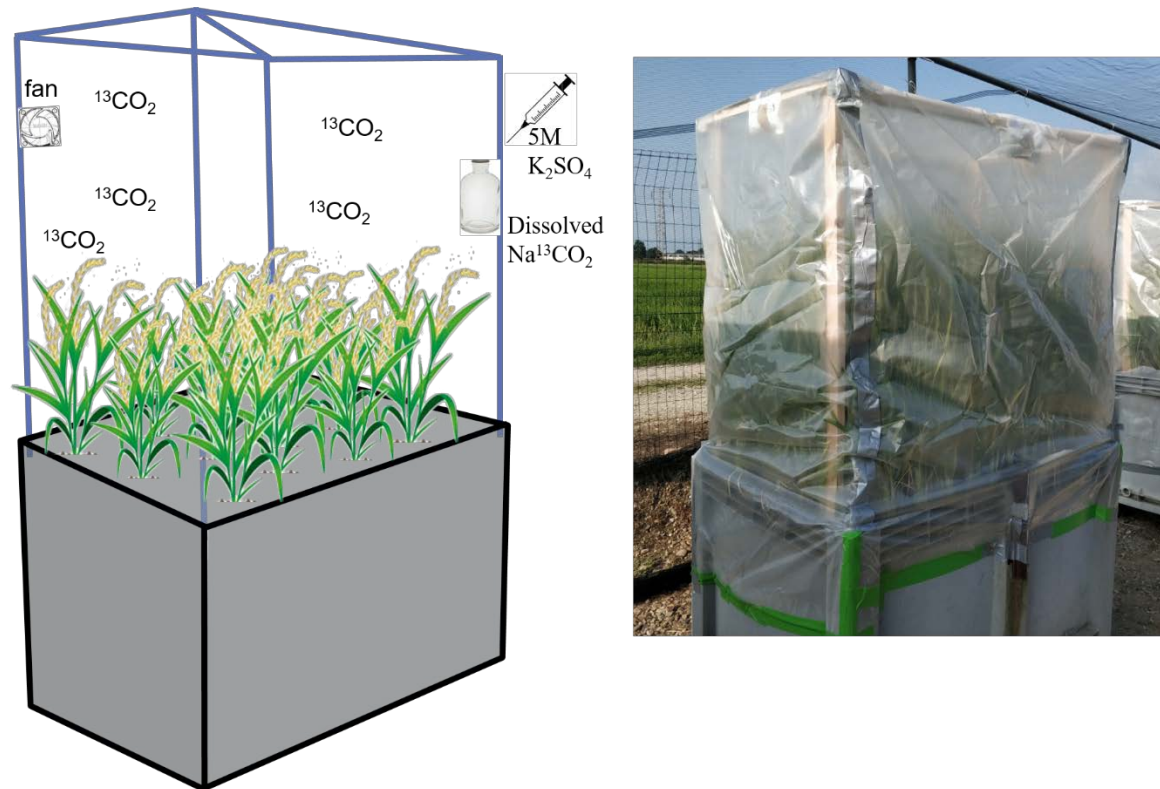


Figure I-2 Experimental set-up of pulse labelling approach.

For investigating the priming effect, a certain amount of ^{13}C -glucose was added to glass serum bottles containing well-mixed paddy soil (Study 4) to mimic labile C input under field conditions. Gas samples in the headspace were collected by syringe using pre-evacuated exetainer glass bottles at defined time intervals after glucose addition. Soils were destructively sampled at defined days to determine the temporal dynamics of different C pools.

2.3 Gas and soil sampling

For Study 1, 2-cylinder passive diffusion soil gas samplers (described in detail in (Goldberg et al., 2008)) were installed into each mesocosm for collecting the soil gases at 0–10 and 10–20 cm. Briefly, each polyvinyl chloride cylinder (ID 70 mm; OD 79 mm; 0.1 m height) contained 5 m coiled silicon tube (ID 3 mm; OD 5 mm), both ends of which were connected with gas impermeable polyurethane tubes (PU) (ID 1.8 mm; OD 3 mm). The ends of the PU tubes were placed above the soil surface, and two-way valves were attached. During the rice growth, three gas samplings were conducted from 8–12 a.m. at stem elongation (before wet-drying), booting (after the first drying period), and flowering stages (after the second drying period).

Soil pore water samples were collected using Rhizon samplers. One plant per mesocosm container was chosen randomly for plant and soil sampling (Study 1 & 2). Shoots were cut at the base near the soil surface; the root and soil samples were taken from 0–20 cm depth using a Riverside auger.

2.4 Analysis

2.4.1 Isotope analyses

$^{13}\text{C}/^{12}\text{C}$ isotope ratio of CO_2 and CH_4 in soil gases as well as their concentrations were measured using a gas chromatograph-isotope ratio mass spectrometer coupled to a pre-GC concentration interface (Study 1). CO_2 concentrations in the headspace were measured using an Agilent 7890A gas chromatograph equipped with a thermal conductivity detector (Study 4). The ^{13}C isotope composition of CO_2 , solid samples (shoot, root, and soil), and freeze-dried DOC samples were measured using an isotope mass spectrometer (Study 2 & 4).

2.4.2 Microbial community composition

Lipid extraction and PLFA analysis were used in Study 3 for investigating microbial community structures. The PLFA method is a rapid and sensitive method to detect changes in the microbial community in soil (Frostegård et al., 2011). Different fatty acids were stated to indicate specific groups of microorganisms, including G+ bacteria, gram-negative (G-) bacteria, fungi, and actinomycetes. Detailed classifications are described in supplementary methods in Study 3. PLFA methyl esters were separated and identified using a gas chromatograph fitted with a MIDI Sherlock microbial identification system.

2.4.3 Soil analysis

Dissolved organic C (DOC) concentrations in pore water samples were measured using an N/C analyzer (Study 1). Un-fumigated samples extracted using 0.05 M K_2SO_4 were defined as soil DOC. Extracts were measured by a total organic C (TOC) analyzer. Microbial biomass carbon (MBC) and nitrogen (MBN) were extracted following the fumigation-extraction method (Brookes et al., 1985; Wu et al., 1990). MBC and MBN were calculated based on differences in the DOC and dissolved N concentrations of non-fumigated and fumigated samples divided by the extraction efficiency of 0.45 and 0.54 for C and N, respectively (Study 3 & 4).

Soil pH was determined with a pH meter in a soil/water ratio of 1:2.5. Soil organic C content was determined using the dry combustion method in an elemental analyzer. Soil alkali-hydrolyzable nitrogen content (available N) was determined using alkali solution diffusion absorption (Study 3 & 4).

3. Results and discussion

3.1 CH₄ turnover, photosynthesized C allocation and rice yield affected by AWD and sulfate fertilizer (Study 1 & 2)

Natural C isotope fractionation has proven to be a promising approach for distinguishing CH₄ processes (production and oxidation) within paddy soils under field conditions. Compared to 51 mg C L⁻¹ at the flowering stage under flooded conditions, CH₄ concentrations under AWD declined to less than 0.1% (Study 1). Simultaneously, relative ¹³C enrichment in CH₄ and depletion in CO₂ under AWD indicated the consumption of CH₄, i.e. CH₄ oxidation (Figure I-1 & 3, pathway III). In addition, in Study 2, AWD alone caused an increase in root relative to shoot biomass (Table I-1, $P < 0.05$); moreover, it potentially lowered grain production, yet not significant.

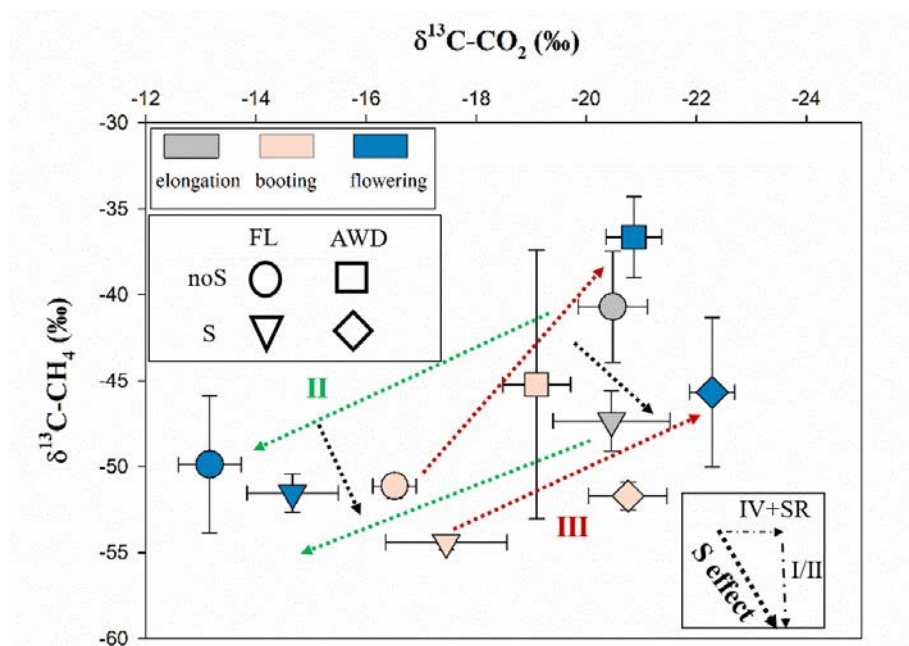


Figure I-3 Cross plot of $\delta^{13}\text{C-CO}_2$ and $\delta^{13}\text{C-CH}_4$ at three rice growth stages under two fertilization treatments and water regimes (mean \pm SE). Circles demonstrate data under flood conditions without S fertilization, down triangles – flood with S, squares – wet-dry regime without S, diamonds – wet-dry regime with S. Dashed arrows show the direction of cross-plot parameters in paddy soil: (I) acetoclastic methanogenesis caused $\delta^{13}\text{C-CH}_4$ depletion; (II) hydrogenotrophic methanogenesis caused $\delta^{13}\text{C-CH}_4$ depletion and $\delta^{13}\text{C-CO}_2$ enrichment; (III) $\delta^{13}\text{C-CH}_4$ enrichment and $\delta^{13}\text{C-CO}_2$ depletion by CH₄ oxidation pathway; (IV) $\delta^{13}\text{C-CO}_2$ depletion caused by sulfate reduction pathway plus soil respiration (SR) including root- and microbial respiration; and sulfate-induced $\delta^{13}\text{C-CH}_4$ depletion. For the stem elongation stage, $n=6$ as there were similar water-logged conditions. For booting and flowering stages, $n=3$.

Sulfate fertilization was reported to reduce CH₄ production as sulfate-reducing bacteria (SRB) stimulated by sulfate addition have a higher affinity for substrates than methanogenic archaea (MA) (Holmer and Kristensen, 1994; Ji et al., 2018). The

absence of a decline in CH₄ concentrations in sulfate treatments in Study 1 was explained by ample organic substrate from the straw amendment. However, sulfate fertilizer had obvious effects on plant biomass (Table I-1). Of particular interest is, under AWD, sulfate fertilizer was able to balance root/shoot ratio and thus stabilized grain productions (Table I-1).

In addition, $\delta^{13}\text{C}$ values in CO₂ were relatively enriched under flooded conditions, and the enrichment increased through the rice growth stages (Figure I-1, pathway II). We suggest that the possible mechanism for this ¹³C-enrichment is a continuously increasing contribution from the hydrogenotrophic methanogenesis, as all other processes would cause ¹³C depletion in CO₂ due to microbial discrimination against heavier ¹³C either in ¹³C-depleted CH₄ or in C₃-derived substrates.

Pulse labelling results showed similar assimilation patterns in all treatments: most of assimilates (>50%) were retained aboveground, and the allocation in roots peaked at day 4; no detective enrichment was found in soils (Fig II.2-3 in Study 2). It was suggested that this minor difference could be due to short pulse labelling time and too low translocation downwards at the flowering stage.

Table I-1 Biomass productions after harvest in 2018 (mean \pm SE, n=3). Root biomass was estimated using the equation: root biomass = straw biomass * root to shoot ratio (mean values in Fig II.2-1).

Yield	noS+FL	S+FL	noS+AWD	S+AWD
Grain (g)	930 \pm 32a	932 \pm 31a	895 \pm 19a	930 \pm 23a
Straw (g)	787 \pm 35b	1068 \pm 46a	782 \pm 24b	993 \pm 13a
G/S	1.18 \pm 0.01a	0.87 \pm 0.04b	1.15 \pm 0.01a	0.94 \pm 0.03b
Root production (g)	202 \pm 7c	297 \pm 10a	263 \pm 7b	283 \pm 3ab

3.2 Microbial communities across the soil profile altered by long-term fertilization (Study 3)

Over the long term, both mineral and organic fertilizers were estimated to help sequester C at the rate of 0.046–0.4 g kg⁻¹ yr⁻¹ (Tian et al., 2015). Aiming to investigate the effects of long-term fertilizer on soil microorganisms, which play important roles for soil C turnover, soil samples were directly collected from a paddy field and analyzed for microbial biomass and community composition. Microbial biomass decreased from 0 to 40 cm (with actinomycetes < G+ bacteria < G- bacteria < fungi) due to lowering soil aeration and substrate availability along soil depths (Kögel-Knabner et al., 2010; Jones et al., 2018).

Over the long term, G+ bacteria benefited the most from mineral fertilizer than the other microbial groups. (Fig I-4). This result was supported by some studies in paddy soil (Daquiado et al., 2016; Tang et al., 2018) and other soil systems (Peacock et al., 2001; Deneff et al., 2009; Wang et al., 2014). However, it contradicted other studies (Zhang et al., 2012b; Dong et al., 2014) and requires further investigations on the underlying mechanisms.

Partial replacement of mineral fertilizer with straw particularly enhanced the abundances of fungi at 10–20 cm soil depth, which is explained by the important role of fungi in straw decomposition (Frey et al., 2003; Li et al., 2020). Manure replacement further enhanced the abundance of G+ bacteria at 0–30 cm soil depth, which may be attributed to the vital role of G+ bacteria in the turnover of organic N (Enggrob et al., 2020).

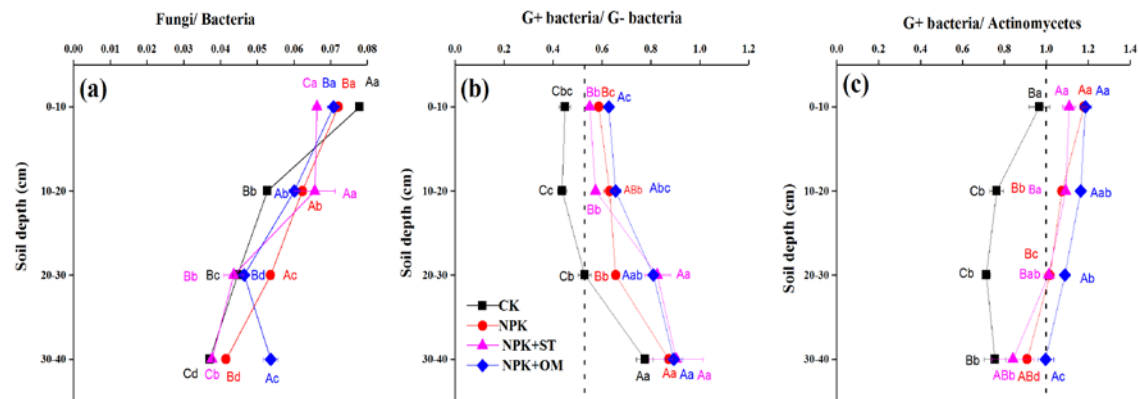


Figure I-4 Changes to the microbial community in paddy soil at different soil depths and under different fertilization regimes based on: (a) ratio of fungal to bacterial phospholipid fatty acids (PLFAs); (b) ratio of G+ to G- bacterial PLFAs; and (c) ratio of G+ bacteria to actinomycete PLFAs (n = 3).

3.3 Soil priming effect patterns in top- and subsoil altered by fertilization (Study 4)

Our findings demonstrate that the structure of the microbial community is strongly impacted by long-term fertilization, independent of fertilizer type (Study 3). In turn, the changes of microbial activity and communities can affect SOM stabilization through accelerating or decelerating SOM mineralization, i.e. PE (Kuzyakov et al., 2000). Four depths of paddy soils were incubated with or without the addition of ^{13}C -labelled glucose to simulate easily available plant C input to the soil for investigating PE patterns.

At day 2 the percentage primed MBC (PE_{MBC}) was negative (-6 – -5%) at 0–10 cm soil depth in all the glucose-treated soils (Fig II.4-4a); organic fertilization (ST and OM) soils had negative PE_{MBC} at deeper soil depths (10–20 and 10–30 cm, respectively). After glucose addition, there are two main microbial process groups that can cause native MBC loss (negative PE_{MBC}): 1) the increase of microbial activity induced more respiration; 2) added substrate was incorporated into microbial biomass and substituted native biomass. Simultaneously, the intensity of PE_{MBC} was positively correlated with relative microbial biomass growth (Fig II.4-4b). These results suggested that in soil that is not C-deficient (receive C through rhizodeposition at 0–10 cm and organic fertilization at deeper depths), microorganisms focused on renewing old C with new C (apparent PE) rather than investing in growth shortly after substrate addition, resulting in slower biomass formation.

The highest PE_{CO_2} was observed shortly after adding glucose in all soils and depths (Fig I-5). In addition, NPK soils had the lowest PE_{CO_2} compared to unfertilized and organic fertilized soils at 0–30 cm. These results are in accordance with the N mining mechanism stating that in soil with balanced nutrients condition (NPK), microbial activity is low together with lower PE; whereas under low nutrients (unfertilized) or extra C (organic fertilized) conditions, PE will be higher as microorganisms produce extracellular enzymes to mine other nutrients (Phillips *et al.*, 2011). Interestingly, SOM-derived DOC relative to the control, i.e., primed DOC, was much higher in topsoil than in subsoil (Fig II.4-3a). If those increased DOC were caused by N mining, topsoil that showed higher DOC release should be expected to have higher PE_{CO_2} due to stronger SOM decomposition (Fontaine *et al.*, 2011).

We propose that biotic and/or abiotic desorption of mineral-bound OC is a key mechanism explaining the SOM-derived DOC increase at day 2. In paddy soils, there are many ways of organic C release as microorganisms utilize glucose. First, microbial Fe reduction under anaerobic condition can release organic C after desorption from Fe oxides (Rasmussen *et al.*, 2006; Dong *et al.*, 2017; Jeewani *et al.*, 2020; Liu *et al.*, 2022b). Second, glucose addition may disrupt mineral–organic associations via an immediate, abiotic mechanism (Keiluweit *et al.*, 2015). Also, anionic intermediates such as formate and acetate with higher sorption capacity on Fe oxides may displace the OC that was originally absorbed (Adhikari *et al.*, 2019; He *et al.*, 2020). After glucose addition, those SOM-derived organic C appeared to be the direct source for positive PE_{CO_2} rather than organic C release from SOM decomposition by stimulating microbial activity (Fig I-5). At the later incubation, we propose that organic C resorption accounts for negative PE_{CO_2} commonly observed in paddy soils: organic C may rebind or co-precipitate with iron oxides or other newly formed minerals such as FeS (Ayotade, 1977; Maguffin *et al.*, 2020) thus reducing Fe(II) and SOM-derived DOC contents (Figs. II.4-5b & 5c). The rebound or co-precipitated organic C is inaccessible for microorganisms and result in negative PE_{CO_2} .

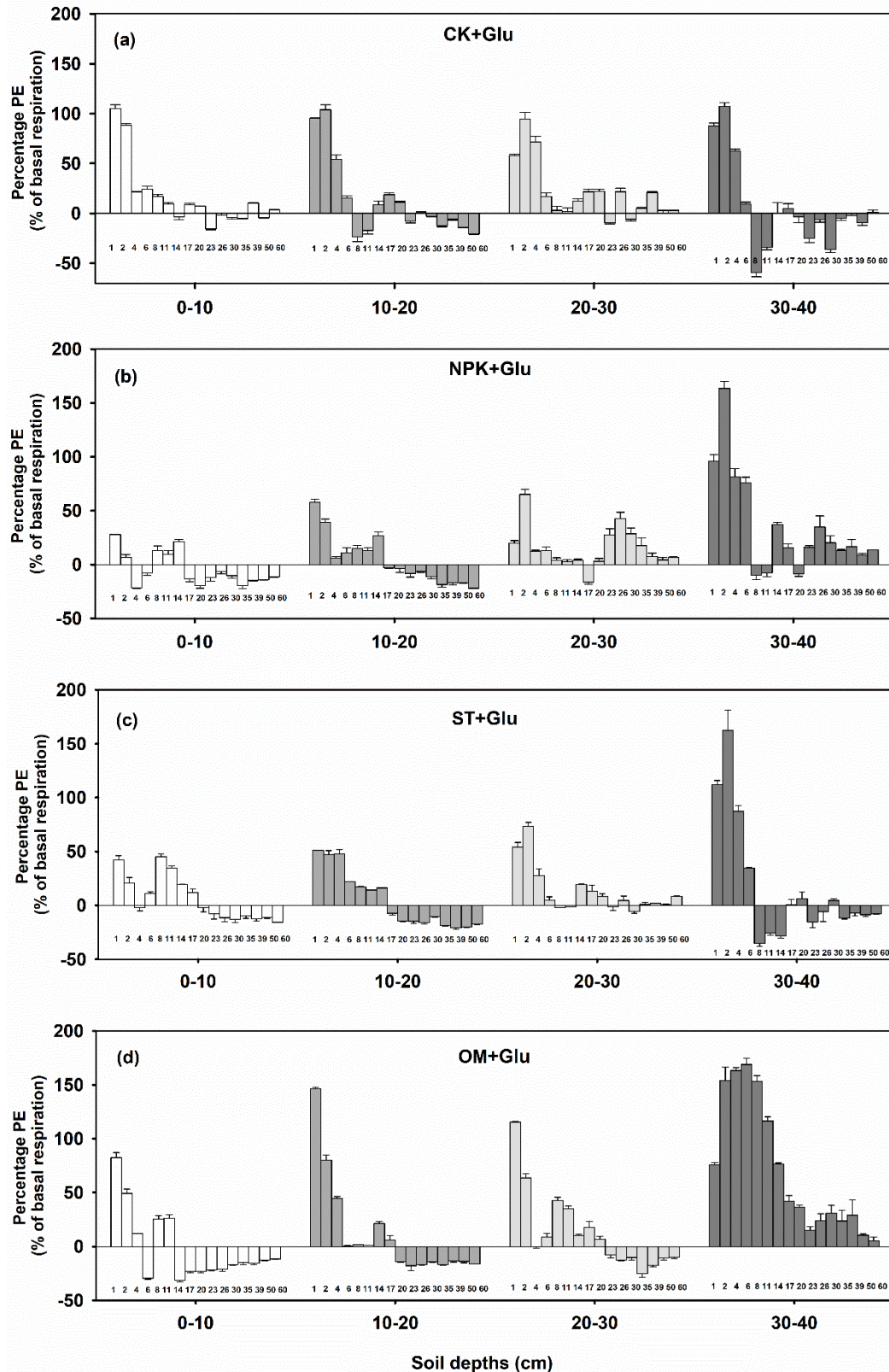


Figure I-5 Percentage priming effect (% of basal respiration per day) in 60-days incubated paddy soil under long-term fertilization regimes at different soil depths (mean \pm SE, $n=3$). Numbers under each bar represented the days after incubation.

4 Conclusions and outlook

The present thesis leads to the following conclusions:

- (1) AWD reduced CH₄ concentrations by suppressing methanogenesis, together with increasing oxidation. In addition, the time and magnitude of AWD should be carefully considered as it may reduce rice grain yield.
- (2) Sulfate fertilization had no effect on reducing CH₄ concentrations in this paddy soil amended with rice straw. However, sulfate fertilizer positively affected rice plant biomass and grain yield.
- (3) With rice growth, hydrogenotrophic methanogenesis obviously contributed to CH₄ production under flooded conditions.
- (4) Long-term mineral and organic fertilization increased microbial biomass and prevented its decreases vertically; in addition, the structure of the microbial community is strongly impacted by long-term fertilization, independent of fertilizer type.
- (5) Microorganisms focused on renewing their C (apparent PE) rather than investing in growth in soil depth without C deficiency.
- (6) A possible mineral-related mechanism was suggested to explain the negative PE commonly observed in paddy soils after 20 days of incubation.

These conclusions are of particulate relevance of further investigations for two reasons:

- (1) Our field-based studies demonstrate both the short-term microbial responses and long-term community shifts to inevitable human managements in paddy soil. Water management and fertilization are expected to largely affect rice plants and microbial activities, thus altering CO₂ and CH₄ turnover and influencing yield. These results call for further integrated investigations on eco-managements balancing sustainable rice yield and soil C stock.
- (2) Our priming effect study draws attention to an integrated mechanism of C turnover in submerged paddy soils. Considering complex mineral-associated mechanisms (substrate desorption and resorption with soil matrix) in further investigations is crucial due to its importance in affecting substrate availability to microorganisms and thus altering soil C stock.

5 Contributions to the included manuscripts

Study 1 Alternating wet-dry cycles rather than sulfate fertilization control pathways of methanogenesis and methane turnover in rice straw-amended paddy soil

Q. Liu: 60% (experimental design, accomplishment of experiment, laboratory analyses, data preparation, manuscript preparation)

M. Romani: 5% (accomplishment of experiment, comments to improve the manuscript)

J. Wang: 5% (experimental design)

B. Planer-Friedrich: 10% (experimental design, comments to improve the manuscript)

J. Pausch: 10% (experimental design, comments to improve the manuscript)

M. Dorodnikov: 10% (discussion of experimental design, comments to improve the manuscript)

Study 2 Effect of alternating wet-dry cycles and sulfate fertilization on plant-soil C allocation and rice yield

Q. Liu: 60% (experimental design, accomplishment of experiment, laboratory analyses, data preparation, manuscript preparation)

J. Pausch: 40% (experimental design, accomplishment of experiment, comments to improve the manuscript)

Study 3 Vertical and horizontal shifts in the microbial community structure of paddy soil under long-term fertilization regimes

Q. Liu: 40% (accomplishment of experiment, data preparation, manuscript preparation)

C.T. Atere: 15% (accomplishment of experiment, comments to improve the manuscript)

Z. Zhu: 10% (experimental design and field work, comments to improve the manuscript)

M. Shahbaz: 5% (comments to improve the manuscript)

X. Wei: 5% (comments to improve the manuscript)

J. Pausch: 15% (comments to improve the manuscript)

J. Wu: 5% (comments to improve the manuscript)

T. Ge: 5% (experimental design, comments to improve the manuscript)

Study 4 Mineral bound organic carbon explain the negative priming effect in paddy soils

Q. Liu: 40% (discussion of experimental design, data preparation, manuscript preparation)

Z. Zhu: 10% (experimental design, comments to improve the manuscript)

K. Abdalla: 10% (comments to improve the manuscript)

T. Ge: 5% (experimental design)

J. Wu: 5% (experimental design)

H. Tang: 5% (experimental design)

Y. Kuzyakov: 10% (discussion of experimental design, comments to improve the manuscript)

J. Pausch: 15% (discussion of experimental design, comments to improve the manuscript)

Acknowledgments

I am honoured to have stayed in Bayreuth for my Ph.D. There are many thanks I want to say to all the important people I met during my time here. First of all, I want to thank my supervisor Prof. Johanna Pausch for her full support. I am satisfied with my happy four years as she left me enough personal space for working and writing. Then I would like to thank our technicians, Ilse Thaufelder and Angelika Mergner, for their help with my experiments. I remembered the most frequent sentence Ilse said to me except “how are you?” was: “This is expensive.” I hope Johanna can get more and more projects funded, and then Ilse can be more generous on the budget. Buy! Buy! Buy!

I still remember the day I arrived at the Bayreuth train station Johanna and Yue Sun (Suri) came together to pick me up. The next day, Suri and Saskia Klink visited the city centre to help me get familiar with Bayreuth. We ordered ice cream, and Saskia taught me to pronounce “ü” in German as we sat not far from “Müller” in Rotmain Centre. I feel sorry that I forgot how I first met Manal Dafallah. Manal is a superwoman in my heart as she came here to study Ph.D. while raising three cute girls with long fluffy hairs. Meanwhile, she can bake various delicious cakes. Our group was occupied with ladies first, and more and more manpower joined us: Khatab Abdalla, Hongfei Liu, Peter Stimmler, and Andreas Wild. I guess it’s enough to mention their names here.

Thank Maxim Dorodnikov for his nice supervision for my Italian experiment. He spent valuable time helping us measure gas samples in Göttingen and commenting on the manuscript. I would also like to thank Prof. Britta Planer-Friedrich for her huge efforts in revising my manuscript. Her comments are super helpful in improving my manuscript. Next, I want to express my gratitude to Marco Romani, Shuai Zhang, and other Italian colleagues in Ente Nazionale Risi for their help on my experiment and daily life. I am glad that our cooperation was very successful! Here, I want to acknowledge my scholarship granted by the China Scholarship Council (CSC). I also want to thank Mohsen Zare and Mohammed Ali from Soil Physics. Mohsen helped me a lot with the modeling, which is far beyond the scope of my knowledge; when I needed help in the basement, Mohammed always happened to pass by me, and he never refused to give me a hand.

Of course, I want to thank my friends for their company during these four years: Bouchra Marouane, Taotao Lu, Katharina Blaurock, Xingyu Liu, Usman Munir, Karel As (they are all from Hydrology); and my Chinese friends Shuang Wei, Jing An, Guan Cai, and Gaochao Cai. Especially, I want to thank Bouchra for her frequent invitation for dinner and for shopping with her Bobi Blue (Blue is the last name I named) car. Suri worried a lot that I would be lonely after she left Bayreuth; however, I am independent enough to live without her company.

Last but not least, I appreciate all the supports and help from my master supervisors Prof. Tida Ge and Prof. Zhenke Zhu. They care about me and always try their best to help me even though I started my Ph.D. in Germany.

I miss my family and Chinese food, especially after being stuck in Germany for almost two years...I believe that one day I will miss the people and food here, just like I miss home now.

References

- Adhikari, D., Dunham-Cheatham, S.M., Wordofa, D.N., Verburg, P., Poulson, S.R., Yang, Y., 2019. Aerobic respiration of mineral-bound organic carbon in a soil. *Science of The Total Environment* 651, 1253-1260.
- Ayotade, K.A., 1977. Kinetics and reactions of hydrogen sulphide in solution of flooded rice soils. *Plant and Soil* 46, 381–389.
- Batjes, N.H., 1996. Total carbon and nitrogen in the soils of the world. *European journal of soil science* 47, 151-163.
- Blagodatskaya, E.V., Blagodatsky, S.A., Anderson, T.H., Kuzyakov, Y., 2007. Priming effects in Chernozem induced by glucose and N in relation to microbial growth strategies. *Applied Soil Ecology* 37, 95-105.
- Blagodatskaya, E., Kuzyakov, Y., 2008. Mechanisms of real and apparent priming effects and their dependence on soil microbial biomass and community structure: critical review. *Biology and Fertility of Soils* 45, 115-131.
- Brookes, P.C., Landman, A., Pruden, G., Jenkinson, D.S., 1985. Chloroform fumigation and the release of soil-nitrogen - a rapid direct extraction method to measure microbial biomass nitrogen in soil. *Soil Biology and Biochemistry* 17, 837-842.
- Cai, Z., Xing, G., Yan, X., Xu, H., Tsuruta, H., Yagi, K., Minami, K., 1997. Methane and nitrous oxide emissions from rice paddy fields as affected by nitrogen fertilisers and water management. *Plant and Soil* 196, 7-14.
- Calvin, M., 1962. The Path of Carbon in Photosynthesis: The carbon cycle is a tool for exploring chemical biodynamics and the mechanism of quantum conversion. *Science* 135, 879-889.
- Chen, R., Senbayram, M., Blagodatsky, S., Myachina, O., Dittert, K., Lin, X., Blagodatskaya, E., Kuzyakov, Y., 2014. Soil C and N availability determine the priming effect: microbial N mining and stoichiometric decomposition theories. *Global Change Biology* 20, 2356-2367.
- Chidthaisong, A., Inubushi, K., Muramatsu, Y., Watanabe, I., 1996. Production potential and emission of methane in flooded rice soil microcosms after continuous application of straws. *Microbes and Environments* 3, 73-78.
- Conrad, R., 2005. Quantification of methanogenic pathways using stable carbon isotopic signatures: a review and a proposal. *Organic Geochemistry* 36, 739-752.
- Corton, T., Bajita, J., Grospe, F., Pamplona, R., Assis, C., Wassmann, R., Lantin, R., Buendia, L., 2000. Methane emission from irrigated and intensively managed rice fields in Central Luzon (Philippines). *Nutrient cycling in Agroecosystems* 58, 37-53.
- Cui, J., Zhu, Z., Xu, X., Liu, S., Jones, D.L., Kuzyakov, Y., Shibistova, O., Wu, J., Ge, T., 2020. Carbon and nitrogen recycling from microbial necromass to cope with C:N stoichiometric imbalance by priming. *Soil Biology and Biochemistry* 142.
- Daquiado, A.R., Kuppusamy, S., Kim, S.Y., Kim, J.H., Yoon, Y.-E., Kim, P.J., Oh, S.-H., Kwak, Y.-S., Lee, Y.B., 2016. Pyrosequencing analysis of bacterial community diversity in long-term fertilized paddy field soil. *Applied Soil Ecology* 108, 84-91.
- Denef, K., Roobroeck, D., Manimel Wadu, M.C.W., Lootens, P., Boeckx, P., 2009. Microbial community composition and rhizodeposit-carbon assimilation in differently managed temperate grassland soils. *Soil Biology and Biochemistry* 41, 144-153.
- Dong, W.-Y., Zhang, X.-Y., Dai, X.-Q., Fu, X.-L., Yang, F.-T., Liu, X.-Y., Sun, X.-M., Wen, X.-F., Schaeffer, S., 2014. Changes in soil microbial community composition

- in response to fertilization of paddy soils in subtropical China. *Applied Soil Ecology* 84, 140-147.
- Dong, Y., Sanford, R.A., Chang, Y.J., McInerney, M.J., Fouke, B.W., 2017. Hematite Reduction Buffers Acid Generation and Enhances Nutrient Uptake by a Fermentative Iron Reducing Bacterium, *Orenia metallireducens* Strain Z6. *Environmental Science & Technology* 51, 232-242.
- Enggrob, K.L., Larsen, T., Peixoto, L., Rasmussen, J., 2020. Gram-positive bacteria control the rapid anabolism of protein-sized soil organic nitrogen compounds questioning the present paradigm. *Scientific Report* 10, 15840.
- Fairhurst, T., Dobermann, A., 2002. Rice in the global food supply. *World* 5, 454,349-511,675.
- Feng, J., Chen, C., Zhang, Y., Song, Z., Deng, A., Zheng, C., Zhang, W., 2013. Impacts of cropping practices on yield-scaled greenhouse gas emissions from rice fields in China: A meta-analysis. *Agriculture, Ecosystems & Environment* 164, 220-228.
- Fontaine, S., Henault, C., Amor, A., Bdioui, N., Bloor, J.M.G., Maire, V., Mary, B., Revaillet, S., Maron, P.A., 2011. Fungi mediate long term sequestration of carbon and nitrogen in soil through their priming effect. *Soil Biology and Biochemistry* 43, 86-96.
- Frey, S.D., Six, J., Elliott, E.T., 2003. Reciprocal transfer of carbon and nitrogen by decomposer fungi at the soil–litter interface. *Soil Biology and Biochemistry* 35, 1001-1004.
- Frostegård, Å., Tunlid, A., Bååth, E., 2011. Use and misuse of PLFA measurements in soils. *Soil Biology and Biochemistry* 43, 1621-1625.
- Goldberg, S.D., Knorr, K.-H., Gebauer, G., 2008. N₂O concentration and isotope signature along profiles provide deeper insight into the fate of N₂O in soils. *Isotopes in Environmental and Health Studies* 44, 377-391.
- Groot, T., Van Bodegom, P., Harren, F., Meijer, H., 2003. Quantification of methane oxidation in the rice rhizosphere using ¹³C-labelled methane. *Biogeochemistry* 64, 355-372.
- He, Y., Cheng, W., Zhou, L., Shao, J., Liu, H., Zhou, H., Zhu, K., Zhou, X., 2020. Soil DOC release and aggregate disruption mediate rhizosphere priming effect on soil C decomposition. *Soil Biology and Biochemistry* 144.
- Holmer, M., Kristensen, E., 1994. Coexistence of sulfate reduction and methane production in an organic-rich sediment. *Marine Ecology-Progress Series* 107, 177-177.
- Houghton, R., 1999. The annual net flux of carbon to the atmosphere from changes in land use 1850–1990. *Tellus B* 51, 298-313.
- Huang, X., Wang, C., Liu, Q., Zhu, Z., Lynn, T.M., Shen, J., Whiteley, A.S., Kumaresan, D., Ge, T., Wu, J., Naeth, M.A., 2018. Abundance of microbial CO₂-fixing genes during the late rice season in a long-term management paddy field amended with straw and straw-derived biochar. *Canadian Journal of Soil Science* 98, 306-316.
- Hussain, S., Peng, S., Fahad, S., Khaliq, A., Huang, J., Cui, K., Nie, L., 2015. Rice management interventions to mitigate greenhouse gas emissions: a review. *Environ Sci Pollut Res Int* 22, 3342-3360.
- Hütsch, B.W., Augustin, J., Merbach, W., 2002. Plant rhizodeposition—an important source for carbon turnover in soils. *Journal of Plant Nutrition and Soil Science* 165, 397-407.
- Jeewani, P.H., Gunina, A., Tao, L., Zhu, Z., Kuzyakov, Y., Van Zwieten, L.,

- Guggenberger, G., Shen, C., Yu, G., Singh, B.P., Pan, S., Luo, Y., Xu, J., 2020. Rusty sink of rhizodeposits and associated keystone microbiomes. *Soil Biology and Biochemistry* 147.
- Ji, Y., Liu, P., Conrad, R., 2018. Change of the pathway of methane production with progressing anoxic incubation of paddy soil. *Soil Biology and Biochemistry* 121, 177-184.
- Jones, D.L., Magthab, E.A., Gleeson, D.B., Hill, P.W., Sánchez-Rodríguez, A.R., Roberts, P., Ge, T., Murphy, D.V., 2018. Microbial competition for nitrogen and carbon is as intense in the subsoil as in the topsoil. *Soil Biology and Biochemistry* 117, 72-82.
- Keiluweit, M., Bougoure, J.J., Nico, P.S., Pett-Ridge, J., Weber, P.K., Kleber, M., 2015. Mineral protection of soil carbon counteracted by root exudates. *Nature Climate Change* 5, 588-595.
- Knudson, L., 1920. The secretion of invertase by plant roots. *American Journal of Botany* 7, 371-379.
- Kögel-Knabner, I., Amelung, W., Cao, Z., Fiedler, S., Frenzel, P., Jahn, R., Kalbitz, K., Kölbl, A., Schloter, M., 2010. Biogeochemistry of paddy soils. *Geoderma* 157, 1-14.
- Krzycki, J.A., Kenealy, W.R., Deniro, M.J., Zeikus, J.G., 1987. Stable carbon isotope fractionation by *Methanosarcina barkeri* during methanogenesis from acetate, methanol, or carbon dioxide-hydrogen. *Applied and Environmental Microbiology* 53, 2597-2599.
- Kuzyakov, Y., 2006. Sources of CO₂ efflux from soil and review of partitioning methods. *Soil Biology and Biochemistry* 38, 425-448.
- Kuzyakov, Y., Friedel, J.K., Stahr, K., 2000. Review of mechanisms and quantification of priming effects. *Soil Biology and Biochemistry* 32, 1485-1498.
- Lal, R., 2005. World crop residues production and implications of its use as a biofuel. *Environment International* 31, 575-584.
- Lal, R., 2008. Carbon sequestration. *Philos Trans R Soc Lond B Biol Sci* 363, 815-830.
- Li, X., Li, Z., Zhang, X., Xia, L., Zhang, W., Ma, Q., He, H., 2020. Disentangling immobilization of nitrate by fungi and bacteria in soil to plant residue amendment. *Geoderma* 374.
- Linguist, B., Van Groenigen, K.J., Adviento - Borbe, M.A., Pittelkow, C., Van Kessel, C., 2012a. An agronomic assessment of greenhouse gas emissions from major cereal crops. *Global Change Biology* 18, 194-209.
- Linguist, B.A., Adviento-Borbe, M.A., Pittelkow, C.M., van Kessel, C., van Groenigen, K.J., 2012b. Fertilizer management practices and greenhouse gas emissions from rice systems: A quantitative review and analysis. *Field Crops Research* 135, 10-21.
- Liu, Q., Li, Y., Liu, S., Gao, W., Shen, J., Zhang, G., Xu, H., Zhu, Z., Ge, T., Wu, J., 2022. Anaerobic primed CO₂ and CH₄ in paddy soil are driven by Fe reduction and stimulated by biochar. *Science of Total Environment* 808, 151911.
- Liu, Y., Ge, T., van Groenigen, K.J., Yang, Y., Wang, P., Cheng, K., Zhu, Z., Wang, J., Li, Y., Guggenberger, G., Sardans, J., Penuelas, J., Wu, J., Kuzyakov, Y., 2021. Rice paddy soils are a quantitatively important carbon store according to a global synthesis. *Communications Earth & Environment* 2.
- Maguffin, S.C., Abu-Ali, L., Tappero, R.V., Pena, J., Rohila, J.S., McClung, A.M., Reid, M.C., 2020. Influence of manganese abundances on iron and arsenic solubility in rice paddy soils. *Geochimica et Cosmochimica Acta* 276, 50-69.
- Mason-Jones, K., Schmücker, N., Kuzyakov, Y., 2018. Contrasting effects of organic

- and mineral nitrogen challenge the N-Mining Hypothesis for soil organic matter priming. *Soil Biology and Biochemistry* 124, 38-46.
- Michael, J.W., Eckhard, F., 1985. Methane oxidation in sediment and water column environments-Isotope evidence. *Organic Geochemistry* 10, 759-768.
- Miura, Y., Kanno, T., 1997. Emissions of trace gases (CO₂, CO, CH₄, and N₂O) resulting from rice straw burning. *Soil science and plant nutrition* 43, 849-854.
- Oertel, C., Matschullat, J., Zurba, K., Zimmermann, F., Erasmi, S., 2016. Greenhouse gas emissions from soils—A review. *Geochemistry* 76, 327-352.
- Pan, F.-F., Yu, W.-T., Ma, Q., Zhou, H., Jiang, C.-M., Xu, Y.-G., Ren, J.-F., 2017. Influence of ¹⁵N-labeled ammonium sulfate and straw on nitrogen retention and supply in different fertility soils. *Biology and Fertility of Soils* 53, 303-313.
- Peacock, A.g., Mullen, M., Ringelberg, D., Tyler, D., Hedrick, D., Gale, P., White, D., 2001. Soil microbial community responses to dairy manure or ammonium nitrate applications. *Soil Biology and Biochemistry* 33, 1011-1019.
- Phillips, R.P., Finzi, A.C., Bernhardt, E.S., 2011. Enhanced root exudation induces microbial feedbacks to N cycling in a pine forest under long-term CO₂ fumigation. *Ecol Lett* 14, 187-194.
- Qiu, H., Zheng, X., Ge, T., Dorodnikov, M., Chen, X., Hu, Y., Kuzyakov, Y., Wu, J., Su, Y., Zhang, Z., 2017. Weaker priming and mineralisation of low molecular weight organic substances in paddy than in upland soil. *European Journal of Soil Biology* 83, 9-17.
- Rasmussen, C., Southard, R.J., Horwath, W.R., 2006. Mineral control of organic carbon mineralization in a range of temperate conifer forest soils. *Global Change Biology* 12, 834-847.
- Ro, S., Seanjan, P., Tulaphitak, T., Inubushi, K., 2011. Sulfate content influencing methane production and emission from incubated soil and rice-planted soil in Northeast Thailand. *Soil Science and Plant Nutrition* 57, 833-842.
- Saunois, M., Stavert, A.R., Poulter, B., Bousquet, P., Canadell, J.G., Jackson, R.B., Raymond, P.A., Dlugokencky, E.J., Houweling, S., Patra, P.K., Ciais, P., Arora, V.K., Bastviken, D., Bergamaschi, P., Blake, D.R., Brailsford, G., Bruhwiler, L., Carlson, K.M., Carrol, M., Castaldi, S., Chandra, N., Crevoisier, C., Crill, P.M., Covey, K., Curry, C.L., Etiope, G., Frankenberg, C., Gedney, N., Hegglin, M.I., Höglund-Isaksson, L., Hugelius, G., Ishizawa, M., Ito, A., Janssens-Maenhout, G., Jensen, K.M., Joos, F., Kleinen, T., Krummel, P.B., Langenfelds, R.L., Laruelle, G.G., Liu, L., Machida, T., Maksyutov, S., McDonald, K.C., McNorton, J., Miller, P.A., Melton, J.R., Morino, I., Müller, J., Murguía-Flores, F., Naik, V., Niwa, Y., Noce, S., O'Doherty, S., Parker, R.J., Peng, C., Peng, S., Peters, G.P., Prigent, C., Prinn, R., Ramonet, M., Regnier, P., Riley, W.J., Rosentreter, J.A., Segers, A., Simpson, I.J., Shi, H., Smith, S.J., Steele, L.P., Thornton, B.F., Tian, H., Tohjima, Y., Tubiello, F.N., Tsuruta, A., Viovy, N., Voulgarakis, A., Weber, T.S., van Weele, M., van der Werf, G.R., Weiss, R.F., Worthy, D., Wunch, D., Yin, Y., Yoshida, Y., Zhang, W., Zhang, Z., Zhao, Y., Zheng, B., Zhu, Q., Zhu, Q., Zhuang, Q., 2020. The Global Methane Budget 2000–2017. *Earth System Science Data* 12, 1561-1623.
- Scharlemann, J.P.W., Tanner, E.V.J., Hiederer, R., Kapos, V., 2014. Global soil carbon: understanding and managing the largest terrestrial carbon pool. *Carbon Management* 5, 81-91.
- Schonheit, P., Kristjansson, J.K., Thauer, R.K., 1982. Kinetic mechanism for the ability

- of sulfate reducers to out-compete methanogens for acetate. *Archives of Microbiology* 132, 285-288.
- Smith, M.R., Mah, R.A., 1980. Acetate as Sole Carbon and Energy-Source for Growth of *Methanosarcina* Strain-227. *Applied and Environmental Microbiology* 39, 993-999.
- Tang, H.M., Xu, Y.L., Xiao, X.P., Li, C., Li, W.Y., Cheng, K.K., Pan, X.C., Sun, G., 2018. Impacts of long-term fertilization on the soil microbial communities in double-cropped paddy fields. *The Journal of Agricultural Science* 156, 857-864.
- Tian, K., Zhao, Y., Xu, X., Hai, N., Huang, B., Deng, W., 2015. Effects of long-term fertilization and residue management on soil organic carbon changes in paddy soils of China: A meta-analysis. *Agriculture, Ecosystems & Environment* 204, 40-50.
- Velthof, G.L., Kuikman, P.J., Oenema, O., 2002. Nitrous oxide emission from soils amended with crop residues. *Nutrient cycling in agroecosystems* 62, 249-261.
- Wang, Q.K., Wang, S.L., He, T.X., Liu, L., Wu, J.B., 2014. Response of organic carbon mineralization and microbial community to leaf litter and nutrient additions in subtropical forest soils. *Soil Biology and Biochemistry* 71, 13-20.
- Wei, L., Zhu, Z., Liu, S., Xiao, M., Wang, J., Deng, Y., Kuzyakov, Y., Wu, J., Ge, T., 2021. Temperature sensitivity (Q) of stable, primed and easily available organic matter pools during decomposition in paddy soil. *Applied Soil Ecology* 157.
- Wei, X., Zhu, Z., Liu, Y., Luo, Y., Deng, Y., Xu, X., Liu, S., Richter, A., Shibistova, O., Guggenberger, G., Wu, J., Ge, T., 2020. C:N:P stoichiometry regulates soil organic carbon mineralization and concomitant shifts in microbial community composition in paddy soil. *Biology and Fertility of Soils* 56, 1093-1107.
- Whalen, S.C., 2005. Biogeochemistry of methane exchange between natural wetlands and the atmosphere. *Environmental Engineering Science* 22, 73-94.
- Whiticar, M.J., 1999. Carbon and hydrogen isotope systematics of bacterial formation and oxidation of methane. *Chemical Geology* 161, 291-314.
- Whiticar, M.J., Faber, E., Schoell, M., 1986. Biogenic methane formation in marine and freshwater environments: CO₂ reduction vs. acetate fermentation— isotope evidence. *Geochimica et Cosmochimica Acta* 50, 693-709.
- Wu, J., Joergensen, R.G., Pommerening, B., Chaussod, R., Brookes, P.C., 1990. Measurement of soil microbial biomass C by fumigation extraction - an automated procedure. *Soil Biology and Biochemistry* 22, 1167-1169.
- Wu, L., Xu, H., Xiao, Q., Huang, Y., Suleman, M.M., Zhu, P., Kuzyakov, Y., Xu, X., Xu, M., Zhang, W., 2020. Soil carbon balance by priming differs with single versus repeated addition of glucose and soil fertility level. *Soil Biology and Biochemistry* 148, 107913.
- Zhang, G., Ji, Y., Ma, J., Xu, H., Cai, Z., Yagi, K., 2012a. Intermittent irrigation changes production, oxidation, and emission of CH₄ in paddy fields determined with stable carbon isotope technique. *Soil Biology and Biochemistry* 52, 108-116.
- Zhang, Q., Shamsi, I.H., Xu, D., Wang, G., Lin, X., Jilani, G., Hussain, N., Chaudhry, A.N., 2012b. Chemical fertilizer and organic manure inputs in soil exhibit a vice versa pattern of microbial community structure. *Applied Soil Ecology* 57, 1-8.
- Zhou, P., Sheng, H., Li, Y., Tong, C., Ge, T., Wu, J., 2016. Lower C sequestration and N use efficiency by straw incorporation than manure amendment on paddy soils. *Agriculture, Ecosystems & Environment* 219, 93-100.

II Manuscript

II.1 Alternating wet-dry cycles rather than sulfate fertilization control pathways of methanogenesis and methane turnover in rice straw-amended paddy soil

Qiong Liu^a, Marco Romani^b, Jiajia Wang^{c,d}, Britta Planer-Friedrich^c, Johanna Pausch^{a*}, Maxim Dorodnikov^{e,f}

Published in Environmental Science & Technology, 2021.
Vol. 55, Page 12075–12083.

^aAgroecology, BayCEER, University of Bayreuth, Bayreuth, 95440, Germany.

^bRice Research Centre, Ente Nazionale Risi, Castello d'Agogna, 27030, Italy.

^cEnvironmental Geochemistry, BayCEER, University of Bayreuth, Bayreuth, 95440, Germany.

^dDepartment of Environmental Science and Engineering, Fudan University, Shanghai 200433, China

^eSoil Science of Temperate Ecosystems, Georg-August University of Göttingen, 37077, Germany.

^fBiogeochemistry of Agroecosystems, Georg-August University of Göttingen, 37077, Germany.

*E-mail: Johanna.Pausch@uni-bayreuth.de

Abstract

Alternate wet-drying (AWD) and sulfate fertilization have been considered as effective methods for lowering CH₄ emissions from paddy soils. However, there is a clear knowledge gap between field studies which focus on quantification of emissions and lab studies that investigate mechanisms. To elucidate mechanisms of CH₄ production and oxidation under field condition, rice was planted in straw-amended mesocosms with or without sulfate fertilization under continuously flooded conditions or two wet-dry-cycles. CO₂ and CH₄ concentrations in soil air and their natural C isotope compositions were measured at stem elongation, booting, and flowering stages. CH₄ concentration reached 51 mg-C L⁻¹ at flowering stage under flooded conditions, while it decreased to 0.04 mg-C L⁻¹ under AWD. Relative ¹³C enrichment in CH₄ and depletion in CO₂ under AWD indicated CH₄ oxidation. Ample organic substrate supply may have reduced competition between sulfate-reducing bacteria and methanogenic archaea and therefore explain the absence of a fall in CH₄ concentrations in sulfate treatments. ¹³C-enrichment in CO₂ over time (6‰ and 7‰ with and without sulfate fertilizer, respectively) under flooded conditions indicates continuous contribution of hydrogenotrophic methanogenesis to CH₄ production with ongoing rice growth. Overall, AWD could more efficiently reduce CH₄ production than sulfate fertilization in rice-straw-amended paddy soils.

Key words: hydrogenotrophic methanogenesis, acetoclastic methanogenesis, CO₂, sulfate reducing bacteria, methanogenic archaea

1. Introduction

Rice feeds more than 50% of the world's population, but, at the same time, rice fields are an important wetland ecosystem contributing to global CH₄ emissions (Linguist et al., 2012a; Zhu et al., 2018; Wei et al., 2019). Previous studies focused on CH₄ production, oxidation potential, and emissions in paddy soils under fertilization (Cai et al., 1997; Zhu et al., 2018), changing temperature (Conrad, 2002), and water management (Adhya et al., 1994; Zhang et al., 2012; Ma et al., 2013). CH₄ production is an anaerobic final process of organic matter degradation or CO₂ reduction and is driven by methanogenic archaea (MA) (Conrad, 2005; Whalen, 2005). Two most important reactions of methanogenesis in paddy soils are acetoclastic methanogenesis (Fig II.1-1, mechanism I) and hydrogenotrophic methanogenesis (mechanism II). In reaction I, CH₄ is produced primarily from the methyl group of acetate (Smith and Mah, 1980). During hydrogenotrophic methanogenesis, CO₂ is reduced to CH₄ with H₂ as the electron donor (Whalen, 2005).

Uncertainty still exists about the contribution of the two methanogenesis pathways to CH₄ production throughout the rice growing season. Hydrogenotrophic methanogenesis dominated in the early stage, whereas the acetoclastic pathway dominated at the end of the season (Krüger et al., 2002; Zhang et al., 2013). Opposite trends were demonstrated by Zhang et al., (2012) claiming an increasing contribution of hydrogenotrophic methanogenesis with rice growth stages. Ji et al., (2018) found that hydrogenotrophic methanogenesis became dominant (>50%) when available carbon decreased in the late incubation phase. Stable isotope fractionation results in a clear $\delta^{13}\text{C}$ differentiation of CO₂ and CH₄ between acetoclastic and hydrogenotrophic methanogenesis (Conrad, 2005). Previous studies demonstrated that discrimination against ¹³C during acetoclastic methanogenesis is rather strong resulting in ¹³C-depleted CH₄ (-50‰~-60‰ vs. PDB) (Whiticar, 1999). An even greater ¹³C-depletion of CH₄ was observed during hydrogenotrophic methanogenesis (down to -110‰ vs. PDB) (Krzycki et al., 1987; Whiticar, 1999). Simultaneously, there was a strong ¹³C-enrichment of residual CO₂ from hydrogenotrophic methanogenesis due to the preferred consumption of lighter ¹²C-CO₂. In contrast, isotopic fractionation of CO₂ produced by acetoclastic methanogenesis was concluded to be low (Conrad, 2005). For a tropical peatland, ¹³C-enrichment of CO₂ relative to the acetate by about 9‰ were reported (Holmes et al., 2015). Isotope fractionation also occurs during CH₄ oxidation, with preferential consumption of lighter ¹²C-CH₄, resulting in a ¹³C-depletion of CO₂ and a ¹³C-enrichment of the remaining CH₄ (mechanism III) (Michael and Eckhard, 1985).

Alternating wet-dry cycles (AWD) have been reported to decrease CH₄ emission by inhibiting methanogens via oxygen (O₂) supply and also by increasing the rate of CH₄ oxidation (Zhang et al., 2012). Sulfate fertilization has also been demonstrated to be an efficient method of suppressing CH₄ emission (Cai et al., 1997; Ro et al., 2011; Linguist et al., 2012b). For example, ammonium sulfate reduced CH₄ emissions over the years and seasons by 25% to 56% compared with urea applied at the same rate (Corton et al., 2000). The underlying mechanism is competition for substrates (both acetate and H₂) between sulfate-reducing bacteria (SRB) and MA (Schonheit et al., 1982; Whiticar et al., 1986; Ro et al., 2011). SRB contribute to carbon isotope fractionation when oxidizing acetate via the acetyl-CoA/carbon monoxide dehydrogenase pathway with ¹³C-depletion of CO₂ (mechanism IV) while there is no discrimination against ¹³C in

the tricarboxylic acid cycle (mechanism V) (Goevert and Conrad, 2008). There is a clear knowledge gap between field studies which focus on quantification of emissions and lab studies that investigate mechanisms. Understanding the mechanisms controlling methanogenesis pathways could help predicting CO₂ and CH₄ emissions in rice fields. In order to better estimate and predict dynamics of CH₄ and CO₂ emission in paddy soils and their dependency on field management, studying mechanisms of CH₄ production in the field is inevitable.

In this study, we set-up a mesocosm experiment with rice plants under field conditions to measure CO₂ and CH₄ dynamics in soil gases and their natural ¹³C-isotope abundance at 0–10 and 10–20 cm soil depths. The main objectives were to compare the efficiency of AWD and sulfate fertilization in decreasing CH₄ production and also to disentangle the CH₄ turnover mechanisms affected by AWD and sulfate addition in paddy soil by distinguishing the differences in δ¹³C-CO₂ and δ¹³C-CH₄ within treatments and growth stages. We hypothesized that 1) AWD decreases CH₄ concentrations after re-flooding due to lower methanogenesis and also higher CH₄ oxidation leading to ¹³C enrichment in CH₄ and depletion in CO₂; 2) sulfate fertilizer decreases CH₄ concentrations by lowering methanogenesis due to the substrate competition between SRB and MA.

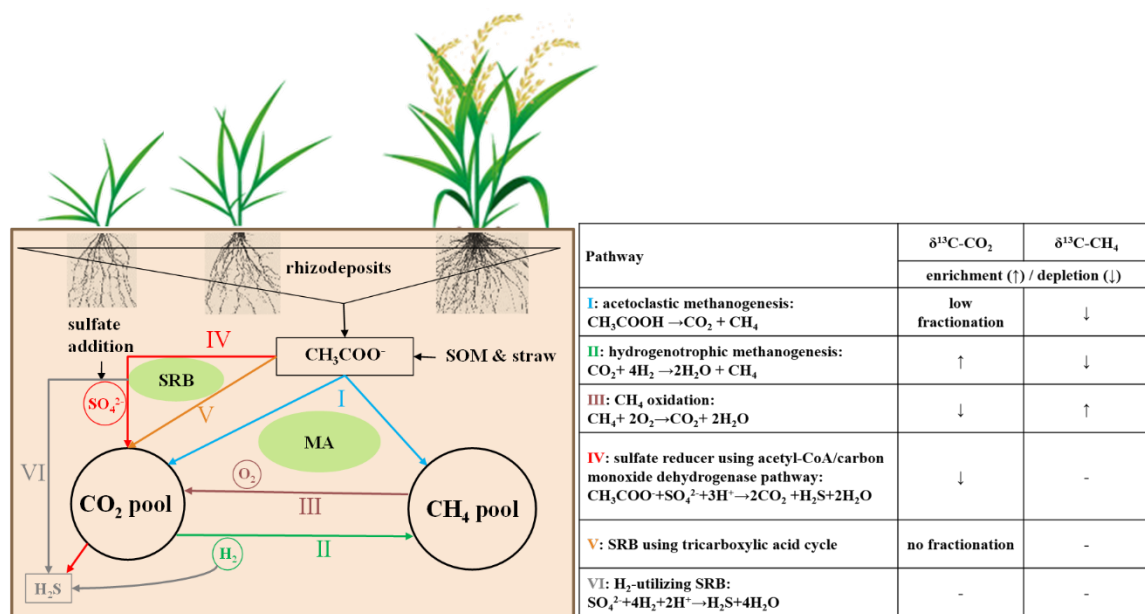


Figure II.1-1 Conceptual framework of the main processes causing ¹³C-isotope fractionation in CO₂ and CH₄ in paddy soils. Arrows in different color and respective Latin numbers represent different C processes in paddy soil. Upward and downward arrows in the table represent the ¹³C-enrichment and depletion during different C processes, respectively.

2. Materials and methods

2.1 Experimental set-up

A large batch of soil was collected from the plough layer (0-30 cm) at a site at Cascina Veronica, close to the town of Garlasco, Pavia, Italy (45°10'39"N, 8°53'48"E) in 2017. The soil was classified as Eutric Gleysol with 15-year rice cultivation history following corn cropping and with $\delta^{13}\text{C}$ value of soil carbon of -21.9‰. The basic chemical properties of the soil were as follows: pH 5.6, total C 2.0%, total N 0.6%, total S 2.6 g kg⁻¹. Mesocosm experiments were established in 2017 under field conditions. Plastic containers (112 cm * 72 cm * 65 cm) were filled with 30 cm of gravel at the bottom and overlaid by 20 cm of mixed soil. Water/dry-seedling and sulfate treatments were conducted with three replicates in a randomized factorial arrangement. More detailed information on the experimental set-up is presented in Supporting Information Table II.1-S1 and elsewhere (Wang et al., 2020).

In 2018, the following treatments were established in these mesocosms: continuous flooding (noS+FL), sulfate fertilizer + continuous flooding (S+FL), wet-dry cycles (noS+AWD), and sulfate fertilizer + wet-dry cycles (S+AWD). After the 2017 rice harvest, the straw from each container was cut into 20 cm pieces and returned to the respective container shortly before sowing in 2018 (Table 1). The amount of straw corresponded to 13.9 ± 0.7 , 13.8 ± 0.3 , 10.1 ± 0.3 , and 13.8 ± 0.1 t dry weight ha⁻¹ for noS+FL, S+FL, noS+AWD, and S+AWD, respectively. The water level was controlled every day in all containers except for AWD treatments. The AWD treatments were kept without irrigation for 9 days (except for rain water) at stem elongation and booting stages and were then rewetted and kept flooded after each drying event (Fig S1). At the beginning of the experiment, 100 kg ha⁻¹ N were added; 30 kg ha⁻¹ N, 41 kg ha⁻¹ K, and 17 kg ha⁻¹ P were applied at tillering stage; 50 kg ha⁻¹ N and 83 kg ha⁻¹ K were added after stem elongation; additional 83 kg ha⁻¹ K were applied at the booting stage. Urea and KCl were used as sources of N and K, respectively, in the treatment without sulfate. (NH₄)₂SO₄ and K₂SO₄ were used as N and K fertilizers, respectively, for S mesocosms. Triple superphosphate was used as a source of P.

Rice (*Oryza sativa* L. cv. Selenio) was germinated in Petri dishes, and 330 of the seedlings were transplanted into each plot at the end of May 2018. All containers were drained and then re-flooded twice, on the day of transplanting due to heavy rain and at tillering stage because rice leaves showed symptoms which may be due to iron toxicity in containers without sulfate fertilizers. Afterwards, all containers were re-fertilized resulting in a final amount of 240 kg ha⁻¹ N, 17 kg ha⁻¹ P, and 290 kg ha⁻¹ K. Correspondingly, the treatments with sulfate fertilizer finally received 396 kg ha⁻¹ S each.

2.2 Soil gas and pore water sampling

2-cylinder passive diffusion soil gas sampler (described in detail in (Goldberg et al., 2008)), was installed into each mesocosm in May 2018 for collecting the soil gases at 0–10 and 10–20 cm. A hole was drilled using a soil corer to a depth of 20 cm. The gas sampler was placed into the hole. During the rice growth, three samplings were conducted from 8–12 a.m. at stem elongation (before wet-drying), booting (after the

first drying period), and flowering stages (after the second drying period) (Fig. S1). Briefly, each polyvinyl chloride (PVC) cylinder (ID 70 mm; OD 79 mm; 0.1 m height) contained 5 m coiled silicon tube (ID 3 mm; OD 5 mm), and both ends of which were connected with gas impermeable polyurethane tubes (PU) (ID 1.8 mm; OD 3 mm). The ends of the PU tubes were placed above the soil surface, and two-way valves were attached (Luer Lock; Value Plastics, Fort Collins, CO, USA). Sampling was performed from the soil surface using 100-mL glass bottles with septa. All bottles were first flushed with N₂ and then evacuated using a vacuum pump. The vacuum was controlled with Tensio Check TC 03S (Tensio-Technik, Geisenheim, Germany). Subsequently, gas was sampled into the bottles directly from each soil depth by attaching the glass bottle to one of the two-way valves, and the other valve was connected with an Argon gasbag in order to compensate for the pressure and flush the soil collectors with CO₂- and CH₄-free gas. The air pressure was measured by the internal sensor connected to a VOLTCRAFT DL-220THP data logger. Soil temperature was measured by digital thermometer (Pearl. GmbH, Buggingen, Germany). At each gas sampling day, plant height was measured by randomly choosing 6 rice plants at each container; in addition, one more measurement was conducted in the middle of stem elongation stage.

Soil pore water was collected using Rhizon samplers (Rhizosphere Research Products, Netherlands) at stem elongation, booting, and flowering stages. The samplers were installed vertically in a soil depth of about 3–4 cm prior to rice transplanting and then left in the soil throughout the season. Pore water (about 10 mL) was firstly extracted by syringe through a three-way valve to flush and purge the sampler before sampling. Then, pore water was collected using 100-mL evacuated glass bottle. The collected pore water samples (about 10 mL) were immediately acidified with 600 µL of 6 M hydrochloric acid for storage before dissolved organic carbon (DOC) measurement.

2.3 Soil and plant sampling

Soil and plant samples were collected after the last soil gas sampling, and one plant per mesocosm container was chosen randomly. Shoots were cut at the base near the soil surface; the root and soil samples were taken from 0–20 cm depth using a Riverside auger (ID 4 cm, Eijkelkamp, Giesbeek, Netherlands). Roots were picked by hand and washed with deionized water. The shoots and roots were oven-dried at 60 °C for 3 days and weighed for biomass determination.

2.4 Analyses and data processing

Since the collected pore water samples were filtered through 0.45 µm in Rhizon samplers, DOC concentrations were directly measured using an N/C analyzer (Multi N/C 2100, Analytik Jena, Germany). Total dissolved S (DTS) was measured in filtered samples (200 nm) by ICP-MS. Redox potential (Eh) was measured immediately on site. ¹³C/¹²C isotope ratio of CO₂ and CH₄ as well as their concentrations were measured using a gas chromatograph-isotope ratio mass spectrometer coupled to a pre-GC concentration interface (PreCon-GC-C-IRMS; Hewlett-Packard GC 5890 series II, Wilmington, DE, USA; PreCon, Combustion Interface II and gas-IRMS delta V; all Thermo Fisher Scientific, Bremen, Germany).

As the bottles with gas samples could not be 100% evacuated, the correct volume of the bottles was calculated (Eq. 1). The gas in bottles was diluted by Argon and it only affected the concentration of the gas (Eq. 2):

$$\text{Corr. } V_{\text{gas bottle}} [\text{mL}] = -P_{\text{gas bottle}} [\text{hPa}] / P_{\text{atmosphere}} [\text{hPa}] * V_{\text{gas bottle}} [\text{mL}] \quad (1)$$

where, Corr. $V_{\text{gas bottle}}$ is the corrected volume of gas bottle [mL], $P_{\text{gas bottle}}$ and $P_{\text{atmosphere}}$ are the negative pressure in the evacuated gas bottle [hPa] and the atmosphere pressure [hPa] when evacuating the gas bottle, respectively, and $V_{\text{gas bottle}}$ is the original volume of gas bottle [mL].

$$\text{Orig. Conc}_{\text{sample}} (\text{ppm}) = \text{Corr. } V_{\text{gas bottle}} [\text{mL}] * \text{Conc}_{\text{sample}} (\text{ppm}) / V_{\text{sample}} [\text{mL}] \quad (2)$$

where, Orig. $\text{Conc}_{\text{sample}}$ and $\text{Conc}_{\text{sample}}$ are the original concentrations of gas in the soil (ppm) and the concentration of gas in the gas bottle (ppm), respectively, and V_{sample} is the gas volume inside the silicon tube buried in the soil [mL].

The $^{13}\text{C}/^{12}\text{C}$ ratio in CH_4 and CO_2 was denoted as $\delta^{13}\text{C}$ in per mil VPDB [‰]:

$$\delta^{13}\text{C} (\text{‰}) = [(R_{\text{sample}} / R_{\text{VPDB}}) - 1] * 1000 \quad (3)$$

where R_{sample} is the isotopic ratio $^{13}\text{C}/^{12}\text{C}$ of CH_4 or CO_2 in the sample, and R_{VPDB} is the isotopic ratio of Vienna Pee Dee Belemnite as the standard for C.

2.5 Statistical evaluation

Data were analyzed by one-way ANOVA for different rice growth stages within each fertilization regime and for different groups of fertilization regime within each growth stage and were compared by Duncan's test in SPSS 19.0 (SPSS Inc., Chicago, IL), with significance defined at $P < 0.05$. Two-way ANOVA with repeated measures was used to test the effect of treatment, growth stage and their interactions for statistical significance. Independent T-test was used for comparing the significant difference between noS and S treatments at stem elongation stage, as there were similar water-logged conditions at this stage.

3. Results

3.1. Plant properties and pore water DOC

Plant height was similar for all treatments at stem elongation (46 DAT) (Fig II.1-2a). With the rice growth, S addition stimulated the plant height by 10.5%, 8.8%, and 2.7% compared with the noS+FL during the elongation (54 DAT), booting, and flowering stages, respectively. The effect of water regimes remained insignificant along the growth stages. Higher shoot, root, and total plant biomass were observed at flowering stage in treatments with sulfate fertilizer (Fig II.1-2b, $P > 0.05$). S fertilizer and AWD increased root to shoot ratio at flowering stage ($P > 0.05$). After the harvest, S mesocosms had significantly higher straw production compared with noS (Table II.1-1, $P < 0.05$). Soil pore water DOC contents increased from stem elongation to flowering stage (Fig II.1-3, $P < 0.05$). Compared with noS, sulfate fertilizer significantly increased pore water DOC under both FL and AWD conditions.

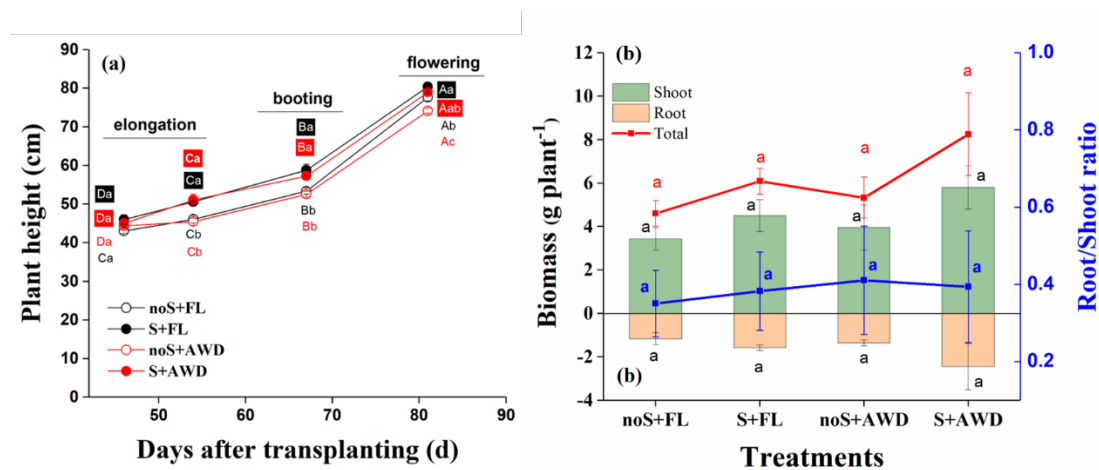


Figure II.1-2 Rice plant height over rice growth season (n=6) (a), plant biomass and root to shoot ratio at flowering stage (n=3) (b) (mean ± SE). The two wet-dry periods were at 56-63 DAT and 70-77 DAT, respectively.

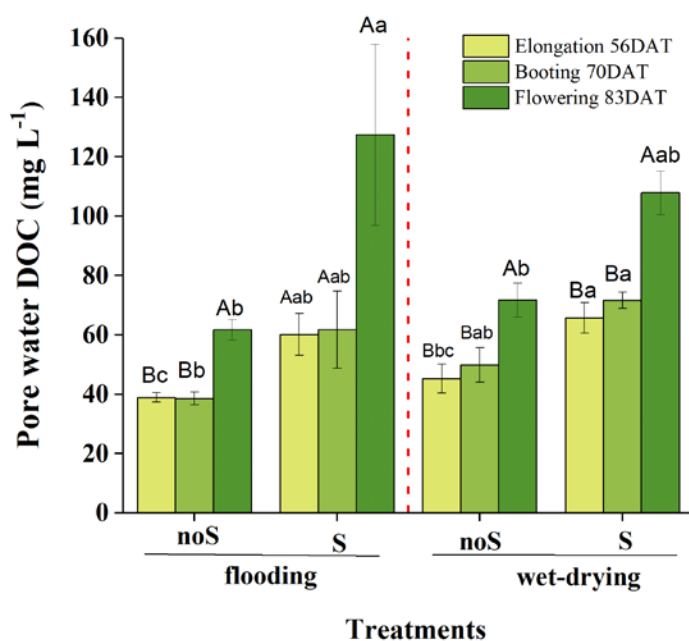


Figure II.1-3 Pore water dissolved organic C concentrations over rice growth season (mean ± SE, n=3).

3.2. CO₂ and CH₄ concentrations in soil air and their isotope ratios under wet-drying and sulfate fertilization treatments

CO₂ and CH₄ concentrations were measured at two depths in the soil profile (0–10, 10–20 cm). The differences between 0–10 and 10–20 cm for CO₂, CH₄, and their δ¹³C-values were insignificant (Fig. II.1-S2, *P*>0.05). Therefore, depth-related data were pooled together and considered jointly for comparisons between treatments and rice growth stages. The maximum difference of soil temperature at three gas sampling days was less than 2 °C (Fig. II.1-S1).

Under continuously flooded condition (FL), CH₄ concentrations increased significantly from stem elongation to flowering stages (from 6 to 64 mg C L⁻¹ and 9 to 51 mg C L⁻¹ with (S) and without (noS) sulfate fertilizer, respectively) (Fig II.1-4a&b, $P < 0.05$). Meanwhile, the $\delta^{13}\text{C-CO}_2$ values were generally increased with rice growth under flooded conditions from -22.0‰ to -14.7‰ and from -19.6‰ to -13.2‰ for S+FL and noS+FL, respectively (Fig II.1-4c, $P < 0.05$). Compared with $\delta^{13}\text{C-CO}_2$, $\delta^{13}\text{C-CH}_4$ values were more depleted (ca. -50‰ on average) and remained relatively constant between growth stages under flooded conditions with and without sulfate addition (Fig II.1-4d).

All mesocosms were kept under flooded conditions during the elongation stage, and, all treatments had similar CH₄ concentrations together with $\delta^{13}\text{C}$ -values except noS+AWD (Fig II.1-4b&d). CO₂ concentrations returned to the same level as elongation stage in AWD treatments three days after re-flooding (Fig II.1-4a), whereas the CH₄ concentrations declined from elongation to flowering stage (Fig II.1-4b, $P < 0.05$).

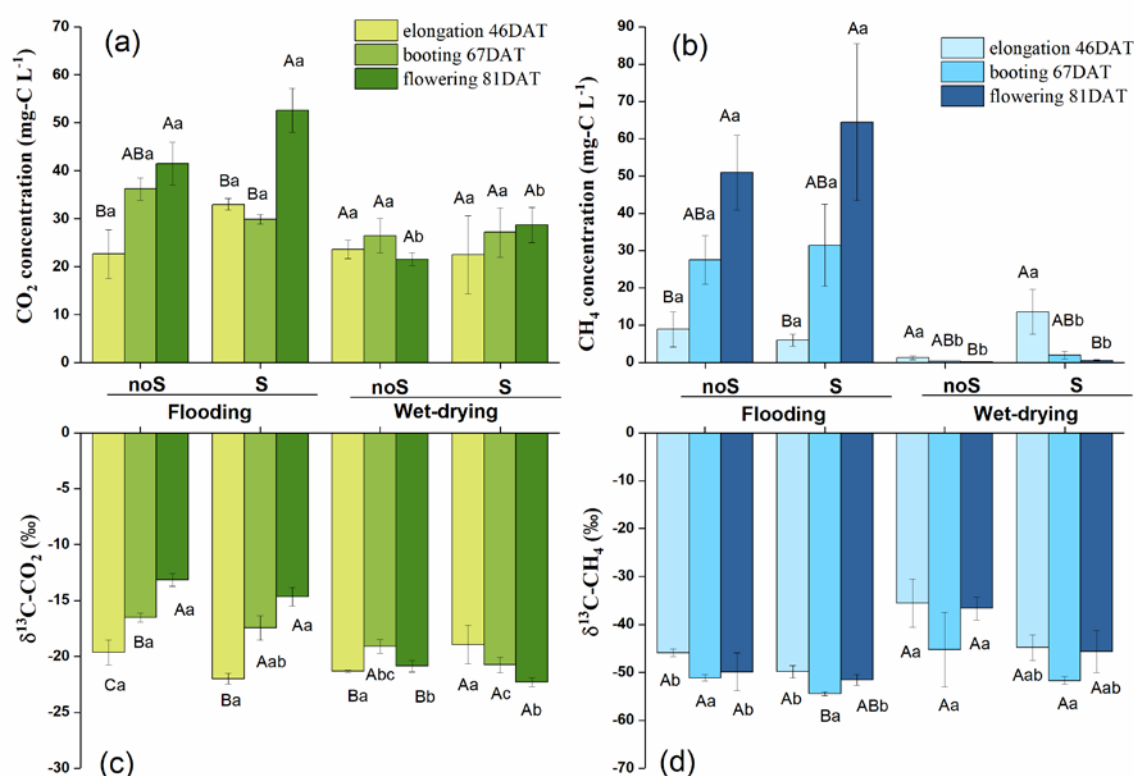


Figure II.1-4 Concentrations of CO₂ (a), CH₄ (b) and delta values of CO₂ (c) and CH₄ (d) in gas bottles in soil depth from 0-20 cm (mean \pm SE, n=3).

When comparing the two water regimes, the CH₄ concentrations drastically dropped under AWD treatment at booting and remained below 0.5 mg C L⁻¹ at the flowering stage (Fig II.1-4b, $P < 0.05$). At booting stage, CO₂ concentrations after the first wet-dry cycle (three days after re-wetting) were similar to that in FL (Fig II.1-4a, $P > 0.05$). 48% of CO₂ concentrations were recovered three days after the second wet-dry cycle at flowering stage as compared with FL (Fig II.1-4a, $P < 0.05$). Meanwhile, the $\delta^{13}\text{C-CO}_2$ values were more depleted (Fig II.1-4c, $P < 0.05$) and $\delta^{13}\text{C-CH}_4$ values were more

enriched under AWD, compared with FL (Fig. 4d). In two-way ANOVA with repeated measures (Table II.1-S2), the interaction of treatments and growth stages on CO₂ and CH₄ concentrations and $\delta^{13}\text{C-CO}_2$ were significant: $F(6, 16)=3.498, P=0.021$; $F(6, 16)=5.986, P=0.002$; and $F(6, 16)=10.29, P<0.001$, respectively.

3.3. Relationship between $\delta^{13}\text{C-CO}_2$ and $\delta^{13}\text{C-CH}_4$

FL caused pronounced ¹³C enrichment in CO₂ and slight to moderate depletion in CH₄ similarly under S and noS fertilization from stem elongation to the flowering stage (Fig II.1-5, green dashed arrows).

Under AWD, a shift in the ¹³C-depleted CO₂ and ¹³C-enriched CH₄ occurred for both S and noS treatments after the first wet-dry cycle (3‰-6‰ ¹³C enrichment, and 3‰ depletion in CH₄ and CO₂, respectively), and from the first to second wet-dry cycle (6‰-9‰ ¹³C enrichment, and 2‰ depletion in CH₄ and CO₂, respectively) (Fig II.1-5, brown dashed arrows).

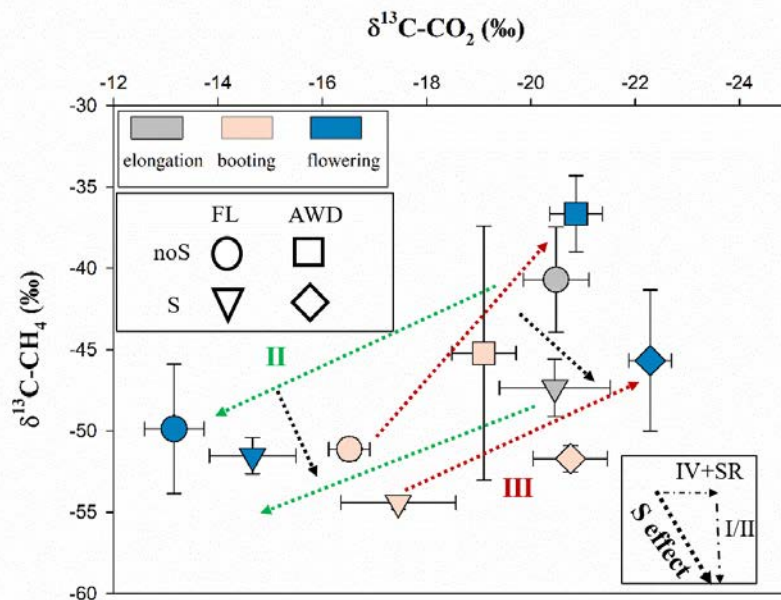


Figure II.1-5 Cross plot of $\delta^{13}\text{C-CO}_2$ and $\delta^{13}\text{C-CH}_4$ at three rice growth stages under two fertilization treatments and water regimes (mean \pm SE). Dashed arrows show the direction of cross-plot parameters in paddy soil: (green) hydrogenotrophic methanogenesis caused $\delta^{13}\text{C-CH}_4$ depletion and $\delta^{13}\text{C-CO}_2$ enrichment (pathway II); (brown) $\delta^{13}\text{C-CH}_4$ enrichment and $\delta^{13}\text{C-CO}_2$ depletion by CH₄ oxidation pathway III; (black) $\delta^{13}\text{C-CO}_2$ depletion caused by sulfate reduction pathway IV plus soil respiration (SR) including root- and microbial respiration; and sulfate induced $\delta^{13}\text{C-CH}_4$ depletion. For the stem elongation stage, data of wet-drying treatments were combined with flooding of respective S treatments (grey circle and triangle, n = 6) as there were similar water-logged conditions at this stage. For booting and flowering stages, n = 3.

Sulfate addition during the stem elongation stage, before AWD and FL were imposed, showed depleted $\delta^{13}\text{C}$ in CH_4 compared with noS. During the booting and flowering stages, the trend of ^{13}C -depletion in CH_4 after S fertilization remained. Simultaneously, there was a ^{13}C -depletion in CO_2 for booting and flowering stages under AWD and FL (Fig II.1-5, black dashed arrows).

Table II.1-1 Total straw production after harvest in 2017 and 2018 (mean \pm SE, n=3).

Treatments in 2017	noS+water-seeded	S+ water-seeded	noS+dry-seeded	S+ dry seeded
Straw (g)	1076 \pm 58a	1072 \pm 22a	785 \pm 25b	1068 \pm 7a
Treatments in 2018	noS+FL	S+FL	noS+AWD	S+AWD
Straw (g)	787 \pm 35b	1068 \pm 46a	782 \pm 24b	993 \pm 13a

4. Discussion

In this study, we investigated the efficiency of AWD and sulfate fertilization on CH_4 reduction in soil gases at 0–20 cm depths. CH_4 concentrations strongly declined after AWD regardless of sulfate fertilization. However, sulfate addition did not decrease CH_4 concentrations at any of the rice growing stages in both FL and AWD conditions (Fig. 4b). Before escaping to the atmosphere, CO_2 and CH_4 undergoes various biogeochemical and physical reactions within soils, including production, oxidation, transport upward (bubbles and diffusion), and further oxidation at the soil-atmosphere interface and in the rhizosphere. Most of those processes can affect natural ^{13}C isotope signals due to isotope fractionation. Here, CO_2 and CH_4 were sampled belowground with passive diffusion gas samplers, so we focused on CH_4 production and oxidation within the soil profile, i.e., on CH_4 turnover. Understanding the mechanisms involved in methanogenesis pathways will help in predicting CH_4 production under environmental and land use changes.

4.1. Effect of wet-dry cycles and sulfate fertilization on CH_4 and CO_2 production

Water management is a common practice to effectively reduce CH_4 fluxes (Berger et al., 2013). As expected, AWD also directly reduced CH_4 concentrations in soil air (Fig II.1-4b, $P < 0.05$). This low concentration was caused by two reasons. First, the shift from flooded to dry soil conditions introduces atmospheric O_2 and directly suppresses methanogens activity by increasing soil aeration (Zhang et al., 2013). Second, the introduced O_2 can simultaneously stimulate an increase in methanotrophic abundance thereby increasing CH_4 oxidation (Ma and Lu, 2011; Ma et al., 2013). For paddy soils, CH_4 oxidation has been shown to cause an ^{13}C enrichment in remaining CH_4 by 15‰ (Zhang et al., 2015). Relatively enriched $\delta^{13}\text{C}$ in CH_4 (2-6‰) after first AWD in our study indicated an oxidative pattern in CH_4 turnover (Fig II.1-1, pathway III; Fig II.1-

5, brown dashed arrows). Even stronger oxidation of CH₄ (6-9‰) could be observed after second AWD at later growing stages (flowering compared with booting, Fig II.1-5).

Simultaneously, δ¹³C in CO₂ was noticeably depleted (3‰ and 2‰ after the first and the second AWD, respectively) as a result of CH₄ oxidation. CO₂ concentrations at booting and flowering stages, which should be considered as newly generated CO₂ after re-flooding (22 to 29 mg C L⁻¹), reached up to 50% of those from flooded containers that had CO₂ accumulation (30 to 53 mg C L⁻¹) (Fig II.1-4a). This high CO₂ production rate can be partially explained by CH₄ oxidation after soil aeration; In addition, AWD enhanced root biomass (Fig 2b, yet not significant for each plant), and also it was reported to increase root activity (Tian et al., 2013), thereby enhancing root-derived CO₂. Consequently, it can also lead to ¹³C depletion in CO₂ due to a higher contribution of root-derived CO₂ with more negative δ¹³C values (~-27‰) as compared to bulk soil CO₂ (Fig II.1-4c, *P*<0.05; Fig II.1-5, black dashed arrow). Short-term reduction in the soil water content in our study caused a strong decrease in measured belowground CH₄ concentrations (Fig II.1-4b). This is consistent with our first hypothesis: less CH₄ produced together with more CH₄ oxidized may have caused this decline in CH₄ concentration after AWD.

Sulfate fertilization was previously reported to reduce CH₄ production (Minamikawa et al., 2005; Ro et al., 2011), as SRB stimulated by sulfate addition have a higher affinity for the substrates (both acetate and H₂) than MA under anaerobic conditions (Holmer and Kristensen, 1994; Ji et al., 2018). Sulfate reduction is also the more energetically efficient process (based on Free-Gibbs energy) compared with methanogenesis (Muyzer and Stams, 2008). This means, sulfate reduction should theoretically outcompete CH₄ production under anaerobic conditions. The soil used in the present study had rather low total S background (2.6 g kg⁻¹), which means the addition of sulfate with fertilizers should have effects on suppressing CH₄ production. The total dissolved S contents in pore water were obviously higher in S treatments at early rice growth stage (Fig. II.1-S3b, *P*<0.05). Our findings contradicted the proposed hypothesis 2 that sulfate fertilization should suppress CH₄ production. We suggest the following explanations.

First, straw addition could have promoted CH₄ production. Previous studies have demonstrated that 6 t ha⁻¹ rice straw addition increased CH₄ emissions by a factor of 1.8 to 3.3 compared with those without straw application (Schütz et al., 1989; Yagi and Minami, 1990). Extra carbon from straw can stimulate the abundance of hydrogenotrophic methanogens *Methanocella* and also acetate-utilizing *Methanosarcina* and *Methanotrix* (Conrad, 2002; Ji et al., 2018). As all containers were amended with more than 10 t ha⁻¹ of straw, such a large amount of organic C could compensate the substrate competition between SRB and MA. Simultaneously, it could also stimulate growth of methanogens and, therefore, promote CH₄ production.

Sulfate fertilizers as such had positive effects on rice plants, confirmed by the enhanced plant height and straw production (Fig II.1-2 & Table II.1-1, *P*<0.05). Higher root biomass (indicated by significantly higher straw production combined with higher root to shoot ratio) could release more rhizodeposits and increase substrate availability for microorganisms (Li and Yagi, 2004; Ge et al., 2012; Atere et al., 2017). DOC concentrations in pore water increased after sulfate addition (Fig. II.1-3), confirming that microbes are less C-limited. In addition, methanogens are active only at very low

Eh conditions (Whiticar, 1999). Though the difference was small, S-treated mesocosms always exhibited lower Eh through the whole rice growing stages in our experimental mesocosms in the previous year (2017) (Wang et al., 2020) and also in this study (2018) (Table II.1-S3). Methanogens benefited from decreasing Eh and therefore enhanced CH₄ production, despite higher root biomass after S-fertilization could also introduce higher O₂ and create an aerobic rhizosphere soil environment (Whalen, 2005). Hence, less competition between SRB and MA due to large organic C input in combination with more rhizodeposits release after sulfate addition may have contributed to the consistently high CH₄ concentration in soil (Fig II.1-b). In addition, S-treated mesocosms always showed a trend of depleted $\delta^{13}\text{C}$ -CH₄ from elongation to flowering stage under both FL and AWD conditions, which indicated a shift in methanogenesis pathways due to S fertilizer (Fig II.1-5, black dashed arrows).

4.2. Rice growth effects on methanogenesis pathways

Under flooded conditions in the current experiment, $\delta^{13}\text{C}$ values in CO₂ were relatively enriched and the enrichment increased through the rice growth stages (Fig II.1-4c; Fig II.1-5, green dashed arrows). We suggest that the most possible mechanism for this ¹³C-enrichment is a continuously increasing contribution from the hydrogenotrophic methanogenesis. In this process, MA strongly discriminates against heavier ¹³C during CO₂ reduction with hydrogen, and the remaining $\delta^{13}\text{C}$ in CO₂ becomes enriched (Hornibrook ER, 1999). Isotopic fractionation in CO₂ caused by the acetoclastic methanogenesis is controversially discussed in literature. It was suggested for a tropical peatland that this pathway also caused a ¹³C fractionation between acetate and the produced CO₂ by about 9‰ (Holmes et al., 2015). In contrast, (Ji et al., 2018) used CH₃F to inhibit acetoclastic methanogenesis and suggested that this pathway did not cause ¹³C enrichment in CO₂. $\delta^{13}\text{C}$ values in CO₂ increased (became less negative) in an anaerobic incubation experiment with paddy soil, whereas ¹³C in CH₄ was highly depleted with values of -60‰ (Zhang et al., 2013). Similarly, ¹³C enrichment in CO₂ patterns were also shown in paddy soils with or without straw in an anaerobic incubation (see Fig 2 in (Ji et al., 2018)). Under field conditions, isotopic fractionation can reflect naturally occurring processes and mechanisms of carbon turnover. In addition, the CO₂ sources are more diverse in mesocosm systems: root respiration, decomposition of soil organic matter and straw, CH₄ oxidation. But all these processes would rather cause ¹³C depletion in CO₂ due to microbial discrimination against heavier ¹³C either in naturally ¹³C-depleted CH₄ or in respective C₃-derived substrates. The difference of soil temperature at three gas samplings from stem elongation to flowering stages was small (around 26 °C), which excluded δ -value change due to temperature variation. Together with the ¹³C-enrichment of CO₂, hydrogenotrophic methanogenesis can cause a strong ¹³C-depletion of CH₄. In line with this our data also showed 2‰-5‰ decline of $\delta^{13}\text{C}$ -CH₄ down to -54‰ (S+FL), yet not significant. We could not fully distinguish between both processes, but based on the above-mentioned points, we suggest that with the rice growth, hydrogenotrophic pathway continuously contributed to CH₄ production.

Our field-based study confirmed that wet-dry cycles reduced CH₄ concentrations by suppressing methanogenesis, together with increasing oxidation shown by ¹³C enrichment in CH₄ and ¹³C depletion in CO₂, whereas sulfate fertilization had no effect

on the CH₄ concentrations in this paddy soil amended with rice straw. Sulfate addition affects CH₄ production mainly through substrate competition between SRB and MA; this may not be the case in soils with ample C availability. Therefore, straw amendment and sulfate-induced rhizodeposition could explain the absence of a fall in CH₄ production. At later stages of rice growth, the contribution of the hydrogenotrophic methanogenesis to CH₄ production under flooded conditions was obvious as indicated by ¹³C enrichment in CO₂ with consistent CH₄ depletion. However, the results found here still have some limitations. We noted that the data in this study were collected from one rice season in 2018, which may reduce the representativeness of the results; In addition, efflux results would improve our understanding of linking CO₂ and CH₄ concentrations produced *in situ* to that escaped to the atmosphere (efflux). Further studies should consider efflux data at different growth seasons simultaneously to get a better understanding of CO₂ and CH₄ emission mechanisms in paddy fields. From the broader agroecological perspective, understanding the shifts in the methanogenesis pathways during rice growth in paddy fields may help to better control greenhouse gas emissions through adaptations of management practices.

Acknowledgments

We would like to thank Shuai Zhang for his help on collecting samples. We are also grateful to Gianluca Beltarre, Umberto Rolla, Eleonora Miniotti, Daniele Tenni, Stefano Afric and other colleagues in Italian rice research center for their professional scientific support and also non-academic friendly help during this experiment in 2018. Finally, we want to thank Prof. Dr. Gerhard Gebauer and his team of the Laboratory of Isotope Biogeochemistry at the University of Bayreuth for the abundance analysis of the carbon isotopes of gas samples. Qiong Liu's financial support was granted by the China Scholarship council (CSC).

References

- Adhya, T.K., Rath, A.K., Gupta, P.K., Rao, V.R., Das, S.N., Parida, K.M., Parashar, D.C., Sethunathan, N., 1994. Methane emission from flooded rice fields under irrigated conditions. *Biology and Fertility of Soils* 18, 245-248.
- Atere, C.T., Ge, T., Zhu, Z., Tong, C., Jones, D.L., Shibistova, O., Guggenberger, G., Wu, J., 2017. Rice rhizodeposition and carbon stabilisation in paddy soil are regulated via drying-rewetting cycles and nitrogen fertilisation. *Biology and Fertility of Soils* 53, 407-417.
- Berger, S., Jang, I., Seo, J., Kang, H., Gebauer, G., 2013. A record of N₂O and CH₄ emissions and underlying soil processes of Korean rice paddies as affected by different water management practices. *Biogeochemistry* 115, 317-332.
- Cai, Z., Xing, G., Yan, X., Xu, H., Tsuruta, H., Yagi, K., Minami, K., 1997. Methane and nitrous oxide emissions from rice paddy fields as affected by nitrogen fertilisers and water management. *Plant and Soil* 196, 7-14.
- Conrad, R., 2002. Control of microbial methane production in wetland rice fields. *Nutrient Cycling in Agroecosystems* 64, 59-69.
- Conrad, R., 2005. Quantification of methanogenic pathways using stable carbon isotopic signatures: a review and a proposal. *Organic Geochemistry* 36, 739-752.
- Corton, T., Bajita, J., Grospe, F., Pamplona, R., Assis, C., Wassmann, R., Lantin, R., Buendia, L., 2000. Methane emission from irrigated and intensively managed rice fields in Central Luzon (Philippines). *Nutrient cycling in Agroecosystems* 58, 37-53.
- Ge, T., Yuan, H., Zhu, H., Wu, X., Nie, S.a., Liu, C., Tong, C., Wu, J., Brookes, P., 2012. Biological carbon assimilation and dynamics in a flooded rice – Soil system. *Soil Biology and Biochemistry* 48, 39-46.
- Goevert, D., Conrad, R., 2008. Carbon isotope fractionation by sulfate-reducing bacteria using different pathways for the oxidation of acetate. *Environmental Science & Technology* 42, 7813-7817.
- Goldberg, S.D., Knorr, K.-H., Gebauer, G., 2008. N₂O concentration and isotope signature along profiles provide deeper insight into the fate of N₂O in soils. *Isotopes in Environmental and Health Studies* 44, 377-391.
- Holmer, M., Kristensen, E., 1994. Coexistence of sulfate reduction and methane production in an organic-rich sediment. *Marine Ecology-Progress Series* 107, 177-177.
- Holmes, M.E., Chanton, J.P., Tfaily, M.M., Ogram, A., 2015. CO₂ and CH₄ isotope compositions and production pathways in a tropical peatland. *Global Biogeochemical Cycles* 29, 1-18.
- Hornibrook ER, L.F., Fyfe WS, 1999. Evolution of stable carbon isotope compositions for methane and carbon dioxide in freshwater wetlands and other anaerobic environments. *Geochimica et Cosmochimica Acta* 64, 1013–1027.
- Ji, Y., Liu, P., Conrad, R., 2018. Change of the pathway of methane production with progressing anoxic incubation of paddy soil. *Soil Biology and Biochemistry* 121, 177-184.
- Krüger, M., Eller, G., Conrad, R., Frenzel, P., 2002. Seasonal variation in pathways of CH₄ production and in CH₄ oxidation in rice fields determined by stable carbon isotopes and specific inhibitors. *Global Change Biology* 8, 265-280.
- Krzycki, J.A., Kenealy, W.R., Deniro, M.J., Zeikus, J.G., 1987. Stable carbon isotope fractionation by *methanosarcina barkeri* during methanogenesis from acetate,

- methanol, or carbon dioxide-hydrogen. *Appl Environ Microb* 53, 2597-2599.
- Li, Z., Yagi, K., 2004. Rice root-derived carbon input and its effect on decomposition of old soil carbon pool under elevated CO₂. *Soil Biology and Biochemistry* 36, 1967-1973.
- Linquist, B., Groenigen, K.J., Adviento-Borbe, M.A., Pittelkow, C., Kessel, C., 2012a. An agronomic assessment of greenhouse gas emissions from major cereal crops. *Global Change Biology* 18, 194-209.
- Linquist, B.A., Adviento-Borbe, M.A., Pittelkow, C.M., van Kessel, C., van Groenigen, K.J., 2012b. Fertilizer management practices and greenhouse gas emissions from rice systems: A quantitative review and analysis. *Field Crops Research* 135, 10-21.
- Ma, K., Conrad, R., Lu, Y., 2013. Dry/Wet cycles change the activity and population dynamics of methanotrophs in rice field soil. *Appl Environ Microb* 79, 4932-4939.
- Ma, K., Lu, Y., 2011. Regulation of microbial methane production and oxidation by intermittent drainage in rice field soil. *FEMS Microbiol Ecol* 75, 446-456.
- Michael, J.W., Eckhard, F., 1985. Methane oxidation in sediment and water column environments-Isotope evidence. *Organic Geochemistry* 10, 759-768.
- Minamikawa, K., Sakai, N., Hayashi, H., 2005. The effects of ammonium sulfate application on methane emission and soil carbon content of a paddy field in Japan. *Agriculture, Ecosystems & Environment* 107, 371-379.
- Muyzer, G., Stams, A.J., 2008. The ecology and biotechnology of sulphate-reducing bacteria. *Nat Rev Microbiol* 6, 441-454.
- Ro, S., Seanjan, P., Tulaphitak, T., Inubushi, K., 2011. Sulfate content influencing methane production and emission from incubated soil and rice-planted soil in Northeast Thailand. *Soil Science and Plant Nutrition* 57, 833-842.
- Schonheit, P., Kristjansson, J.K., Thauer, R.K., 1982. Kinetic mechanism for the ability of sulfate reducers to out-compete methanogens for acetate. *Archives of Microbiology* 132, 285-288.
- Schütz, H., Holzapfel-Pschorn, A., Conrad, R., Rennenberg, H., Seiler, W., 1989. A 3-year continuous record on the influence of daytime, season, and fertilizer treatment on methane emission rates from an Italian rice paddy. *Journal of Geophysical Research: Atmospheres* 94, 16405-16416.
- Smith, M.R., Mah, R.A., 1980. Acetate as sole carbon and energy-source for growth of *Methanosarcina* strain-227. *Applied and Environmental Microbiology* 39, 993-999.
- Tian, J., Dippold, M., Pausch, J., Blagodatskaya, E., Fan, M., Li, X., Kuzyakov, Y., 2013. Microbial response to rhizodeposition depending on water regimes in paddy soils. *Soil Biology and Biochemistry* 65, 195-203.
- Wang, J., Kerl, C.F., Hu, P., Martin, M., Mu, T., Brüggewirth, L., Wu, G., Said-Pullicino, D., Romani, M., Wu, L., Planer-Friedrich, B., 2020. Thiolated arsenic species observed in rice paddy pore waters. *Nature Geoscience* 13, 282-287.
- Wei, X., Zhu, Z., Wei, L., Wu, J., Ge, T., 2019. Biogeochemical cycles of key elements in the paddy-rice rhizosphere: Microbial mechanisms and coupling processes. *Rhizosphere* 10, 100145.
- Whalen, S.C., 2005. Biogeochemistry of methane exchange between natural wetlands and the atmosphere. *Environmental Engineering Science* 22, 73-94.
- Whiticar, M.J., 1999. Carbon and hydrogen isotope systematics of bacterial formation and oxidation of methane. *Chemical Geology* 161, 291-314.
- Whiticar, M.J., Faber, E., Schoell, M., 1986. Biogenic methane formation in marine and freshwater environments: CO₂ reduction vs. acetate fermentation— isotope evidence. *Geochimica et Cosmochimica Acta* 50, 693-709.

- Yagi, K., Minami, K., 1990. Effect of organic matter application on methane emission from some Japanese paddy fields. *Soil Science and Plant Nutrition* 36, 599-610.
- Zhang, G., Ji, Y., Ma, J., Xu, H., Cai, Z., Yagi, K., 2012. Intermittent irrigation changes production, oxidation, and emission of CH₄ in paddy fields determined with stable carbon isotope technique. *Soil Biology and Biochemistry* 52, 108-116.
- Zhang, G., Liu, G., Zhang, Y., Ma, J., Xu, H., Yagi, K., 2013. Methanogenic pathway and fraction of CH₄ oxidized in paddy fields: seasonal variation and effect of water management in winter fallow season. *PLoS One* 8, e73982.
- Zhang, G., Yu, H., Fan, X., Liu, G., Ma, J., Xu, H., 2015. Effect of rice straw application on stable carbon isotopes, methanogenic pathway, and fraction of CH₄ oxidized in a continuously flooded rice field in winter season. *Soil Biology and Biochemistry* 84, 75-82.
- Zhu, Z., Ge, T., Liu, S., Hu, Y., Ye, R., Xiao, M., Tong, C., Kuzyakov, Y., Wu, J., 2018. Rice rhizodeposits affect organic matter priming in paddy soil: The role of N fertilization and plant growth for enzyme activities, CO₂ and CH₄ emissions. *Soil Biology and Biochemistry* 116, 369-377.

Supplementary materials

Table II.1-S1 Fertilization information of the field experiment in 2017 and 2018.

Year	2017 ^a	2018
Cultivation areas	0.78 m ²	0.78 m ²
Seedlings per mesocosm	340	330
treatments	Water seeded with or without sulfate	continuous flooding with or without sulfate (noS+FL, S+FL)
	Dry seeded with or without sulfate	alternate wet-drying with or without sulfate (noS+AWD, S+AWD)
Fertilization	180 kg N ha ⁻¹ , 124 kg K ha ⁻¹ , 17 kg P ha ⁻¹	240 kg N ha ⁻¹ , 290 kg K ha ⁻¹ , 17 kg P ha ⁻¹
Amount of S from sulfate fertilizer	81 mg S/kg (293 kg S ha ⁻¹)	124 mg S/kg (396 kg S ha ⁻¹)
Rice straw addition per mesocosm	200 g	785–1076 g

a. Data from 2017 are taken from Wang, J.; Kerl, C. F.; Hu, P.; Martin, M.; Mu, T.; Brüggewirth, L.; Wu, G.; Said-Pullicino, D.; Romani, M.; Wu, L.; Planer-Friedrich, B. Thiolated arsenic species observed in rice paddy pore waters. *Nature Geoscience* 2020, 13 (4), 282-287. DOI:10.1038/s41561-020-0533-1.

Table II.1-S2 Summary results from a two-way ANOVA with repeated measures of CO₂ and CH₄ concentrations and their isotope composition, plant height and pore water DOC contents at different rice growth stages. Basis of results for Figures II.1-2, 3 and 4.

Variables	Treatment effect		Stage effect		Treatment* Stage effect	
	<i>F</i>	<i>P</i>	<i>F</i>	<i>P</i>	<i>F</i>	<i>P</i>
δ ¹³ C-CO ₂	16.417	0.001	12.146	0.001	10.29	<0.001
CO ₂ concentration	6.306	0.017	8.084	0.004	3.498	0.021
δ ¹³ C-CH ₄	4.713	0.035	5.928	0.012	0.385	0.878
CH ₄ concentration	8.926	0.006	9.754	0.002	5.985	0.002
Plant height	39917.7	0.001	1250.6	<0.001	2.245	0.055
Pore water DOC	4.233	0.046	41.59	<0.001	2.953	0.076

Table II.1-S3 Redox potential values (Eh) in pore water (mV) in 2017 and 2018 (mean ± SD, n=3). noS+FL: continuous flooding; S+FL: sulfate fertilizer + continuous flooding; noS+AWD: wet-dry cycles, and S+AWD: sulfate fertilizer + wet-dry cycles.

Sampling time in 2017	noS+ water-seeded	S+ water-seeded	noS+ dry-seeded	S+ dry-seeded
tillering	181±85	123±25	212±44	207±59
elongation	168±62	131±36	163±9	135±30
booting	185±56	159±24	162±11	127±47
flowering	122±5	92±16	180±98	89±30
Sampling time in 2018	noS+FL	S+FL	noS+AWD	S+AWD
elongation	157 ± 6	168 ± 66	175 ± 15	166 ± 35
booting	163 ± 22	148 ± 7	168 ± 6	149 ± 23
flowering	189 ± 6	173 ± 3	184 ± 3	171 ± 7

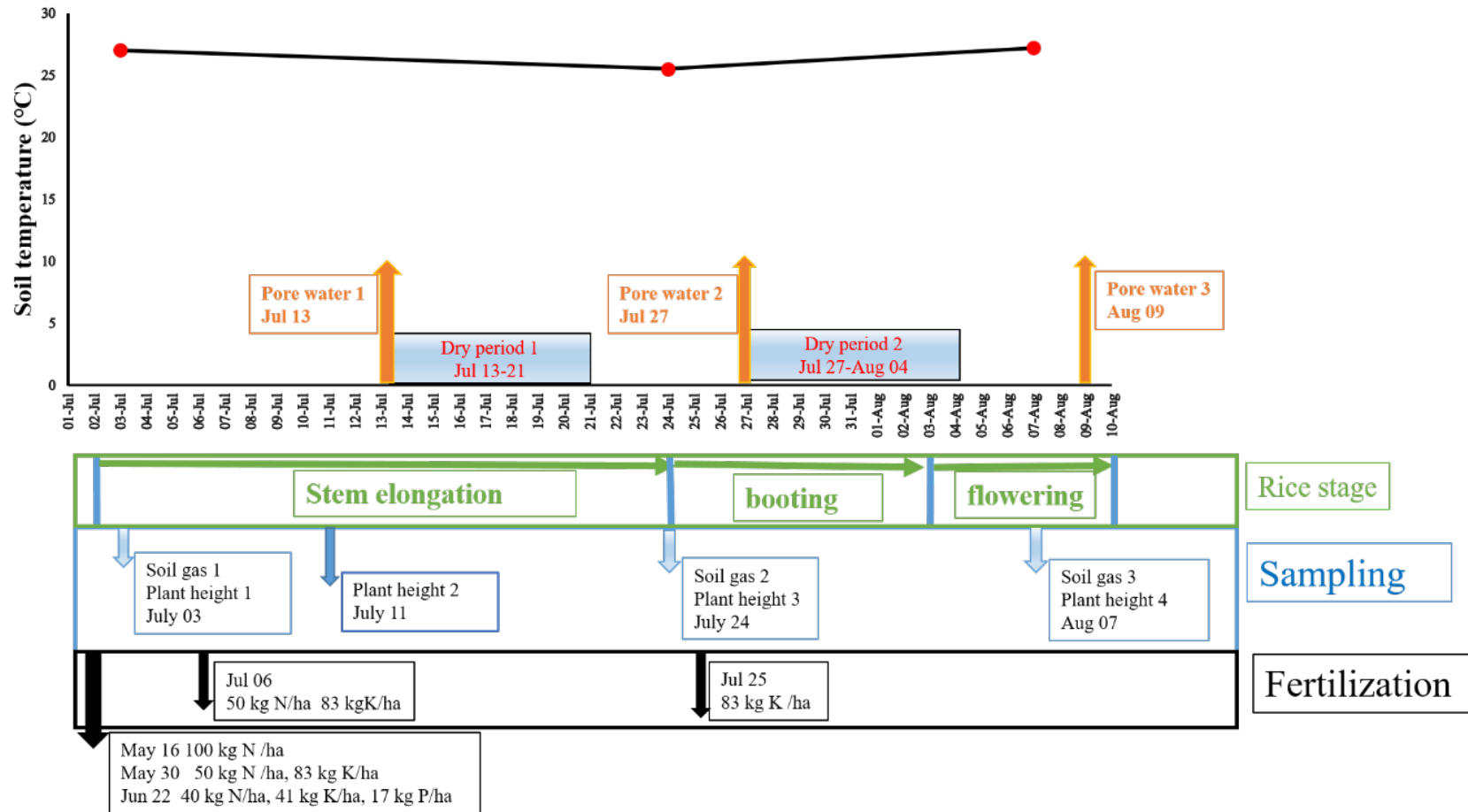


Figure II.1-S1 Fertilization, rice growth stages and sampling time schedules of the field experiment in 2018. For details, please refer to the text in Materials and methods.

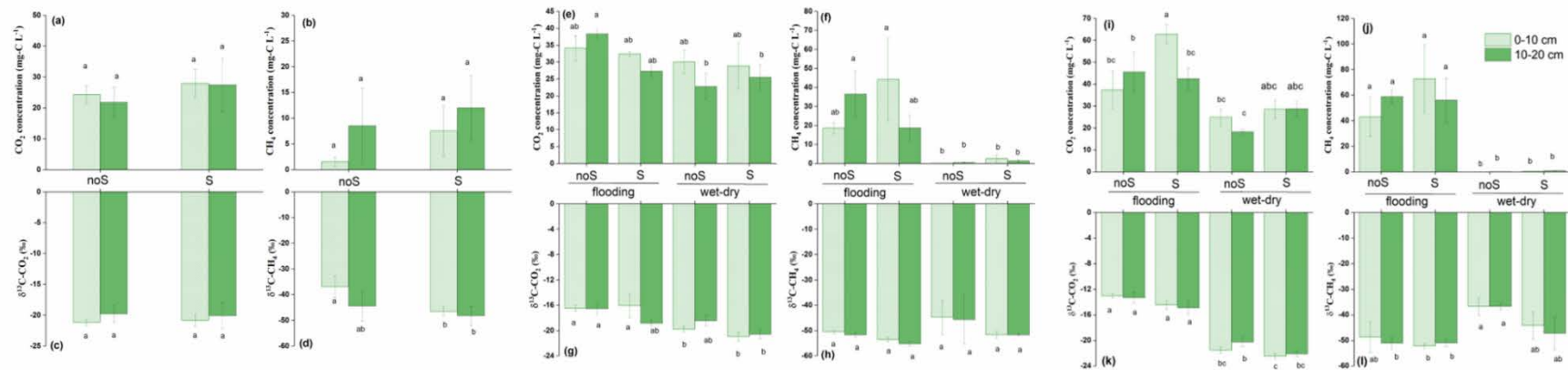


Figure II.1-S2 Mean concentration of CO₂, CH₄ and their mean delta values (a) CO₂, (b) CH₄ concentrations and mean delta values of CO₂ (c) and CH₄ (d) before drying conducted (stem elongation stage, 54 DAT), and mean concentration of CO₂ (e, i), CH₄ (f, j) and mean delta values of CO₂ (g, k) and CH₄ (h, l) after wet-drying conducted at booting and flowering stages, respectively, in gas bottles at 0–10 cm and 10–20 cm soil depth (mean ± SE, n=6).

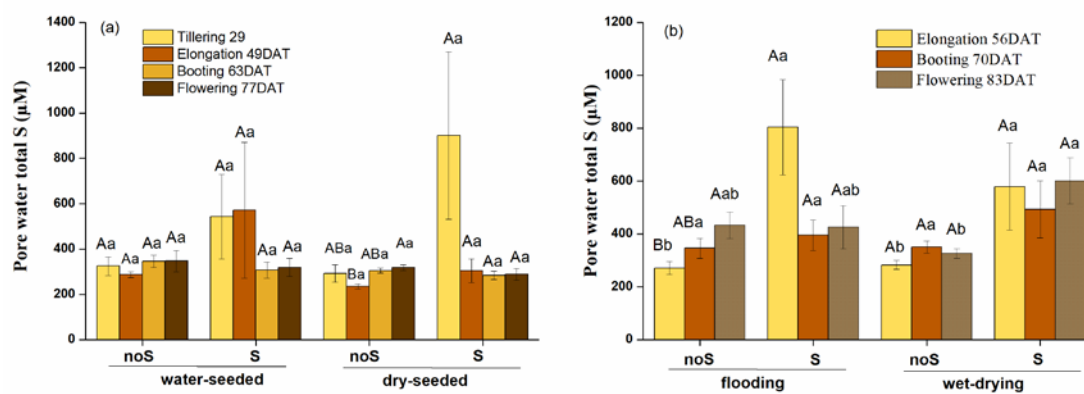


Figure II.1-S3 Pore water total dissolved sulfur concentrations over rice growth season in 2017 (a) and 2018 (b) (mean \pm SE, n=3).

II.2 Effect of alternating wet-dry cycles and sulfate fertilization on plant-soil C allocation and rice yield

Qiong Liu^{a*}, Johanna Pausch^a

In preparation for short communication

^aAgroecology, BayCEER, University of Bayreuth, Bayreuth, 95440, Germany.

*E-mail: Qiong.liu@uni-bayreuth.de

Abstract

Alternating wet-dry cycles (AWD) and sulfate fertilization were reported to efficiently reduce CH₄ emissions from paddy soils. However, it is not fully understood how those management practices and their combination affect photosynthetic C allocation and rice yield. To investigate the underlying mechanisms, rice mesocosms with and without sulfate fertilization under flooded conditions and two wet-dry-cycles were pulse labelled with ¹³CO₂ at the flowering stage. Results showed similar assimilation patterns in all treatments: more than 50% of the assimilates were retained in aboveground biomass after pulse labelling. The ¹³C translocation to roots was peaked at day 4 and then gradually decreased. In addition, no ¹³C enrichment in soils was detectable due to low assimilates allocated downwards at this growing stage. AWD alone enhanced the root to shoot biomass ratio and lowered grain production, yet not significant. Sulfate fertilizer increased the root to shoot ratio under flooded conditions, whereas under AWD conditions, it increased shoot biomass and balanced the grain production compared to no sulfate addition. Overall, our results implied the positive effect of sulfate fertilizer on rice plant biomass and grain yield, whereas AWD alone may reduce grain yield. In addition, the effects of AWD and sulfate fertilization on plants are likely to be more pronounced at the vegetative or reproductive stage, as no difference in ¹³C allocation was detectable at the flowering stage.

Key words: pulse labelling, wet-drying, sulfate fertilizer, rice grain, paddy soil

1. Introduction

Rice feeds more than 2.7 billion people, accounting for half of the world's population (Fairhurst and Dobermann, 2002). Artificial paddy soils, where rice is grown, cover more than 163 million ha contributing to ~9% of the world's cropland area (Oertel et al., 2016). Meanwhile, the first 100 cm soil depths were estimated to contain ~1.2% of the global soil organic C pool (Liu et al., 2021b). The C flow in the plant-soil system is highly complex, being highly variable in time and space. In paddy soils, the fertilization effect on CH₄ emissions had been well reported. Sulfate fertilization (e.g. ammonium sulfate) was reported to efficiently decrease CH₄ emission compared to urea fertilizer (Cai et al., 1997; Minamikawa et al., 2005; Linquist et al., 2012). The underlying mechanism is competition for substrates (both acetate and H₂) between sulfate-reducing bacteria (SRB) and methanogenic archaea (MA) (Schonheit et al., 1982; Whiticar et al., 1986; Ro et al., 2011). Water management is another important factor for sustaining food production, especially for crops grown in semi-aquatic condition such as paddy rice. However, fully flooded water supply favors the performance of microorganisms such as methanogens and causes CH₄ emissions (Hussain et al., 2015). In addition, water status can affect microbial community which utilizes plant-derived C in paddy soils. Fungi and gram-negative bacteria were found to be more active under controlled water conditions (Yao et al., 2012; Tian et al., 2013).

Fertilization and water management could also affect the dynamics of CO₂, which is a greenhouse gas that should be carefully considered. Ammonium sulfate was reported to stimulate soil C decomposition (Minamikawa et al., 2005). Alternating wet-drying (AWD) and non-flooded regimes can increase root activity and thus release more photosynthates into soil, stimulating roots and rhizomicrobial respiration (Tian et al., 2012). However, how these two managements and their combination affect photosynthetic C allocation and rice yield remained limited. Our former study found the positive effect of sulfate fertilizer on rice plant biomass and height compared to urea (Liu et al., 2021a). It was suggested that S fertilizer could enhance N uptake by plants (Salvagiotti and Miralles, 2008; Salvagiotti et al., 2009) and help plant development (Capaldi et al., 2015). For mitigating global warming, a comprehensive understanding of both CH₄ and CO₂ dynamics and soil C storage are essential. In addition, the final rice production should also be considered for ensuring sustainable food demand.

Considering these facts, rice plants in mesocosms were pulse labelled with ¹³CO₂ and the newly assimilated C incorporation into plants and soil was traced afterward. The objectives of this study were: (1) to assess the photosynthetic C allocation in the plant-soil system under sulfate fertilizer and AWD management; (2) to evaluate the effect of AWD and sulfate fertilizer on final yield. We hypothesized that 1) sulfate and AWD increased C allocation into soil due to enhanced root and microbial activity; 2) sulfate and AWD increased rice yield due to positive effects on plants and microorganisms.

2. Materials and methods

2.1 Experimental set-up

A large batch of soil was collected from the plough layer (0-30 cm) at a site at Cascina Veronica, close to the town of Garlasco, Pavia, Italy (45°10'39"N, 8°53'48"E) in 2017. The soil was classified as Eutric Gleysol with 15-year rice cultivation history following

corn cropping. Mesocosm containers (112 cm * 72 cm * 65 cm) with the following treatments were established with three replicates in a randomized factorial arrangement in 2018: continuous flooding (noS+FL), sulfate fertilizer + continuous flooding (S+FL), wet-dry cycles (noS+AWD), and sulfate fertilizer + wet-dry cycles (S+AWD). More detailed information on the experimental set-up and fertilizers application are presented in Liu et al., (2021a) and Wang et al., (2020). The basic chemical properties of the soil were as follows: pH 5.6, total C 2.0%, total N 0.6%, total S 2.6 g kg⁻¹. Urea and KCl were used as sources of N and K, respectively, in the treatment without sulfate. (NH₄)₂SO₄ and K₂SO₄ were used as N and K fertilizers, respectively, for S mesocosms. Triple superphosphate was used as a source of P. The water level was controlled every day in all containers except for AWD treatments. AWD treatments were kept without irrigation for 9 days (except for rainwater) at stem elongation and booting stages and were then rewetted and kept flooded after each drying event.

2.2 Pulse labelling and sampling

Pulse labelling technology was used to provide information on the allocation of recently assimilated C to different C pools and to study the dynamics of C allocation between pools. After the second wet-dry cycle at flowering stage (82 days after transplanting, DAT), each mesocosm container was covered with labelling chamber (1.13 * 0.72 * 1 m³) consisting of wood frames stringed with transparent low-density polyethylene (LDPE) foil with a total light transmission of ~90%. The edges of the LDPE foils were sealed with tapes for air leaks. The ¹³CO₂ was released in each chamber by adding an excess of 5 M H₂SO₄ to 5 g of 99% ¹³C-enriched Na₂CO₃ dissolved in water. Plants were labelled for 2.5 hours (8 a.m.-1 p.m.) due to hot weather and then chambers were removed.

At the day before labelling, one sampling was conducted for ¹³C natural abundance measurements. After pulse labelling, soil and plants samples were taken shortly, and 1, 2, 4, 8, 14 days afterwards, resulting in 7 sampling times. For each sampling, one plant per mesocosm container was randomly chosen: shoots were cut at the base near the soil surface; root and soil samples were taken from 0–20 cm depth using a Riverside auger (ID 4 cm, Eijkelkamp, Giesbeek, Netherlands). Roots were picked out from soil by hand and washed with deionized water. Shoots, roots and soils were oven-dried at 60 °C for 3 days, weighed for biomass, and ball-milled for isotope measurement. Rice straw and grains were collected and weighed after the harvest.

2.3 Analyses and data processing

The stable ¹³C isotope composition of shoot, root, and soil samples was analyzed using a Carlo Elba 1108 elemental analyzer interfaced to a Thermo Finnigan Delta Plus XP isotope ratio mass spectrometer.

The incorporation of excess ¹³C in shoots, roots, and soil samples (excess ¹³C amount) was calculated as follows:

$$\text{Excess } ^{13}\text{C amount} = (\text{atom}\% ^{13}\text{C}_L - \text{atom}\% ^{13}\text{C}_{UL}) / 100 * \text{TC}_{\text{sample}} \quad (1)$$

where atom% ¹³C_L and atom% ¹³C_{UL} are the atom% ¹³C in labelled and unlabelled samples, respectively, and TC_{sample} represents the total C amount of each labelled

sample.

Total root production was estimated as follows:

$$\text{Root production} = \text{Straw production} * (\text{Root/Shoot Ratio}) \quad (2)$$

where Root/Shoot Ratio is the mean value of the ratio of root biomass to shoot biomass in Fig II.2-1. Straw production is the straw biomass collected after harvest in Table II.2-1.

2.4 Statistical evaluation

Data was analyzed by one-way ANOVA for different treatments within sampling time and was compared by Duncan's test in SPSS 19.0 (SPSS Inc., Chicago, IL), with significance defined at $P < 0.05$.

3. Results

3.1 Plant biomass and yield

Under flooded conditions, the root, shoot, and the total plant biomass were higher after sulfate fertilization, compared with control (noS + FL) (Fig 1, $P > 0.05$). Simultaneously, the straw production and the estimated root production were significantly higher in sulfate treatments; in addition, the grain to straw ratio was significantly lower after sulfate fertilization (Table 1, $P < 0.05$). AWD alone (noS + AWD) increased both root and shoot biomass and largely enhanced the root to shoot ratio compared to control. However, it slightly reduced grain production, yet not significant ($P > 0.05$).

Under AWD, sulfate fertilizer enhanced shoot biomass and reduced the root to shoot ratio. Straw production was significantly higher than noS + AWD ($P < 0.05$). In addition, the grain to straw ratio was significantly lower after sulfate fertilization. Compared to S + FL, AWD didn't affect plant biomass. In addition, it lowered both the straw and root productions without affecting grain yield.

3.2 Total ^{13}C amount in the plant-soil system

After pulse labelling, the ^{13}C assimilated in shoot was gradually decreased with time from day 0 to day 4 and remained constant afterward. At day 14 after labelling, more than 50% of assimilates remained in the shoot biomass (Fig 2a). ^{13}C allocation into roots peaked at day 4 for all treatments except for S+FL and then gradually decreased (Fig 2b). Similar to ^{13}C patterns in the root, the ^{13}C -root to ^{13}C -shoot ratio increased with time, peaked at day 4, and gradually decreased (Fig 2c). No ^{13}C translocation was detectable to soils after labelling.

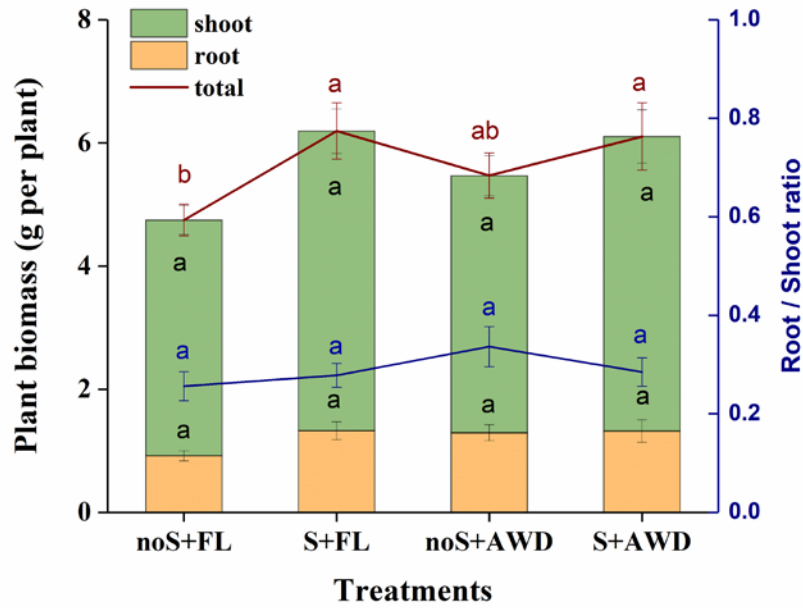


Figure II.2-1 Plant biomass and the root to shoot ratio at flowering stage (mean \pm SE, $n=21$, 3 replicates * 7 sampling times). The two wet-dry periods were 56-63 DAT and 70-77 DAT, respectively. Small letters indicate significant differences at $P < 0.05$ based on Duncan's test within treatments.

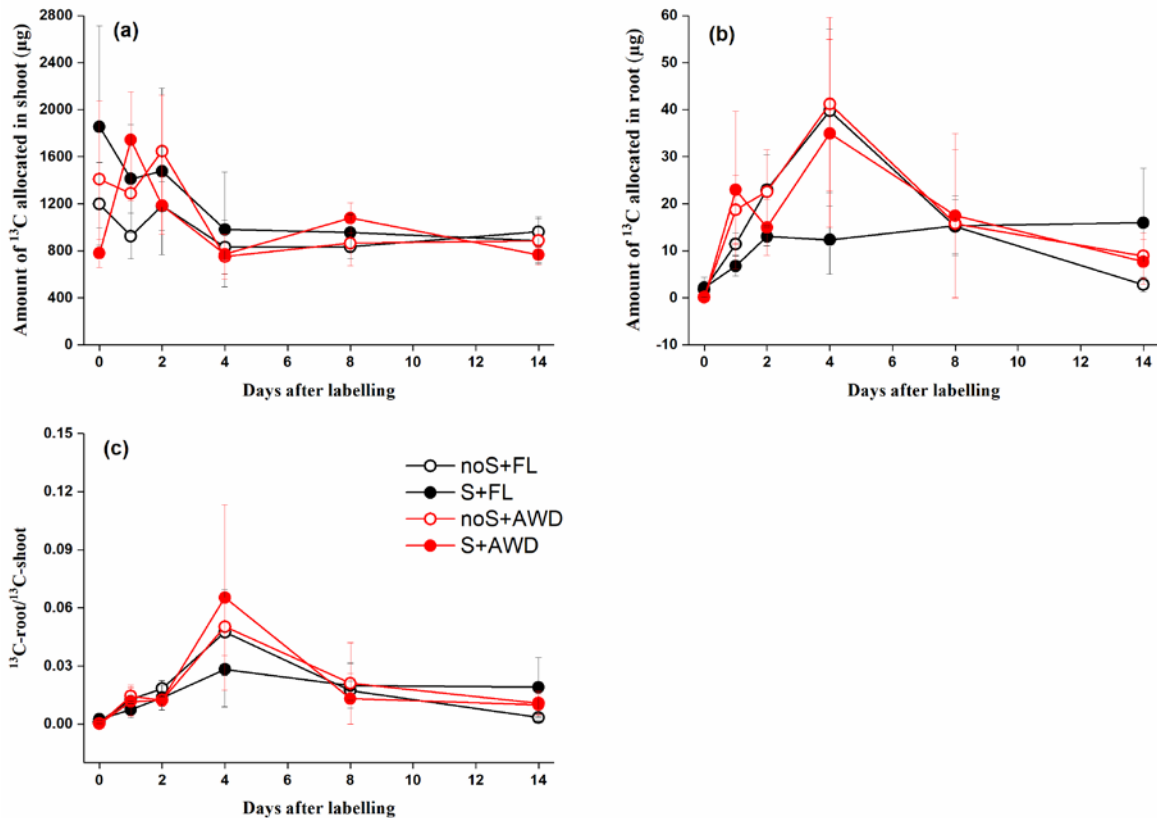


Figure II.2-2 The assimilated ¹³C allocation in rice plants (a) ¹³C in shoot; (b) ¹³C in root; (c) ¹³C-root to ¹³C-shoot ratio after ¹³C pulse labelling under different treatments (mean \pm SE, $n=3$).

Table II.2-1 Biomass productions after harvest in 2018 (mean \pm SE, n=3).

Yield	noS+FL	S+FL	noS+AWD	S+AWD
Grain (g)	930 \pm 32a	932 \pm 31a	895 \pm 19a	930 \pm 23a
Straw (g)	787 \pm 35b	1068 \pm 46a	782 \pm 24b	993 \pm 13a
G/S	1.18 \pm 0.01a	0.87 \pm 0.04b	1.15 \pm 0.01a	0.94 \pm 0.03b
Root production (g)	202 \pm 7c	297 \pm 10a	263 \pm 7b	283 \pm 3ab

4. Discussion

4.1. Photosynthetic C allocation

Pulse labelling can efficiently provide information on the allocation of recently assimilated C to different C pools and compare the allocation and dynamics of ^{13}C in rice under AWD and sulfate fertilization. However, no ^{13}C assimilation difference was observed within treatments in our study, which may be caused by two reasons. First, we conducted pulse labelling for paddy mesocosms under field conditions for 2.5 h only due to high air temperature. In former studies, a labelling time of 5~7-hours was applied for paddy soil in pot experiments (Tian et al., 2012; Tian et al., 2013; Zhu et al., 2016; Xiao et al., 2019). 2.5 h may be too short to see the allocation difference especially under hot weather conditions as plants are not able to assimilate all the tracer. Shortly after pulse labelling, the amount of ^{13}C assimilated in shoot was around 0.78–1.85 mg (45–62% of ^{13}C recovered relative to the added tracer) in our results, which is far less than 11.6–13.8 mg after 6 h of pulse labelling in Yuan et al., (2016). Second, most of assimilates were retained in shoots 14 days after pulse labelling, and no incorporation into soil was observed (Fig 2a). Consistent with our results, the newly allocated C to shoot decreased with time after 5 hours of pulse labelling (Tian et al., 2012). However, the allocation into root followed a power function increase with time, which was contradictory to our results that it peaked at day 4 and generally decreased (Fig 2b). Yuan et al., (2016) found ^{13}C incorporation rate into soil microbial groups increased with rice maturity (maximum 63 DAT in their study). Our pulse labelling was conducted 82 DAT (the end of flowering stage), which may be too late to see the fast incorporation. Previous studies also suggested that 78–90% of net assimilates would be retained aboveground, and only 1–5% could be incorporated into soil during the maturing stage of rice plant (Lu et al., 2002). Less translocation at flowering and grain-filling stages could be the second reason causing the missing difference. Plants may invest more in flower and fruit production and hence remain more recent assimilates aboveground at this growth stage. (Pausch and Kuzyakov, 2018).

4.2. Effect of AWD and sulfate fertilizer on plant properties

The effect of AWD on rice biomass is contradictory in former studies. AWD was reported to reduce rice root production (Oliver et al., 2019), whereas it increased root activity without affecting biomass (Tian et al., 2013). In our study, two wet-dry cycles highly enhanced root biomass together with potentially reduced grain yield, though not significant ($P>0.05$). (Mishra and Salokhe, 2011) suggested that AWD effects may differ from rice growth stages: AWD increases root length density at vegetative stage whereas at reproductive stage cause opposite results. In addition, different magnitudes

of AWD may have the opposite effect on biomass. Alternate wetting and moderate soil drying (re-watered when soil water potential reached -15 kPa at 15–20 cm depth) can increase root and shoot biomass, whereas severe soil drying (re-watered when soil water potential reached -30 kPa) decrease both root and shoot biomass compared with conventional irrigation (Zhang et al., 2009). Moreover, severe soil drying can reduce grain yield when soil water potential was less than -20 kPa (Carrijo et al., 2017). For optimizing the higher grain yield and lower greenhouse gas emission, the time and magnitude for AWD should be carefully considered.

Consistent with our former study, sulfate fertilizer increased biomass production (straw yield) (Table 1, $P < 0.05$) (Liu et al., 2021a). This result was proximately due to the critical role of S on enhancing N uptake (Salvagiotti and Miralles, 2008; Salvagiotti et al., 2009) and helping plant development (Capaldi et al., 2015). Together with the increased root to shoot ratio, it was estimated that sulfate fertilizer could also benefit microorganisms through increasing root biomass and thus increase rhizodeposits release into soil (Table 1). However, contrary to hypothesis 2, sulfate fertilizer had no effect on rice yield under flooded conditions. Under AWD conditions, sulfate fertilizer lowered the root to shoot ratio by increasing shoot biomass. In addition, the grain production was also increased (Fig 1 & Table 1, $P < 0.05$). Overall, those results may indicate that AWD may reduce rice grain production, while sulfate fertilizer has positive effects on balancing root to shoot biomass ratio and thus stabilizing rice yield. Our results highlighted the positive effect of sulfate fertilizer on both rice plant biomass and grain yield and the importance of time and magnitude of AWD on affecting rice grain yield. Further investigations should include C allocation patterns at various growth stages and CO_2 and CH_4 emission dynamics to assess climate-relevant aspects of agricultural management practices.

Acknowledgments

We are grateful to Prof. Dr. Gerhard Gebauer and his team of the Laboratory of Isotope Biogeochemistry at the University of Bayreuth for the abundance analysis of the carbon isotopes of solid samples. Qiong Liu's financial support is granted by the China Scholarship Council (CSC).

References

- Cai, Z., Xing, G., Yan, X., Xu, H., Tsuruta, H., Yagi, K., Minami, K., 1997. Methane and nitrous oxide emissions from rice paddy fields as affected by nitrogen fertilisers and water management. *Plant and Soil* 196, 7-14.
- Capaldi, F.R., Gratão, P.L., Reis, A.R., Lima, L.W., Azevedo, R.A., 2015. Sulfur Metabolism and Stress Defense Responses in Plants. *Tropical Plant Biology* 8, 60-73.
- Carrijo, D.R., Lundy, M.E., Linquist, B.A., 2017. Rice yields and water use under alternate wetting and drying irrigation: A meta-analysis. *Field Crops Research* 203, 173-180.
- Fairhurst, T., Dobermann, A., 2002. Rice in the global food supply. *World* 5, 454,349-511,675.
- Hussain, S., Peng, S., Fahad, S., Khaliq, A., Huang, J., Cui, K., Nie, L., 2015. Rice management interventions to mitigate greenhouse gas emissions: a review. *Environmental Science and Pollution Research* 22, 3342-3360.
- Linquist, B.A., Adviento-Borbe, M.A., Pittelkow, C.M., van Kessel, C., van Groenigen, K.J., 2012. Fertilizer management practices and greenhouse gas emissions from rice systems: A quantitative review and analysis. *Field Crops Research* 135, 10-21.
- Liu, Q., Romani, M., Wang, J., Planer-Friedrich, B., Pausch, J., Dorodnikov, M., 2021a. Alternating Wet-Dry Cycles Rather than Sulfate Fertilization Control Pathways of Methanogenesis and Methane Turnover in Rice Straw-Amended Paddy Soil. *Environmental Science & Technology* 55, 12075-12083.
- Liu, Y., Ge, T., van Groenigen, K.J., Yang, Y., Wang, P., Cheng, K., Zhu, Z., Wang, J., Li, Y., Guggenberger, G., Sardans, J., Penuelas, J., Wu, J., Kuzyakov, Y., 2021b. Rice paddy soils are a quantitatively important carbon store according to a global synthesis. *Communications Earth & Environment* 2.
- Lu, Y., Watanabe, A., Kimura, M., 2002. Input and distribution of photosynthesized carbon in a flooded rice soil. *Global Biogeochemical Cycles* 16, 32-31-38.
- Minamikawa, K., Sakai, N., Hayashi, H., 2005. The effects of ammonium sulfate application on methane emission and soil carbon content of a paddy field in Japan. *Agriculture, Ecosystems & Environment* 107, 371-379.
- Mishra, A., Salokhe, V.M., 2011. Rice root growth and physiological responses to SRI water management and implications for crop productivity. *Paddy and Water Environment* 9, 41-52.
- Oertel, C., Matschullat, J., Zurba, K., Zimmermann, F., Erasmi, S., 2016. Greenhouse gas emissions from soils—A review. *Geochemistry* 76, 327-352.
- Oliver, V., Cochrane, N., Magnusson, J., Brachi, E., Monaco, S., Volante, A., Courtois, B., Vale, G., Price, A., Teh, Y.A., 2019. Effects of water management and cultivar on carbon dynamics, plant productivity and biomass allocation in European rice systems. *Science of The Total Environment* 685, 1139-1151.
- Pausch, J., Kuzyakov, Y., 2018. Carbon input by roots into the soil: Quantification of rhizodeposition from root to ecosystem scale. *Glob Chang Biol* 24, 1-12.
- Ro, S., Seanjan, P., Tulaphitak, T., Inubushi, K., 2011. Sulfate content influencing methane production and emission from incubated soil and rice-planted soil in Northeast Thailand. *Soil Science and Plant Nutrition* 57, 833-842.
- Salvagiotti, F., Castellarín, J.M., Miralles, D.J., Pedrol, H.M., 2009. Sulfur fertilization improves nitrogen use efficiency in wheat by increasing nitrogen uptake. *Field Crops Research* 113, 170-177.
- Salvagiotti, F., Miralles, D.J., 2008. Radiation interception, biomass production and grain yield as affected by the interaction of nitrogen and sulfur fertilization in wheat. *European Journal of Agronomy* 28, 282-290.

- Schonheit, P., Kristjansson, J.K., Thauer, R.K., 1982. Kinetic mechanism for the ability of sulfate reducers to out-compete methanogens for acetate. *Arch. Microbiol.* 132, 285-288.
- Tian, J., Dippold, M., Pausch, J., Blagodatskaya, E., Fan, M., Li, X., Kuzyakov, Y., 2013. Microbial response to rhizodeposition depending on water regimes in paddy soils. *Soil Biology and Biochemistry* 65, 195-203.
- Tian, J., Pausch, J., Fan, M., Li, X., Tang, Q., Kuzyakov, Y., 2012. Allocation and dynamics of assimilated carbon in rice-soil system depending on water management. *Plant and Soil* 363, 273-285.
- Wang, J., Kerl, C.F., Hu, P., Martin, M., Mu, T., Brüggewirth, L., Wu, G., Said-Pullicino, D., Romani, M., Wu, L., Planer-Friedrich, B., 2020. Thiolated arsenic species observed in rice paddy pore waters. *Nature Geoscience* 13, 282-287.
- Whiticar, M.J., Faber, E., Schoell, M., 1986. Biogenic methane formation in marine and freshwater environments: CO₂ reduction vs. acetate fermentation—*isotope evidence*. *Geochimica et Cosmochimica Acta* 50, 693-709.
- Xiao, M., Zang, H., Ge, T., Chen, A., Zhu, Z., Zhou, P., Atere, C.T., Wu, J., Su, Y., Kuzyakov, Y., 2019. Effect of nitrogen fertilizer on rice photosynthate allocation and Carbon input in paddy soil. *European Journal of Soil Science*.
- Yao, H., Thornton, B., Paterson, E., 2012. Incorporation of ¹³C-labelled rice rhizodeposition carbon into soil microbial communities under different water status. *Soil Biology and Biochemistry* 53, 72-77.
- Yuan, H., Zhu, Z., Liu, S., Ge, T., Jing, H., Li, B., Liu, Q., Lynn, T.M., Wu, J., Kuzyakov, Y., 2016. Microbial utilization of rice root exudates: ¹³C labeling and PLFA composition. *Biology and Fertility of Soils* 52, 615-627.
- Zhang, H., Xue, Y., Wang, Z., Yang, J., Zhang, J., 2009. An Alternate Wetting and Moderate Soil Drying Regime Improves Root and Shoot Growth in Rice. *Crop Science* 49, 2246-2260.
- Zhu, Z., Ge, T., Xiao, M., Yuan, H., Wang, T., Liu, S., Atere, C.T., Wu, J., Kuzyakov, Y., 2016. Belowground carbon allocation and dynamics under rice cultivation depends on soil organic matter content. *Plant and Soil* 410, 247-258.

II.3 Vertical and horizontal shifts in the microbial community structure of paddy soil under long-term fertilization regimes

Qiong Liu^{a,b,c}, Cornelius Talade Atere^{b,d}, Zhenke Zhu^{b,*}, Muhammad Shahbaz^e, Xiaomeng Wei^b, Johanna Pausch^c, Jinshui Wu^b, Tida Ge^b

Published in *Applied Soil Ecology* as short communication, 2022
Vol. 169, 104248.

^a State Key Laboratory of Soil and Sustainable Agriculture, Institute of Soil Science, Chinese Academy of Sciences, Nanjing, 210008, China

^b Key Laboratory of Agro-ecological Processes in Subtropical Region & Changsha Research Station for Agricultural and Environmental Monitoring, Institute of Subtropical Agriculture, Chinese Academy of Sciences, Hunan 410125, China

^c Department of Agroecology, BayCEER, University of Bayreuth, Bayreuth 95447, Germany

^d Department of Soil Science and Land Resources Management, Faculty of Agriculture, Obafemi Awolowo University, Ile-Ife 220005, Nigeria

^e Centre for Environmental and Climate Science, Lund University, 223 62 Lund, Sweden

*Corresponding author

Institute of Subtropical Agriculture, Chinese Academy of Sciences, Changsha, Hunan Province 410125, China

E-mail: zhuzhenke@isa.ac.cn (Zhenke Zhu)

Abstract

Knowledge remains limited on how the structure of microbial community in paddy soils changes in relation to different types of fertilizers with same amount of nutrients. Thus, here, soil samples were collected at 0–10, 10–20, 20–30, and 30–40 cm depths from a paddy field subjected to four long-term fertilization treatments (no fertilization, mineral fertilization, mineral fertilization combined with rice straw, and chicken manure) and analyzed for microbial biomass and community composition. In unfertilized soils, microbial biomass decreased from 0 to 40 cm (with actinomycetes < Gram-positive (G+) bacteria < Gram-negative (G-) bacteria < fungi). This ordering was retained after fertilization, but the decline with depth was less pronounced. Both mineral and mineral plus organic fertilization increased the biomass of G+ bacteria compared to G- bacteria (22.7–56.2% increase) and actinomycetes (14.8–52.5% increase). Thus, over the long term, G+ bacteria benefited the most from mineral fertilizer than the other microbial groups. The partial replacement of mineral fertilizer with manure primarily enhanced the abundance of G+ bacteria at 0–30 cm soil depth, whereas replacement with straw enhanced the abundance of fungi at 10–20 cm soil depth. Our findings demonstrate that the structure of the microbial community is strongly impacted by long-term fertilization, independent of fertilizer type.

Key words: mineral fertilizer; microbial community composition; straw addition; soil depth; organic manure; paddy soil

1. Introduction

Paddy soil covers an estimated 161 million ha worldwide and fulfills more than half of the world population's food demands. Mineral and organic fertilizers are usually applied separately or in combination to paddy fields to enhance soil organic carbon (C) content and soil fertility (Yan et al., 2007; Liu et al., 2014; Zhang et al., 2016; Wei et al., 2021). For instance, the combined use of 70% manure and 30% mineral fertilizer improve rice yields and microbial diversity, especially that of bacteria (Chen et al., 2017). Thus, fertilization strategies might strongly affect the composition and functioning of the microbial community (Wang et al., 2017; Liu et al., 2019). Gram-negative (G⁻) bacteria appear to preferentially use labile plant-derived C, whereas Gram-positive (G⁺) bacteria are able to utilize recalcitrant compounds (Kramer and Gleixner, 2008; Fanin et al., 2019). In contrast, amendment with biochar reduces the relative abundance of G⁺ bacteria (Luo et al., 2017a), whereas both sucrose and straw addition strongly promote G⁻ bacteria and actinomycetes (Luo et al., 2017b). In paddy soils, straw residue and manure promote the growth of G⁻ bacteria over that of G⁺ bacteria (Zhang et al., 2012; Tang et al., 2018). Shoot- and root-C greatly increased the amount of microbial phospholipid fatty acids (PLFAs), which are indicative of fungi and actinomycetes (Zhu et al., 2017). In paddy soils, mineral fertilizer either increases the ratio of G⁺ to G⁻ bacteria (Zhang et al., 2007) or has no effect (Zhang et al., 2012; Dong et al., 2014).

Many studies have focused on evaluating microbial communities in topsoil (as a function of tillage or direct fertilization), because community composition is more variable in the surface horizons (generally at 0–20 cm) (Eilers et al., 2012). However, nutrients can translocate vertically from the top layer to the deeper soil layers (Kramer et al., 2013), with up to 30% of microbial biomass occurring in the C horizon (deeper than 50 cm) (van Leeuwen et al., 2017). Hence, soil depth should be considered an important environmental gradient that structures microbial communities in soil. However, information remains limited on how the microbial community changes vertically in paddy soil, especially in systems that receive long-term fertilization with different type of fertilizers, but with an equal amount of nutrient supply.

Thus, here, we investigated how the structure of the microbial community responds to the application of different fertilizers in paddy soils. We examined how the ratios of fungi to bacteria, G⁺ to G⁻ bacteria, and G⁺ bacteria to actinomycetes, respond to different types of fertilizers at 10-cm intervals to a depth of 40 cm in a paddy soil system. We hypothesized that: (1) the G⁺ to G⁻ bacteria ratio increases with soil depth because of decreasing nutrient availability; (2) mineral fertilizer has no effect on the G⁺ to G⁻ bacteria ratio; and (3) organic fertilizers (straw and manure) enhance the abundance of G⁻ bacteria over G⁺ bacteria because of high organic C input, whereas straw enhances the abundance of actinomycetes over G⁺ bacteria because of the prevalence of recalcitrant C.

Soil was sampled from four soil layers (0–10, 10–20, 20–30, and 30–40 cm) during the May of 2017 (before transplanting early rice) in a field used for long-term fertilization experimental trials in Ningxiang, Hunan Province, China (111°54'–112°18'E, 28°07'–28°37'N). The experiment was commenced in 1986 on soil formed from river alluvium. The main physical and chemical properties of the soil at the start of the experiment were pH of 5.8, 17.1 g kg⁻¹ soil organic C, 1.8 g kg⁻¹ total N, 144.0 mg kg⁻¹

available N, and 12.8 mg kg⁻¹ Olsen-P. Four fertilization regimes were established: no fertilizer (CK), mineral fertilizer (NPK) (urea, superphosphate, and potassium chloride), rice straw combined with mineral fertilizer (NPK + ST), and 70% NPK + 30% chicken manure (NPK + OM). The total amount of fertilizer was identical for each treatment in each season. Microbial biomass and community composition were measured using chloroform fumigation extraction and PLFA analysis, respectively. Further details on the experimental design, methods, and statistical analyses are provided in the supplementary methods.

2. Results

All fertilizer types increased total microbial PLFAs compared to unfertilized soil (CK); and all specific microbial PLFAs (G⁻ and G⁺ bacteria, actinomycetes, and fungi) decreased from the soil surface (0 cm depth) to 40 cm depth (Table II.3-S1). The relative abundance of specific microbial PLFAs declined in CK from 0 to 40 cm depth in the following order: actinomycetes (91.2%) < G⁺ bacteria (93.1%) < G⁻ bacteria (96.0%) < fungi (97.2%). This ordering was retained after mineral and mineral plus organic fertilization; however, the decline in abundance was not as prominent: NPK (86.6% [actinomycetes] to 94.4% [fungi]), NPK + ST (88.2 [actinomycetes] to 95.4% [fungi]), and NPK + OM (84.0 [actinomycetes] to 90.8% [fungi]) (Table II.3-S1, $P < 0.05$).

All types of fertilizers enhanced the abundance of bacteria more than that of fungi at a soil depth of 0–10 cm and significantly decreased the ratio of fungi to bacteria in relation to CK (7–15% decline compared to CK). Moreover, this ratio was significantly decreased from the soil depth of 0–10 cm to 10–20 cm except NPK+ST (Fig II.3-1a, $P < 0.05$). Both mineral and organic fertilizers significantly increased the ratio of G⁺ to G⁻ bacteria (24–44%, 23–56%, and 40–56% increase compared to CK for NPK, NPK+ST, and NPK+OM, respectively) in 0–10, 10–20, and 20–30 cm soil depths (Fig II.3-1b, $P < 0.05$). The ratio of G⁺ bacteria to actinomycetes exceeded 1.0 after fertilization at these soil depths (Fig II.3-1c, $P < 0.05$).

All specific microbial PLFAs were significantly affected by treatments, soil depths, and their combinations (Adonis analysis: all outputs were $P < 0.05$). However, the explanation rate (R^2) for soil depth exceeded 0.6, while that of fertilizer treatment (including combinations) was < 0.1 (Table II.3-S3). Redundancy analysis showed that soil organic C and pH significantly contributed to the structure of soil microbial communities, explaining 87% and 3.7% of the variance in the first two axes, respectively (Fig II.3-2a & Table II.3-S2, $P < 0.05$). In particular, soil pH was only significantly correlated with the microbial communities in the top soil (0–20 cm), explaining 4.9% of total variation (Fig II.3-2b, $P < 0.05$).

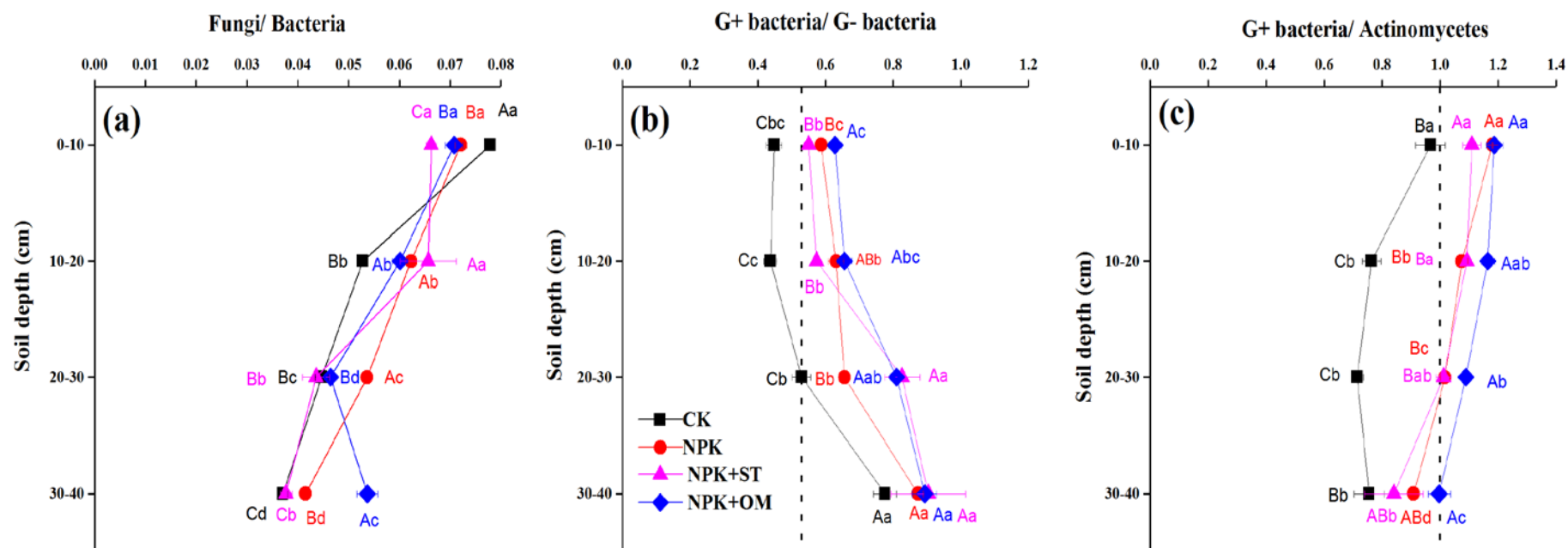


Figure II.3-1 Changes to the microbial community in paddy soil at different soil depths and under different fertilization regimes based on: (a) ratio of fungal to bacterial phospholipid fatty acids (PLFAs); (b) ratio of gram-positive (G+) to gram-negative (G-) bacterial PLFAs; and (c) ratio of gram-positive to actinomycete PLFAs (n=3).

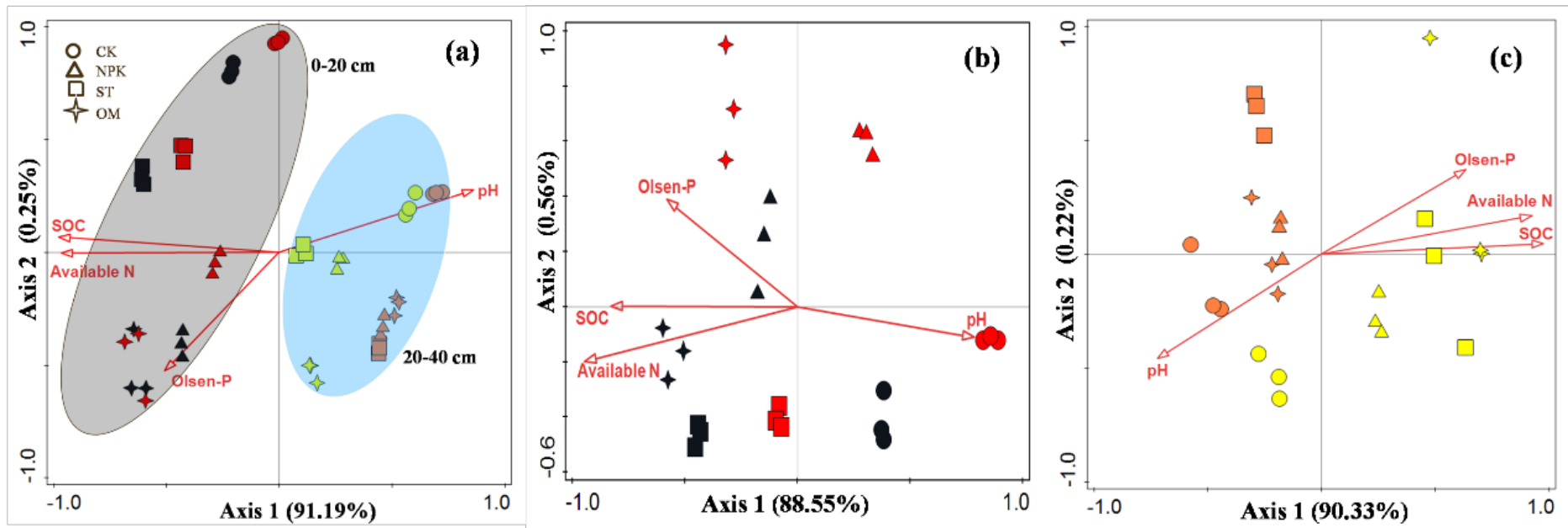


Figure II.3-2 Redundancy analysis of phospholipid fatty acid content from soil samples: (a) 0–40 cm, (b) 0–20 cm, and (c) 20–40 cm. SOC: soil organic carbon. Data for depths of 0–10 cm (black), 10–20 cm (red), 20–30 cm (yellow), and 30–40 cm (orange) are shown.

3. Discussion

3.1 Microbial abundance along the soil depth gradient

Compared with the decline in microbial biomass along the soil depth gradient, the effect of nutrient input by fertilization on microbial biomass was small, as indicated by the low explanation rates using Adonis analysis (Table II.3-S1 & S3). Many factors contribute towards the decline in microbial biomass with soil depth, including lower soil aeration (due to the “plough pan”), and lower substrate availability (Kögel-Knabner et al., 2010; Jones et al., 2018). The abundance and activity of fungi are considered low in paddy soils because of prolonged anaerobic conditions (Yao et al., 2012; Yuan et al., 2016). However, previous studies demonstrated that fungi could assimilate rhizodeposits in paddy soils (Ge et al., 2016; Wang et al., 2016) because fungal hyphae are directly connected to rice roots (Yuan et al., 2016; Huang et al., 2020; Shahbaz et al., 2021). In paddy soils, over 50% of the total root biomass is allocated in the first 5 cm of the surface soil (Li et al., 2004; Li and Yagi, 2004). Rice roots release oxygen through aerenchyma and benefit fungi by creating an aerobic environment in the rhizosphere. Our results showed that fungal PLFAs exhibited the highest decline (24–69%) between soil depths of 0–10 and 10–20 cm, except when NPK+ST was added (Table II.3-S1 & Fig II.3-1a, $P < 0.05$). This phenomenon was proximately attributed to soil aeration declining with depth. Consistent with our hypothesis 1, the G+ to G– bacteria ratio increased with soil depth (Fig II.3-1b, $P < 0.05$). G– bacteria preferentially use labile compounds such as rhizodeposits, whereas G+ bacteria can use recalcitrant compounds from SOM (Fanin et al., 2019). The decline in available C and N content along the soil depths might explain the faster decline in the abundance of G– bacteria compared to G+ bacteria because the growth of microorganisms is related to nutrient availability (Table II.3-S1) (Loeppmann et al., 2016; van Leeuwen et al., 2017). Actinomycetes are well known for their key role in degrading complex compounds (Acosta-Martínez et al., 2008), with their abundance showing the lowest decrease with increasing soil depth when compared to other groups.

The reduced influence of rice plants with increasing soil depth was clearly demonstrated by the different microbial compositions in the 0–20 and 20–40 cm soil layers (Fig II.3-2a). Rhizodeposits contain various organic acids, such as oxalic acid (Keiluweit et al., 2015) and acetate (John et al., 2003), which contribute towards lowering soil pH. In addition, N fertilizer causes soil acidification during N cycling (Zhou et al., 2013). Supporting these previous studies, we observed that pH was lower in the top soil and that it mainly corresponded to changes in the microbial community in the 0–20 cm soil layer (Fig II.3-2a & b, $P < 0.05$). In addition, higher available N content in parallel to lower soil pH was recorded in the fertilized treatments of our study, especially in the 0–30 cm soil layer (Table II.3-S2, $P < 0.05$).

3.2 Dependence of microbial community structure on fertilization strategies

All types of fertilizers more strongly promoted G+ bacteria in paddy soils over other microbes (Fig II.3-1b & c, $P < 0.05$). This finding supported those from previous studies showing that the G+ to G– bacteria ratio increases after mineral fertilization (Daquiado et al., 2016; Tang et al., 2018). However, some studies found no stronger promotion of

G+ bacteria by mineral fertilizers in paddy soils (Zhang et al., 2012; Dong et al., 2014). The stronger promotion of G+ bacteria has also been documented in other soil systems. For example, mineral N fertilizer increased the ratio of G+ to G- bacteria in forest soils after 120 days of incubation (Wang et al., 2014b). In two other studies, NPK fertilizer increased the relative abundance of G+ bacterial PLFAs in grasslands (Denef et al., 2009) and corn fields (Peacock et al., 2001). Thus, over the long term, G+ bacteria benefit the most from mineral fertilizer-derived nutrients in paddy soils. Contrary to our hypothesis, the partial replacement of mineral fertilizer with chicken manure increased the abundance of G+ bacteria more than that of G- bacteria at all evaluated soil depths. This phenomenon might be attributed to the important role of G+ bacteria in the turnover of organic N (Enggrob et al., 2020).

Straw replacement increased the abundance of G- bacteria in the 0–20 cm soil layer (Fig II.3-1b, $P > 0.05$). This might be because G- bacteria preferentially utilize labile organic C in straw (Peacock et al., 2001). Unexpectedly, straw promoted the abundance of fungal PLFAs in the 10–20 cm soil layer (Table II.3-S1). Straw is a substrate with a high C/N ratio, with fungi being the most important decomposers of straw (Li et al., 2020). Various studies have shown that fungi are key decomposers of cellulose, whereas glucose promotes the abundance of bacteria (Meidute et al., 2008; Wang et al., 2014). Straw clearly caused an increase in the abundance of fungi with straw decomposition appearing to occur in the 10–20 cm soil layer in our study, creating a suitable soil environment for microorganisms. This finding was supported by the lowest metabolic quotient for CO₂ ($q\text{CO}_2$) being recorded at this depth (Fig II.3-S1b, $P < 0.05$) (Anderson and Domsch, 2010). However, the results found here still have some limitations. We noted that the data in this study was collected from one sampling point in 2017, which may reduce the representativeness of the results. The soils were under anoxic or aerobic conditions at different rice growing stages, and it may cause variations of microbial abundances and also compositions. Further studies should include temporal dynamics of microbial compositions to better understand the mechanisms of microbial community changes under long-term fertilization in paddy fields. Moreover, the mechanisms of G+ to G- bacteria ratio change, and also the lowering $q\text{CO}_2$ by straw addition in paddy soils need further study.

4. Conclusions

Our field-based study confirmed that long-term mineral and organic fertilization regimes in paddy soils caused microbial biomass to increase horizontally (through fertilization) and prevented microbial biomass from decreasing vertically, especially under mineral and chicken manure fertilization. Both mineral and mineral plus organic fertilization promoted the abundance of G+ bacteria more than that of G- bacteria and actinomycetes at all depths. However, the abundance of G- bacteria dropped faster than that of G+ bacteria along the soil depth gradient. This result indicated that nutrient input by fertilization has a lower impact than soil depth on the abundance of microbes. Thus, fertilization, whether in mineral or organic form, strongly alters the structure of the microbial community through 0–40 cm soil layer. In conclusion, our results highlight the importance of soil depth and fertilization in structuring soil microbial communities.

Acknowledgments

We thank the Public Service Technology Center, Institute of Subtropical Agriculture, Chinese Academy of Sciences. This work was supported by the National Natural Science Foundation of China (41977093; 41877104), Natural Science Foundation of Hunan Province, China (2019JJ30028), the Youth Innovation Promotion Association of the Chinese Academy of Sciences (2019357), and Hunan Province Base for Scientific and Technological Innovation Cooperation (2018WK4012). We also thank Editage (www.editage.cn) for English language editing.

References

- Acosta-Martínez, V., Dowd, S., Sun, Y., Allen, V., 2008. Tag-encoded pyrosequencing analysis of bacterial diversity in a single soil type as affected by management and land use. *Soil Biology and Biochemistry* 40, 2762-2770.
- Anderson, T.H., Domsch, K.H., 2010. Soil microbial biomass: The eco-physiological approach. *Soil Biology and Biochemistry* 42, 2039-2043.
- Chen, D., Yuan, L., Liu, Y., Ji, J., Hou, H., 2017. Long-term application of manures plus chemical fertilizers sustained high rice yield and improved soil chemical and bacterial properties. *Eur. J. Agron.* 90, 34-42.
- Daquiado, A.R., Kuppusamy, S., Kim, S.Y., Kim, J.H., Yoon, Y.E., Kim, P.J., Oh, S.H., Kwak, Y.S., Lee, Y.B., 2016. Pyrosequencing analysis of bacterial community diversity in long-term fertilized paddy field soil. *Applied Soil Ecology* 108, 84-91.
- Denef, K., Roobroeck, D., Wadu, M.C.M., Lootens, P., Boeckx, P., 2009. Microbial community composition and rhizodeposit-carbon assimilation in differently managed temperate grassland soils. *Soil Biology and Biochemistry* 41, 144-153.
- Dong, W.Y., Zhang, X.Y., Dai, X.Q., Fu, X.L., Yang, F.T., Liu, X.Y., Sun, X.M., Wen, X.F., Schaeffer, S., 2014. Changes in soil microbial community composition in response to fertilization of paddy soils in subtropical China. *Applied Soil Ecology* 84, 140-147.
- Eilers, K.G., Debenport, S., Anderson, S., Fierer, N., 2012. Digging deeper to find unique microbial communities: The strong effect of depth on the structure of bacterial and archaeal communities in soil. *Soil Biology and Biochemistry* 50, 58-65.
- Enggrob, K.L., Larsen, T., Peixoto, L., Rasmussen, J., 2020. Gram-positive bacteria control the rapid anabolism of protein-sized soil organic nitrogen compounds questioning the present paradigm. *Sci Rep*, 10, 15840.
- Fanin, N., Kardol, P., Farrell, M., Nilsson, M.C., Gundale, M.J., Wardle, D.A., 2019. The ratio of Gram-positive to Gram-negative bacterial PLFA markers as an indicator of carbon availability in organic soils. *Soil Biology and Biochemistry* 128, 111-114.
- Ge, T., Li, B., Zhu, Z., Hu, Y., Yuan, H., Dorodnikov, M., Jones, D.L., Wu, J., Kuzyakov, Y., 2016. Rice rhizodeposition and its utilization by microbial groups depends on N fertilization. *Biol. Fertil. Soils* 53, 37-48.
- Huang, J., Liu, W., Deng, M., Wang, X., Wang, Z., Yang, L., Liu, L., 2020. Allocation and turnover of rhizodeposited carbon in different soil microbial groups. *Soil Biology and Biochemistry* 150.
- John, F., Martha, H., Davey, J., Steven, L., 2003. How roots control the flux of carbon to the rhizosphere. *Ecology* 84, 827-837.
- Jones, D.L., Magthab, E.A., Gleeson, D.B., Hill, P.W., Sánchez-Rodríguez, A.R., Roberts, P., Ge, T., Murphy, D.V., 2018. Microbial competition for nitrogen and carbon is as intense in the subsoil as in the topsoil. *Soil Biology and Biochemistry* 117, 72-82.
- Keiluweit, M., Bougoure, J.J., Nico, P.S., Pett-Ridge, J., Weber, P.K., Kleber, M., 2015. Mineral protection of soil carbon counteracted by root exudates. *Nature Climate Change* 5, 588-595.
- Kögel-Knabner, I., Amelung, W., Cao, Z., Fiedler, S., Frenzel, P., Jahn, R., Kalbitz, K., Kölbl, A., Schloter, M., 2010. Biogeochemistry of paddy soils. *Geoderma* 157, 1-14.

- Kramer, C., Gleixner, G., 2008. Soil organic matter in soil depth profiles: Distinct carbon preferences of microbial groups during carbon transformation. *Soil Biology and Biochemistry* 40, 425-433.
- Kramer, S., Marhan, S., Haslwimmer, H., Ruess, L., Kandeler, E., 2013. Temporal variation in surface and subsoil abundance and function of the soil microbial community in an arable soil. *Soil Biology and Biochemistry* 61, 76-85.
- Li, C., Mosier, A., Wassmann, R., Cai, Z., Zheng, X., Huang, Y., Tsuruta, H., Boonjawat, J., Lantin, R., 2004. Modeling greenhouse gas emissions from rice-based production systems: Sensitivity and upscaling. *Global Biogeochemical Cycles* 18.
- Li, X., Li, Z., Zhang, X., Xia, L., Zhang, W., Ma, Q., He, H., 2020. Disentangling immobilization of nitrate by fungi and bacteria in soil to plant residue amendment. *Geoderma* 374.
- Li, Z., Yagi, K., 2004. Rice root-derived carbon input and its effect on decomposition of old soil carbon pool under elevated CO₂. *Soil Biology and Biochemistry* 36, 1967-1973.
- Liu, Y., Ge, T., Ye, J., Liu, S., Shibistova, O., Wang, P., Wang, J., Li, Y., Guggenberger, G., Kuzyakov, Y., Wu, J., 2019. Initial utilization of rhizodeposits with rice growth in paddy soils: Rhizosphere and N fertilization effects. *Geoderma* 2019, 338: 30-39.
- Liu, C., Lu, M., Cui, J., Li, B., Fang, C.M., 2014. Effects of straw carbon input on carbon dynamics in agricultural soils: a meta-analysis. *Global Change Biology* 20, 1366-1381.
- Loeppmann, S., Blagodatskaya, E., Pausch, J., Kuzyakov, Y., 2016. Enzyme properties down the soil profile - A matter of substrate quality in rhizosphere and detritosphere. *Soil Biology and Biochemistry* 103, 274-283.
- Luo, Y., Lin, Q., Durenkamp, M., Kuzyakov, Y., 2017a. Does repeated biochar incorporation induce further soil priming effect? *J. Soils Sediments* 18, 128-135.
- Luo, Y., Lin, Q., Durenkamp, M., Dungait, A.J., Brookes, P.C., 2017b. Soil priming effects following substrates addition to biochar-treated soils after 431 days of pre-incubation. *Biology and Fertility of Soils* 53, 315-326.
- Meidute, S., Demoling, F., Bååth, E., 2008. Antagonistic and synergistic effects of fungal and bacterial growth in soil after adding different carbon and nitrogen sources. *Soil Biology and Biochemistry* 40, 2334-2343.
- Peacock, A.G., Mullen, M., Ringelberg, D., Tyler, D., Hedrick, D., Gale, P., White, D., 2001. Soil microbial community responses to dairy manure or ammonium nitrate applications. *Soil Biology and Biochemistry* 33, 1011-1019.
- Shahbaz, M., Thornton, B., Börjesson, G., 2021. Importance of fungi in a 63 years old long-term field experiment with 20 years of maize growth. *European Journal of Soil Science* 102.
- Tang, H.M., Xu, Y.L., Xiao, X.P., Li, C., Li, W.Y., Cheng, K.K., Pan, X.C., Sun, G., 2018. Impacts of long-term fertilization on the soil microbial communities in double-cropped paddy fields. *The Journal of Agricultural Science* 156, 857-864.
- van Leeuwen, J.P., Djukic, I., Bloem, J., Lehtinen, T., Hemerik, L., de Ruiter, P.C., Lair, G.J., 2017. Effects of land use on soil microbial biomass, activity and community structure at different soil depths in the Danube floodplain. *European Journal of Soil Science* 79, 14-20.
- Wang, J., Chapman, S.J., Yao, H., 2016. Incorporation of ¹³C-labelled rice

- rhizodeposition into soil microbial communities under different fertilizer applications. *Applied Soil Ecology* 101, 11-19.
- Wang, Q.K., Wang, S.L., He, T.X., Liu, L., Wu, J.B., 2014. Response of organic carbon mineralization and microbial community to leaf litter and nutrient additions in subtropical forest soils. *Soil Biology and Biochemistry* 71, 13-20.
- Wang, Y., Hu, N., Ge, T., Kuzyakov, Y., Wang, Z.L., Li, Z., Tang, Z., Chen, Y., Wu, C., Lou, Y., 2017. Soil aggregation regulates distributions of carbon, microbial community and enzyme activities after 23-year manure amendment. *Applied Soil Ecology* 111, 65-72.
- Wei, X., Zhu, Z., Liu, Y., Luo, Y., Deng, Y., Xu, X., Liu, S., Richter, A., Guggenberger, G., Wu, J., Ge, T., 2020. C:N:P stoichiometry regulates soil organic carbon mineralization and concomitant shifts in microbial community composition in paddy soil. *Biology and Fertility of Soils* 56, 1093-1107.
- Yan, D., Wang, D., Yang, L., 2007. Long-term effect of chemical fertilizer, straw, and manure on labile organic matter fractions in a paddy soil. *Biology and Fertility of Soils* 44, 93-101.
- Yao, H., Thornton, B., Paterson, E., 2012. Incorporation of ¹³C-labelled rice rhizodeposition carbon into soil microbial communities under different water status. *Soil Biology and Biochemistry* 53, 72-77.
- Yuan, H., Zhu, Z., Liu, S., Ge, T., Jing, H., Li, B., Liu, Q., Lynn, T.M., Wu, J., Kuzyakov, Y., 2016. Microbial utilization of rice root exudates: ¹³C labeling and PLFA composition. *Biology and Fertility of Soils* 52, 615-627.
- Zhang, J.G., Bo, G.D., Zhang, Z.F., Kong, F.Y., Wang, Y., Shen, G.M., 2016. Effects of straw incorporation on soil nutrients, enzymes, and aggregate stability in tobacco fields of China. *Sustainability*, 8.
- Zhang, Q., Wang, G., Yao, H., 2007. Phospholipid fatty acid patterns of microbial communities in paddy soil under different fertilizer treatments. *Journal of Environmental Sciences* 19, 55-59.
- Zhang, Q.C., Shamsi, I.H., Xu, D.T., Wang, G.H., Lin, X.Y., Jilani, G., Hussain, N., Chaudhry, A.N., 2012. Chemical fertilizer and organic manure inputs in soil exhibit a vice versa pattern of microbial community structure. *Applied Soil Ecology* 57, 1-8.
- Zhou, J., Xia, F., Liu, X., He, Y., Xu, J., Brookes, P.C., 2013. Effects of nitrogen fertilizer on the acidification of two typical acid soils in South China. *Journal of Soils Sediments* 14, 415-422.
- Zhu, Z., Ge, T., Hu, Y., Zhou, P., Wang, T., Shibistova, O., Guggenberger, G., Su, Y., Wu, J., 2017. Fate of rice shoot and root residues, rhizodeposits, and microbial assimilated carbon in paddy soil - part 2: turnover and microbial utilization. *Plant Soil*, 416, 243-257.

Supplementary methods

1.1 Site description and fertilization strategies

The long-term fertilization experiment was started in 1986 in Ningxiang, Hunan Province, China (111°54'–112°18'E, 28°07'–28°37'N). The mean annual temperature and rainfall at the site are 17 °C and 1681 mm, respectively. There were three crops in each year: Chinese *milk vetch* (*Astragalus sinicus* L.), early rice and late rice (*Oryza sativa* L.). Early and late rice was harvested in July and October, respectively. Milk vetch was sown in November and harvested in May of the following year. Four treatments were established: no fertilizer (CK), mineral fertilizer (NPK), rice straw combined with mineral fertilizer (NPK + ST), and 70% NPK + 30% chicken manure (NPK + OM). There were three replications for each treatment, and each plot size was 30 m². The experimental design ensured that uniform amounts of N, P, and K were applied in all fertilization treatments. The nutrients in the mineral fertilizer combined with those from rice straw residue and chicken manure added up to total amounts of 142.5 kg N ha⁻¹, 23.6 kg P ha⁻¹, and 52.3 kg K ha⁻¹ per fertilization treatment per year for the early rice season; and per fertilization treatment per year for the early rice season; and 157.5 kg N ha⁻¹, 18.9 kg P ha⁻¹, and 67.2 kg K ha⁻¹ for the late rice season. The total amount of fertilizer in each fertilization treatment during the milk vetch season was identical to that of the late rice season. Rice straw was returned at a rate of 2775 kg ha⁻¹ a⁻¹ and 3600 kg ha⁻¹ a⁻¹ for the early and late rice seasons, respectively. Decomposed chicken manure was applied at a rate of 2625 kg ha⁻¹ a⁻¹ and 2670 kg ha⁻¹ a⁻¹ for the early and late rice seasons, respectively. Before transplanting seedlings, air-dried rice residue was manually spread on the soil surface and incorporated into the soil at a cultivation depth of 20 cm. For early and late cropped rice, 40% and 30% of mineral N fertilizer, respectively, was applied at sowing, and the remaining N fertilizer was applied by top dressing (7–10 days after transplanting) during the crop growing period. All the P and K fertilizers were applied at sowing. The early rice variety, Xiangzaoxian 45, and late rice variety, Xiangwanxian 13, were used in 2016.

1.2 Soil sampling and chemical analysis

Soil samples were taken from four layers (depths of 0–10, 10–20, 20–30, and 30–40 cm) to assess vertical differences in microbial biomass and community composition under different long-term fertilization regimes. Five soil cores were taken from each plot and thoroughly mixed. The composite soil samples were immediately placed in a gas-permeable plastic bag and stored at 4 °C until analysis. A subset of soil samples was air-dried and passed through a 2-mm sieve to remove coarse plant debris and stones. The physical and chemical properties of the soil were then analyzed.

Microbial biomass carbon (MBC) and nitrogen (MBN) were extracted following the fumigation-extraction method (Brookes et al., 1985; Wu et al., 1990) and were analyzed for C and N using a total organic carbon analyzer (TOC-VWP; Shimadzu Corporation, Kyoto, Japan) and a flow-injection auto-analyzer (Tecator FIA Star 5000 Analyzer, Foss Tecator, Sweden), respectively. MBC and MBN were calculated based on differences in the concentrations of non-fumigated and fumigated samples divided by the extraction efficiency of 0.45 for C and 0.54 for N. Soil pH was determined with a pH meter (Delta 320; Mettler Toledo, Columbus, OH, USA) in a soil/water ratio of 1:2.5. Soil organic C content was determined using the dry combustion method in an elemental analyzer (VarioMAX C/N; Elementar, Langensfeld, Germany). Soil alkali-hydrolysable

nitrogen content (available N) was determined using alkali solution diffusion absorption. Olsen-P was extracted using $0.5 \text{ mol L}^{-1} \text{ NaHCO}_3$ (Olsen et al., 1954).

1.3 Extraction of phospholipid fatty acids (PLFA)

For PLFA extraction, 2 g freeze-dried (2-mm sieved) soil was extracted and derivatized to fatty acid methyl esters following the method of Bligh and Dyer (1959) and adapted by White et al. (1979). In brief, the soil was first extracted twice using 22.8 mL of a single-phase solution of chloroform:methanol:citrate buffer (1:2:0.8 v/v/v, 0.15 M, pH 4.0). The supernatant was transferred to test tubes and split into two phases by adding equal amounts of CHCl_3 and citrate buffer. Phospholipids were then separated from neutral lipids and glycolipids on a silica acid column (Supelco, Bellefonte, PA, USA). Methyl nonadecanoate fatty acid (19:0) was added before derivatization as an internal standard to determine the concentration of phospholipids. Following the methylation of phospholipids, PLFA methyl esters were separated and identified using a gas chromatograph (N6890; Agilent Technologies, Inc., Santa Clara, CA, USA) fitted with a MIDI Sherlock microbial identification system (version 4.5; MIDI, Inc., Newark, DE, USA). Individual PLFAs were quantified from the combined area of the peaks with mass-to-charge values (m/z 44, 45, and 46) relative to the internal standard added to each sample (Thornton et al., 2011). Iso- and anteiso-branched fatty acids (except for 10 Me-branched PLFAs) were used as indicators for G⁺ bacteria, while monounsaturated and cyclopropyl fatty acids were used as indicators for G⁻ bacteria (Wang et al., 2016; Ma et al., 2018). Ten Me-branched PLFAs were used as actinomycete biomarkers, while 18:2 ω 6c and arbuscular mycorrhizal fungi 16:1 ω 5c were used as fungal biomarkers. The sum of G⁺ bacteria, G⁻ bacteria, and actinomycetes was used to calculate the ratios of bacterial PLFAs.

1.4 Measurement of soil respiration

A subsample of air-dried soil was pre-incubated for 14 days at 25 °C under flooded conditions. For each measurement of the respiration rate, approximately 20 g (equivalent dry weight) of each soil sample was incubated in a 500-mL container at 25 °C for 24 h. Afterwards, CO_2 concentrations in the headspace were measured using an Agilent-7890a gas chromatograph equipped with a flame ionization detector (Agilent Technologies, Inc.). Soil respiration rates were calculated from the net accumulation of CO_2 over time. The soil metabolic quotient ($q\text{CO}_2$) was calculated by dividing the soil respiration rate by MBC content (Plaza et al., 2004).

1.5 Statistical analysis

Data were analyzed using one-way analysis of variance (ANOVA) for the four soil depths within each fertilization regime and for the different fertilization regimes within each soil depth. The data were compared using Duncan's test in SPSS 19.0 (SPSS Inc., Chicago, IL, USA). Significance was set at $P < 0.05$. To determine whether fertilization treatment and soil depth significantly influenced microbial composition, permutational multivariate analysis of variance was performed using the Adonis function implemented in the R statistical environment (v 3.5.2). The relationship between microbial composition and physicochemical properties was analyzed using redundancy analysis (RDA) in Canoco 5.0 for Windows (Microcomputer Power, Ithaca, NY, USA).

References

- Bligh, E.G., Dyer, W.J., 1959. A rapid method of total lipid extraction and purification. *Canadian Journal of Biochemistry and Physiology* 37, 911-917.
- Brookes, P.C., Landman, A., Pruden, G., Jenkinson, D.S., 1985. Chloroform fumigation and the release of soil nitrogen: a rapid direct extraction method to measure microbial biomass nitrogen in soil. *Soil Biology and Biochemistry* 17, 837-842.
- Ma, Q., Wu, L., Wang, J., Ma, J., Zheng, N., Hill, P.W., Chadwick, D.R., Jones, D.L., 2018. Fertilizer regime changes the competitive uptake of organic nitrogen by wheat and soil microorganisms: An in-situ uptake test using ^{13}C , ^{15}N labelling, and ^{13}C -PLFA analysis. *Soil Biology and Biochemistry* 125, 319-327.
- Olsen, S.R., Cole, C.V., Watanabe, F.S., Dean, L.A., 1954. Estimation of available phosphorus in soils by extraction with sodium bicarbonate. *US Department of Agriculture* 939, 1-19.
- Plaza, C., Hernandez, D., Garcia-Gil, J.C., Polo, A., 2004. Microbial activity in pig slurry-amended soils under semiarid conditions. *Soil Biology and Biochemistry* 36, 1577-1585.
- Thornton, B., Zhang, Z.L., Mayes, R.W., Hogberg, M.N., Midwood, A.J., 2011. Can gas chromatography combustion isotope ratio mass spectrometry be used to quantify organic compound abundance? *Rapid Commun. Mass Spectrom.* 25, 2433-2438.
- Wang, J., Chapman, S.J., Yao, H., 2016. Incorporation of ^{13}C -labelled rice rhizodeposition into soil microbial communities under different fertilizer applications. *Applied Soil Ecology* 101, 11-19.
- White, D.C., Davis, W.M., Nickels, J.S., King, J.D., Bobbie, R.J., 1979. Determination of the sedimentary microbial biomass by extractable lipid phosphate. *Oecologia*, 40, 51-62.
- Wu, J., Joergensen, R.G., Pommerening, B., Chaussod, R., Brookes, P.C., 1990. Measurement of soil microbial biomass C by fumigation extraction - an automated procedure. *Soil Biology and Biochemistry* 22, 1167-1169.

Table II.3-S1 Total phospholipid fatty acids (PLFAs) (mg C kg⁻¹) in paddy soil under fertilization regimes at different soil depths (mean ± SE, n=3). G⁻: Gram-negative bacteria; G⁺: Gram-positive bacteria.

Treatments	Soil depth (cm)	G ⁻	G ⁺	Actinomycetes	Fungi	General Fame	Total PLFA
CK	0–10	13.2±0.50Ca	5.92±0.47Ca	6.11±0.23Ca	1.96±0.10Ba	10.6±0.56Ca	39.4±1.84Ca
	10–20	5.81±0.15Db	2.54±0.26Db	3.33±0.10Db	0.62±0.01Cb	4.88±0.19Db	17.8±0.72Db
	20–30	1.50±0.08Cc	0.79±0.03Dc	1.11±0.01Cc	0.15±0.01Dc	1.62±0.06Cc	5.32±0.16Cc
	30–40	0.53±0.06Cd	0.41±0.07Cd	0.54±0.05Cd	0.05±0.01Cd	0.59±0.06Cd	2.20±0.25Cd
NPK	0–10	15.6±0.18Ba	9.16±0.12Ba	8.01±0.25Ba	2.35±0.03Ba	13.3±0.40Ba	50.1±0.87Ba
	10–20	9.63±0.19Cb	6.08±0.33Cb	5.66±0.20Cb	1.33±0.05Bb	8.43±0.30Cb	32.4±1.01Cb
	20–30	5.44±0.18Bc	3.57±0.10Cc	3.51±0.01Bc	0.67±0.01Bc	5.09±0.11Bc	19.0±0.47Bc
	30–40	1.12±0.03Bd	0.98±0.01Bd	1.07±0.01Bd	0.13±0.00Bd	1.27±0.04Bd	4.85±0.09Bd
NPK + ST	0–10	17.0±0.06Ba	9.36±0.25Ba	8.44±0.01Ba	2.31±0.02Ba	14.5±0.07Ba	52.8±1.46Ba
	10–20	15.3±0.41Bb	8.79±0.10Ba	8.05±0.13Ba	2.11±0.14Aa	13.9±0.12Ba	50.5±0.79Ba
	20–30	4.96±0.38Bc	4.08±0.27Bb	4.04±0.35Bb	0.57±0.04Cb	5.17±0.43Bb	19.5±1.41Bb
	30–40	0.93±0.12Bd	1.04±0.10Bc	1.00±0.12Bc	0.11±0.02Bc	1.04±0.10Bc	4.02±0.56Bc
NPK+ OM	0–10	19.3±0.90Aa	13.0±0.44Aa	10.2±0.56Aa	2.96±0.24Aa	17.1±1.11Aa	64.1±3.90Aa
	10–20	17.0±0.64Ab	11.1±0.37Aa	9.55±0.30Aa	2.26±0.03Ab	15.3±0.60Aa	57.5±1.90Aa
	20–30	6.89±0.22Ac	5.58±0.18Ab	5.14±0.20BAb	0.82±0.04Ac	6.71±0.27Ab	25.9±0.89Ab
	30–40	1.82±0.05Ad	1.63±0.10Ac	1.63±0.05Ac	0.27±0.01Ad	2.05±0.08Ac	7.65±0.30Ac

Table II.3-S2 Basic physicochemical properties of paddy soil under fertilization regimes at different soil depths (mean \pm SE, n=3). MBC, microbial biomass carbon; MBN, microbial biomass nitrogen; DOC, dissolved organic carbon.

Treatments		pH	Organic C (g kg ⁻¹)	MBC (mg kg ⁻¹)	MBN (mg kg ⁻¹)	Available N (mg kg ⁻¹)	Olsen-P (mg kg ⁻¹)
CK	0–10	7.2 \pm 0.01Ad	18.3 \pm 0.1Ca	740 \pm 33Ca	128 \pm 4ABa	151 \pm 2Da	6.6 \pm 0.6Ca
	10–20	7.4 \pm 0.02Ac	15.8 \pm 0.2Cb	351 \pm 19Db	44 \pm 6Db	108 \pm 1Cb	4.9 \pm 0.2Bb
	20–30	7.5 \pm 0.01Ab	6.48 \pm 0.1Dc	124 \pm 5Dc	16 \pm 3Cc	47 \pm 1Cc	5.6 \pm 0.4Cab
	30–40	7.6 \pm 0.02Aa	5.42 \pm 0.1Bd	59 \pm 2Cd	9 \pm 1Bc	45 \pm 1Bc	6.5 \pm 0.1Ca
NPK	0–10	6.5 \pm 0.01Dd	17.5 \pm 0.5Da	830 \pm 9Ba	100 \pm 7Ba	182 \pm 5Ca	11.4 \pm 0.6Ba
	10–20	6.8 \pm 0.01Cc	16.1 \pm 0.0Cb	527 \pm 5Cb	67 \pm 2Cb	129 \pm 1Bb	9.2 \pm 0.1Bb
	20–30	7.2 \pm 0.02Bb	9.40 \pm 0.1Cc	220 \pm 6Cc	64 \pm 10ABb	71 \pm 1Bc	6.8 \pm 0.8Cc
	30–40	7.3 \pm 0.02Ca	6.09 \pm 0.0Ad	82 \pm 7Bd	22 \pm 3ABc	43 \pm 1Bd	7.0 \pm 0.5BCc
NPK + ST	0–10	6.6 \pm 0.02Cd	22.0 \pm 0.1Ba	881 \pm 27Ba	140 \pm 21ABa	210 \pm 2Ba	10.4 \pm 0.5Bab
	10–20	6.8 \pm 0.01Cc	20.1 \pm 0.3Bb	808 \pm 30Bb	100 \pm 8Bb	185 \pm 1Ab	9.3 \pm 0.2Bbc
	20–30	7.1 \pm 0.01Db	11.9 \pm 0.1Bc	259 \pm 11Bc	45 \pm 5Bc	97 \pm 3Ac	11.0 \pm 0.9Ba
	30–40	7.2 \pm 0.02Da	6.1 \pm 0.1Ad	63 \pm 4BCd	13 \pm 2Bc	50 \pm 1Ad	8.0 \pm 0.1Bc
NPK + OM	0–10	6.7 \pm 0.02Bd	25.5 \pm 0.4Aa	1020 \pm 52Aa	155 \pm 10Aa	251 \pm 1Aa	111 \pm 6Aa
	10–20	6.9 \pm 0.01Bc	25.0 \pm 0.7Aa	869 \pm 22Ab	130 \pm 2Ab	193 \pm 7Ab	117 \pm 4Aa
	20–30	7.2 \pm 0.02Cb	12.1 \pm 0.0Ab	421 \pm 2Ac	82 \pm 7Ac	98 \pm 4Ac	57 \pm 2Ab
	30–40	7.3 \pm 0.02Ba	5.9 \pm 0.2Ac	165 \pm 2Ad	28 \pm 7Ad	42 \pm 2Bd	10 \pm 0.3Ac

Table II.3-S3 Adonis analysis of the effects of treatments and soil depths and their interaction on the specific microbial PLFAs (permutation=999).

	Treatments			Depth			Treatments*Depths		
	<i>F</i>	<i>R</i> ²	<i>P</i>	<i>F</i>	<i>R</i> ²	<i>P</i>	<i>F</i>	<i>R</i> ²	<i>P</i>
G- bacteria	4.564	0.033	0.025	86.7	0.624	0.001	3.70	0.027	0.027
G+ bacteria	9.190	0.071	0.003	68.8	0.535	0.001	6.63	0.052	0.010
Actinomycetes	7.482	0.051	0.006	89.1	0.612	0.001	4.99	0.034	0.014
Fungi	5.316	0.041	0.010	74.67	0.580	0.001	4.57	0.036	0.012

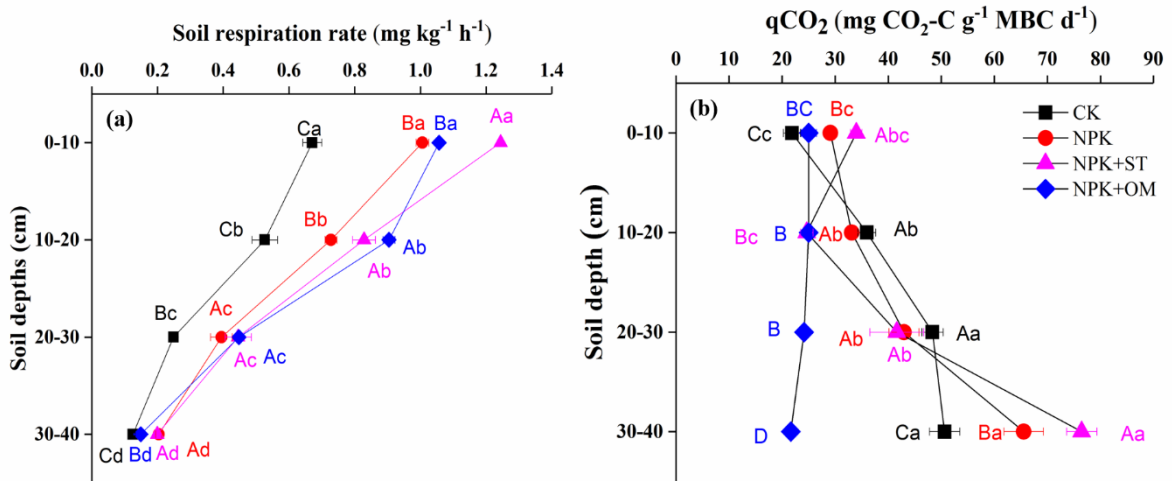


Figure II.3-S1 (a) Soil respiration rate and (b) soil metabolic quotient (qCO₂) in paddy soil under fertilization regimes at different soil depths (n=3).

II.4. Mineral bound organic carbon explains the negative priming effect in paddy soils

Qiong Liu ^{a,b,c,d}, Zhenke Zhu ^{a,b,c*}, Khatab Abdalla ^d, Tida Ge ^{a,b,c}, Jinshui Wu ^c, Haiming Tang ^e, Yakov Kuzyakov ^{f,g}, Johanna Pausch ^d

In preparation

^a State Key Laboratory for Managing Biotic and Chemical Threats to the Quality and Safety of Agro-products, Institute of Plant Virology, Ningbo University, Ningbo 315211, China

^b Key Laboratory of Biotechnology in Plant Protection of MARA and Zhejiang Province, Institute of Plant Virology, Ningbo University, Ningbo 315211, China

^c Key Laboratory of Agro-ecological Processes in Subtropical Region & Changsha Research Station for Agricultural and Environmental Monitoring, Institute of Subtropical Agriculture, Chinese Academy of Sciences, Hunan, 410125, China

^d Agroecology, Bayreuth Center of Ecology and Environmental Research, BayCEER, University of Bayreuth, Bayreuth, 95440, Germany

^e Hunan Soil and Fertilizer Institute, Changsha, China.

^f Department of Soil Science of Temperate Ecosystems, Department of Agricultural Soil Science, University of Goettingen, 37077 Goettingen, Germany

^g Peoples Friendship University of Russia (RUDN University), 117198 Moscow, Russia

* Corresponding Author

E-mail: zhuzhenke@isa.ac.cn

Abstract

While fertilization is critical to increase rice yields, it might alter soil organic matter (SOM) mineralization via priming effect (PE), a major mechanism affecting soil carbon (C) stocks. Here, we investigated PE and its consequences on soil C stocks after long-term fertilization (31 years) in paddy soils amended with mineral and/or organic fertilizers. Soil was collected in 10-cm increments to a depth of 40 cm and incubated for 60 days with ^{13}C -labeled glucose. Shortly after glucose addition, SOM-derived microbial biomass C (MBC) decreased at 0–10 cm in unfertilized and mineral-fertilized soils, and at 0–20, 0–30 cm in straw- and chicken manure-fertilized soils, respectively (apparent PE). Low PE and massive release of SOM-derived dissolved organic C (DOC) in topsoil during first 2 days is explained by mineral-bound organic C release. The released C was decomposed by microorganisms, which increased unlabeled CO_2 efflux and created a positive but low PE. However, after 20 days of incubation, the organic C concentration was reduced by rebinding or co-precipitating to mineral surfaces, which can explain the negative PE at later incubation phases commonly observed in paddy soils. Regardless of fertilizer type, glucose addition to the subsoils (30–40 cm) resulted in a net C loss (6.6–18.8 mg kg^{-1}) after 60 days due to higher PE intensity driven by high abundance of actinomycetes and Gram-positive bacteria. Our study demonstrated the complex mechanisms of C turnover in submerged paddy soils: 1) apparent PE, 2) biotic and/or abiotic release of mineral-bound organic C, 3) negative PE at later incubation phases due to organic C rebinding or co-precipitation to soil minerals. The last two mechanisms alter substrate availability to microorganisms and affect soil C stocks.

Keywords: Fertilization; manure; rice straw; priming effect; soil C; soil depth

1. Introduction

Mineral fertilizers and organic fertilizers such as straw and manure as well as their combinations are commonly applied to paddy soils for efficient and sustainable rice production (Mi *et al.*, 2018). Fertilizers also benefit crops and soil microorganisms by reducing competition with plants for nutrients (Kuzyakov and Xu, 2013). For example, in rice fields, mineral and organic fertilizers increase microbial biomass (Chen *et al.*, 2020) and the ratio of G+ to G- bacteria (Daquiado *et al.*, 2016) over the long term. The ratio of G+ to G- bacteria increases with soil depth due to decreasing nutrient accessibility (Liu *et al.*, 2022a).

Changes in microbial activity and community composition in response to fertilization can affect soil C stocks as microorganisms may accelerate or reduce soil organic matter (SOM) mineralization when fresh organic matter is added to soil (positive and negative priming effect (PE), respectively) (Kuzyakov *et al.*, 2000). Negative PE was explained by utilization of added substrates by soil microorganisms instead of SOM shortly after substrate addition (Blagodatskaya *et al.*, 2007). Positive PE was explained by nutrient mining and stoichiometric decomposition (Fontaine *et al.*, 2011; Chen *et al.*, 2014). In the former mechanism, organic C input creates higher demand for other nutrients such as N and increases SOM decomposition by producing enzymes that mobilize limiting nutrients from organic forms (Fontaine *et al.*, 2011; Wei *et al.*, 2020). In contrast, the latter mechanism suggests that balanced substrate addition or C/N ratios that approach microbial requirements can increase microbial activity and accelerate SOM decomposition (Chen *et al.*, 2014).

Priming effects dynamically change over time, because of alterations in substrate availability and succession of microbial community and functions (Blagodatskaya *et al.*, 2007). Organic C addition triggers microbial metabolism and causes "apparent priming" by short-term (days or weeks) pool substitution. However, in previous incubation studies with paddy soil no consistent short-term pattern of PE direction and intensity was observed after labile C (glucose) input (Cui *et al.*, 2020). For example, negative PE was reported shortly after glucose addition at a rate of 0.5 g kg⁻¹ (equivalent to ~250% MBC) (Wei *et al.*, 2020). While the same amount of acetate induced positive PE (~110% MBC) (Wei *et al.*, 2021).

Unlike apparent priming, the real priming (SOM decomposition) occurs when activated microorganisms deplete readily accessible substrates and secrete extracellular enzymes to mine nutrients (Blagodatskaya and Kuzyakov, 2008; Zhu *et al.*, 2021). Both real and apparent PE mechanisms have been commonly discussed in previous studies, with evidence of apparent priming being more theoretic. Few studies partitioned MBC and dissolved organic C (DOC) into SOM- and substrate-derived C sources as an indicator for pool substitution and hence, apparent priming due to microbial activity. Considering sources of MBC and DOC pools and of CO₂ fluxes would lead to a more comprehensive understanding of the mechanisms and dynamics of PE in rice fields under different management, where microbial community shifts due to long-term fertilization. We incubated soils collected from a long-term field experiment with organic and mineral fertilizer application. Soil samples were collected from four depths and incubated with or without ¹³C-labeled glucose to mimic readily accessible C inputs to paddy fields.

We hypothesized that long-term mineral fertilization reduces PE compared to soils

without fertilizer input as soil microorganisms do not need to mine SOM for nutrients. Accordingly, PE is assumed to increase if both mineral plus organic fertilizers are added (higher C/N ratios due to organic C input) due to the increasing demand for nutrients derived from SOM (nutrient mining mechanism). Consequently, we also hypothesized that lower nutrient availability in subsoil (20–40 cm) result in higher PE than in topsoil (0–20 cm), however, with apparent PE being more pronounced in topsoil due to larger microbial biomass and higher activity.

2. Materials and methods

2.1 Soil sampling and incubation

Paddy soil was collected from 0–10, 10–20, 20–30, and 30–40 cm depth in 2017 from long-term experimental fertilization trials established in 1986 at Ningxiang, Hunan Province, China (111°54'–112°18'E; 28°07'–28°37'N). There were three crops in each year: Chinese milk vetch (*Astragalus sinicus* L.), early rice and late rice (*Oryza sativa* L.). The fertilization regimes were: no fertilizers (CK; control soil without C or nutrient addition); mineral fertilizers (NPK; urea, superphosphate, and potassium chloride); rice straw combined with mineral fertilizers (NPK+ST); and 70% NPK+30% chicken manure (NPK+OM). The fertilization experiments were performed in triplicate and a complete randomized experimental design was used. The design ensured that uniform N, P, and K levels were applied across all fertilized plots. The nutrients in the mineral fertilizer combined with those from rice straw residue and chicken manure added up to total amounts of 142.5 kg N ha⁻¹, 23.6 kg P ha⁻¹, and 52.3 kg K ha⁻¹ per fertilization treatment per year for the early rice season; and per fertilization treatment per year for the early rice season; and 157.5 kg N ha⁻¹, 18.9 kg P ha⁻¹, and 67.2 kg K ha⁻¹ for the late rice season. The total amount of fertilizer in each fertilized soil during the milk vetch season was identical to that of the late rice season. Further details of the experimental design is described in (Liu *et al.*, 2022a). Five soil cores were taken per plot and thoroughly mixed, air-dried, and passed through a 2-mm sieve to remove coarse plant debris and stones. The main soil properties are listed in Table II.4-S1.

Prior to the experiment, the air-dried soils were re-flooded and pre-incubated in the dark at 25 °C for 10 d to avoid a respiration flush due to disturbances. For gas sampling, the pre-incubated soil (each equivalent to 20 g dry weight) was then placed in 500-mL glass serum bottles. Three replicates per soil depth were established: CK soil with or without glucose addition (CK+Glu and CK); NPK soil with or without glucose addition (NPK+Glu and NPK); NPK+ST soil with or without glucose addition (ST+Glu and ST); and NPK+OM soil with or without glucose addition (OM+Glu and OM). Thus, there were 96 incubation bottles in total (four soils × four depths × two glucose levels × 3 replicates). Then ¹³C-labeled glucose (3 atom% ¹³C; Cambridge Isotope Laboratories, Tewksbury, MA, USA) was uniformly added to each bottle at a rate of 100% MBC (Table II.4-S1), thus glucose addition was higher in soils with higher MBC. Deionized water was added to maintain the soil:water ratio at 2:1 and to ensure flooded conditions. The bottles were sealed with butyl rubber stoppers and incubated in the dark at 25 °C for 60 d. For destructive soil sampling, 150 g soil for each fertilization regime and depth with or without glucose addition were placed in 500-mL glass serum bottles and treated as described above. To consider natural C isotope fractionation due to glucose addition throughout the 60-d incubation period, each soil was additionally prepared with

unlabeled glucose for ^{13}C natural abundance measurements.

2.2 Gas and soil sampling

Headspace gas samples (~35 mL) were collected by syringe into pre-evacuated Exetainer glass bottles (Labco, High Wycombe, UK) on days 1, 2, 4, 6, 8, 11, 14, 17, 20, 25, 30, 35, 40, 50, and 60. At each sampling point, the bottles were ventilated and re-sealed with butyl rubber stoppers.

At days 2, 20, and 60, the soil was destructively sampled. The supernatant above the soil surface was poured out, filtered and the dissolved organic carbon (DOC) was measured. Then a portion of the homogenized soil was separated to measure the soil water content, the DOC, and MBC. The remaining soil was air-dried and passed through a 0.15-mm sieve to estimate the amount of ^{13}C in soil organic C.

2.3 Gas and soil analyses

The CO_2 concentrations were measured with an Agilent 7890A gas chromatograph (Agilent Technologies, Palo Alto, CA, USA) fitted with a thermal conductivity detector. The $\delta^{13}\text{C}$ isotope signature of the CO_2 was analyzed with an isotope mass spectrometer (MAT253, Waltham, MA, USA).

Soil organic C was determined with an elemental analyzer (Vario MAX C/N; Langensfeld, Germany). The soil DOC was extracted with 0.05 M K_2SO_4 and measured with a total organic C (TOC) analyzer (TOC-VWP; Kyoto, Japan). The DOC in the supernatant was measured with the same TOC analyzer. The MBC was extracted according to the fumigation-extraction method and calculated from the differences in DOC concentration between the unfumigated and fumigated samples divided by the extraction efficiency (0.45) (Wu *et al.*, 1990). The stable C isotope compositions of the soil organic C and freeze-dried DOC samples were measured with a MAT253 fitted with an elemental analyzer (FLASH 2000; Cambridge UK). The Fe(II) content in the soil and supernatant samples were measured with 0.5 M HCl and the 1,10-phenanthroline colorimetric assay in a UV-visible spectrophotometer (UV-2600; Hongkong, China) (Fadrus and Malý, 1975).

The following equation was used to determine the atom% ^{13}C values of the total MBC (atom% $^{13}\text{C}_{\text{MB}}$):

$$\text{atom\% } ^{13}\text{C}_{\text{MB}} = (C_{\text{F}} * \text{atom\% } ^{13}\text{C}_{\text{F}} - C_{\text{uF}} * \text{atom\% } ^{13}\text{C}_{\text{uF}}) / (C_{\text{F}} - C_{\text{uF}}) \quad (1)$$

where C_{F} and C_{uF} are the total amounts of DOC-C (mg kg^{-1}) in the fumigated and nonfumigated samples, respectively, and atom% $^{13}\text{C}_{\text{F}}$ and atom% $^{13}\text{C}_{\text{uF}}$ are the atom% ^{13}C values of the fumigated and nonfumigated samples, respectively.

The fractions of SOM-derived C (X_{SOM} ; X including CO_2 , DOC, MBC, and soil organic C) and glucose-derived C (X_{glu}) were calculated using a two-pool C isotope-mixing model (Bonde *et al.*, 1992; Cheng, 1996):

$$X_{\text{glu}} = (\text{atom\% } ^{13}\text{C}_{\text{total}} - \text{atom\% } ^{13}\text{C}_{\text{UL}}) / (\text{atom\% } ^{13}\text{C}_{\text{glu}} - \text{atom\% } ^{13}\text{C}_{\text{UL}}) \times X_{\text{total}} \quad (2)$$

where $\text{atom}\% \text{ }^{13}\text{C}_{\text{total}}$ and $\text{atom}\% \text{ }^{13}\text{C}_{\text{UL}}$ are the $\text{atom}\% \text{ }^{13}\text{C}$ values of X derived from labeled glucose-treated and unlabeled glucose-treated soils, respectively, $\text{atom}\% \text{ }^{13}\text{C}_{\text{glu}}$ is the $\text{atom}\% \text{ }^{13}\text{C}$ value of the added labeled glucose, and X_{total} is the total X derived from the glucose-treated soils.

Total X_{SOM} was calculated as follows:

$$X_{\text{SOM}} = X_{\text{total}} - X_{\text{glu}} \quad (3)$$

Percentage PE was calculated as follows:

$$\text{PE} = (X_{\text{SOM,glu}} - X_{\text{SOM,ref}}) \quad (4)$$

$$\text{Percentage PE}_X = \text{PE} / X_{\text{SOM,ref}} \times 100 \quad (5)$$

where $X_{\text{SOM,glu}}$ is the total amount of C (in CO_2 or MBC) derived from SOM mineralization in the glucose-added treatment, and $X_{\text{SOM,ref}}$ is the total amount of C derived from SOM mineralization in the soil without glucose addition.

The relative MBC change was calculated as follows:

$$\text{Relative MBC change} = (\text{MBC}_{\text{glu}} - \text{MBC}_{\text{ref}}) / \text{MBC}_{\text{ref}} \times 100 \quad (6)$$

where MBC_{glu} and MBC_{ref} are the microbial biomass C in the glucose-treated and untreated control soil, respectively.

2.4 Statistical evaluation

One-way ANOVA was used for statistical significance between soil depths within each fertilization regime, and in fertilization regimes within each soil depth, respectively. All the data was compared by Duncan's multiple range test and statistical significance was defined at $p < 0.05$. Two-way ANOVA was used to determine whether fertilization and soil depth significantly influenced glucose-derived CO_2 efflux, total Fe(II) content, or percentage primed MBC. All statistical analyses were conducted in SPSS v. 19.0 (SPSS Inc., Chicago, IL, USA).

3. Results

3.1. CO_2 efflux

In soils with glucose addition, glucose-derived CO_2 efflux initially peaked on day 1 or day 2, rapidly declined until day 11, and slowly decreased thereafter (Fig II.4-1 and S3). By day 20, the mineralization rate of the added glucose was $< 0.7\%$ of total glucose addition per day (Table II.4-S2). By day 60, the mineralization rate of the added glucose was $< 0.15\%$ and accounted for 1.4–11% of the total CO_2 efflux.

3.2. Dynamics of PE based on CO_2

Two distinct periods of PE_{CO_2} were observed across all soils and depths. 1) A positive PE_{CO_2} was detected during the first 6 d and peaked on day 1 or day 2 except at 30–40 cm depth in OM+Glu; 2) Weaker and negative PE_{CO_2} were measured for the later

incubation phases (Fig. II.4-2).

In CK+Glu soil and at all depths, the maximum PE_{CO_2} was 95–107% of the control soil without glucose addition within the first day. Continuously negative PE_{CO_2} were observed at 10–20 cm and 30–40 cm from days 23 to 60 (Fig. II.4-2a). In NPK+Glu and ST+Glu soils, the PE_{CO_2} were generally lower in the topsoil than the subsoil. At the later incubation phase from day 17 to 60, the 0–10 cm and 10–20 cm soil depths showed negative PE_{CO_2} for both soils (Figs. II.4-2b and 2c). The 30–40-cm depth in ST+GLU soil showed a negative PE_{CO_2} after day 8. In OM+GLU soil, negative PE_{CO_2} were observed at days 14, 20, and 23 for 0–10 cm, 10–20 cm, and 20–30 cm soil depths, respectively, until the end of incubation. However, the PE_{CO_2} at 30–40 cm soil depth was positive from the onset of incubation until day 60 (Fig. II.4-2d).

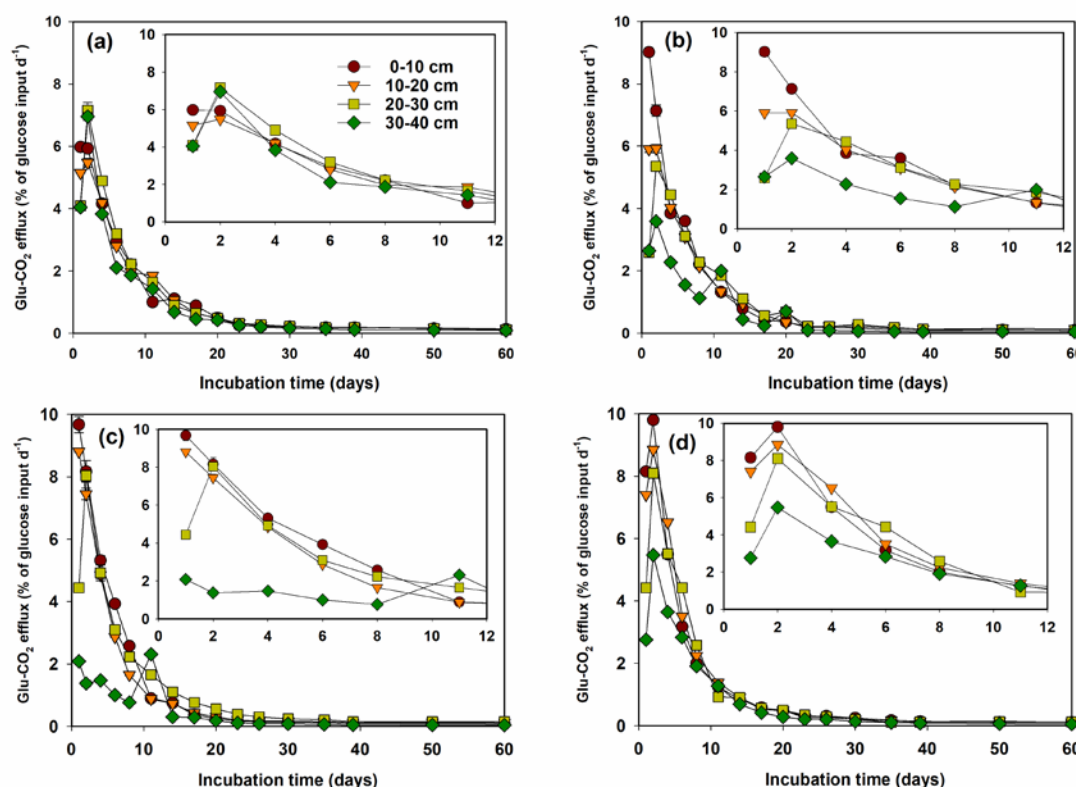


Figure II.4-1 Glucose-derived CO_2 efflux (% of total glucose input per day) in 60-days incubated paddy soil (a) CK+Glu; (b) NPK+Glu; (c) ST+Glu; (d) OM+Glu under long-term fertilization regimes at different soil depths (mean \pm SE, $n=3$). Statistical analysis was presented in supplementary Table II.4-S2.

3.3. Dynamics of DOC, Fe (II) content, and PE based on MBC

Glucose addition increased SOM-derived DOC in all soils and depths by day 2, especially at 0–20 cm (Fig. II.4-3a). At day 2, 10–48% of glucose-derived C remained in the soil and supernatant in the form of DOC. While 8–35% of the glucose-derived C was rapidly detected in the MBC pool except 30–40 cm depth in the OM+Glu soil. Simultaneously, glucose addition increased total MBC by 4–36% compared to that in respective control soil (Fig. II.4-3d).

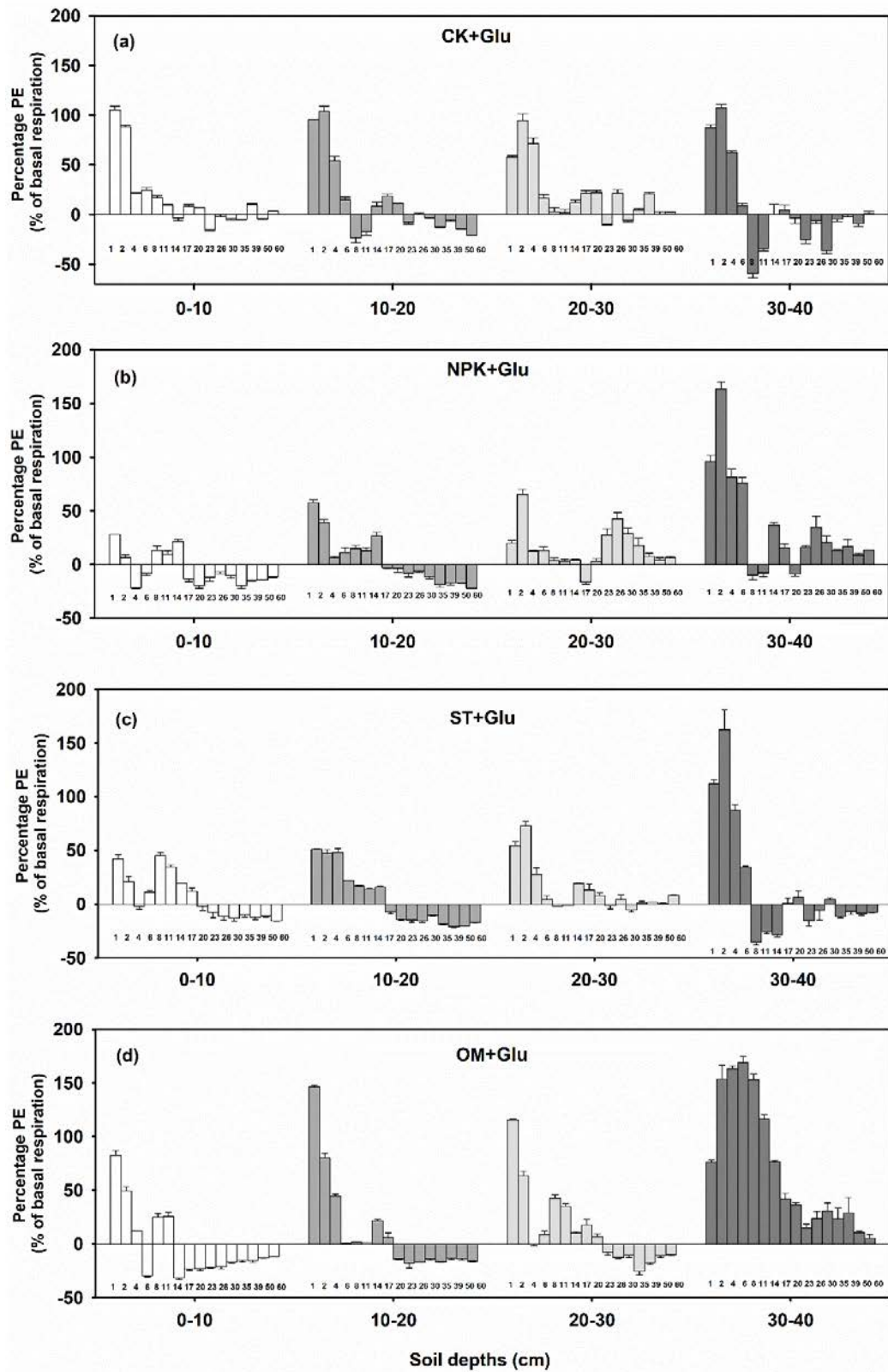


Figure II.4-2 Percentage priming effect (% of basal respiration per day) in 60-days incubated paddy soil under long-term fertilization regimes at different soil depths (mean \pm SE, n=3). Numbers under each bar represented the days after incubation.

PE_{MBC} was negative at 0–10 cm in CK+Glu and NPK+Glu but strongly positive at 10–40 cm soil depth (Fig. II.4-4a). ST+GLU and OM+GLU soils had negative PE_{MBC} in deeper soil depths (0–20 cm and 0–30 cm, respectively). Overall, the PE_{MBC} intensity was positively correlated with total MBC change (Fig. II.4-4b; $P < 0.001$). Glucose addition increased the soil Fe(II) content in the fertilized soils, especially at 0–20 cm soil depth (Fig. II.4-5a).

After 20 d incubation, most of the glucose was consumed and $< 1.3\%$ of the added glucose-derived C was detectable in the DOC pool (Fig. II.4-3b). The total DOC and SOM-derived DOC concentrations decreased from day 2 to day 20. C retention surpassed C loss for all soils and at all depths except ST+GLU at 30–40 cm (Fig. II.4-S4a). The Fe(II) content increased in the control soils but was stable in the glucose-treated soils (Fig. II.4-5b).

At the end of incubation (day 60), 7–46% of the added glucose-derived C was immobilized in the soil (Fig. II.4-S4b). However, C loss through PE_{CO_2} was relatively greater in the subsoil especially at 30–40 cm in fertilized soils. In the glucose-treated soils, the soil Fe(II) content was generally lower than that of the control, especially at 0–20 cm (Fig. II.4-5c).

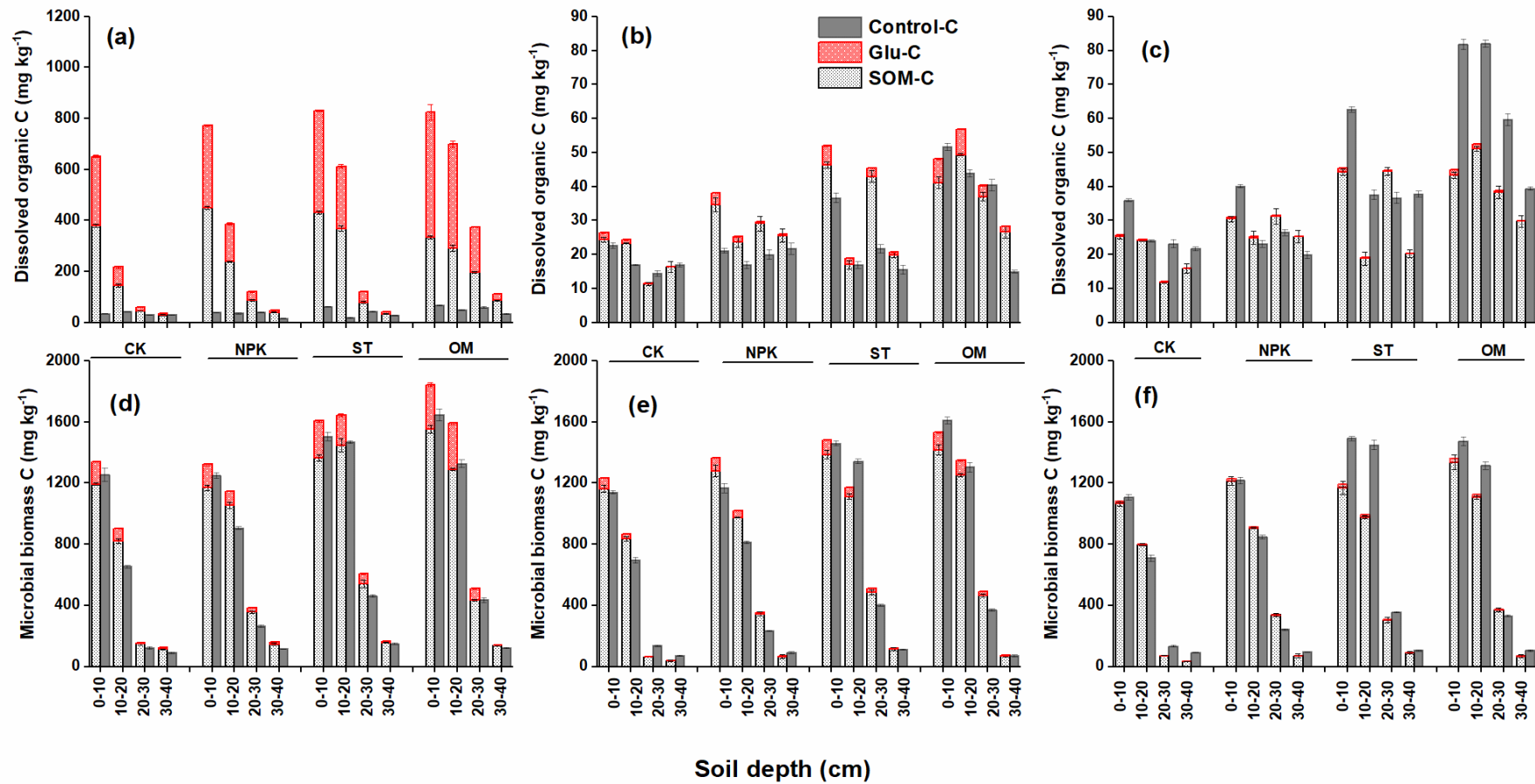


Figure II.4-3 Absolute amount of DOC and MBC derived from soil organic matter (SOM-C) and glucose (Glu-C) (mg kg^{-1}) at day 2 (a, d), day 20 (b, e) and day 60 (c, f) in incubated paddy soil under long-term fertilization regimes at different soil depths (mean \pm SE, $n=3$). Control-C represent the DOC, and MBC contents in the incubated soil without glucose addition at the same sampling day.

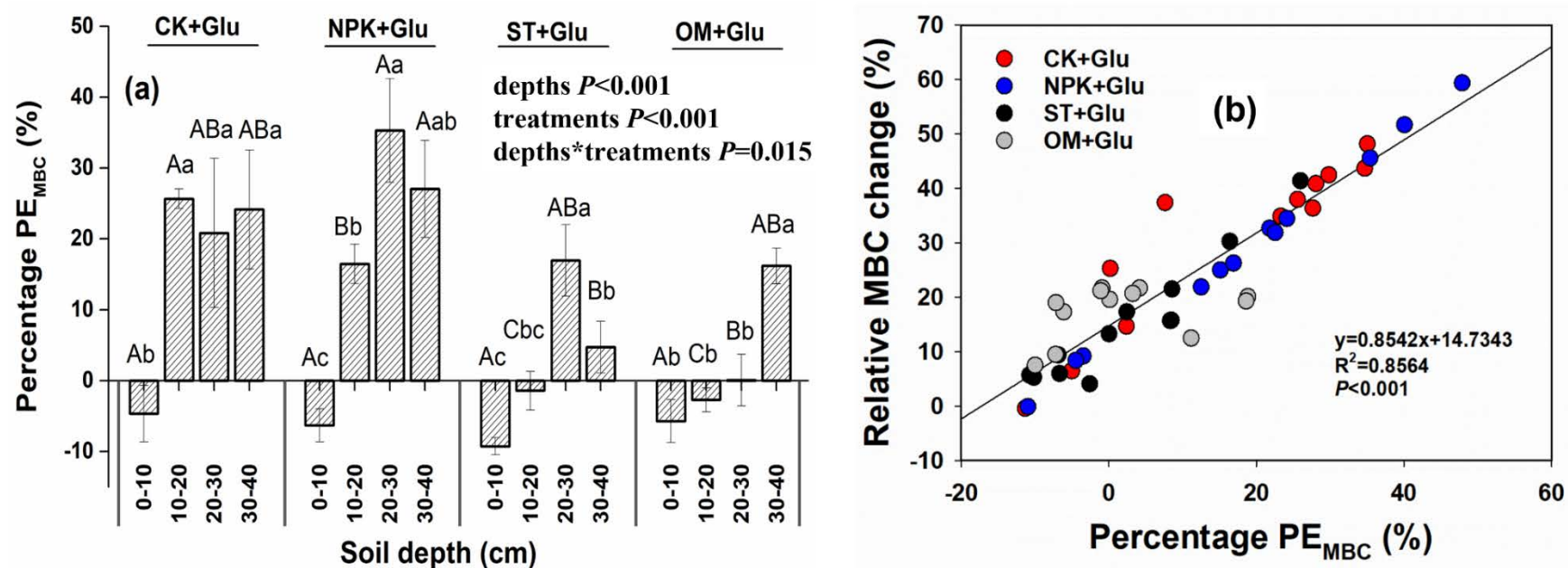


Figure II.4-4 Percentage primed MBC (a, Percentage PE_{MBC}) and the relationship between Percentage PE_{MBC} and glucose-induced MBC change (b) at day 2 in incubated paddy soil under long-term fertilization regimes at different soil depths (mean \pm SE, $n=3$). Lower-case letters represent significant differences between soil depths within the same fertilization regime. Uppercase letters represent significant differences between fertilization regimes within the same soil depth.

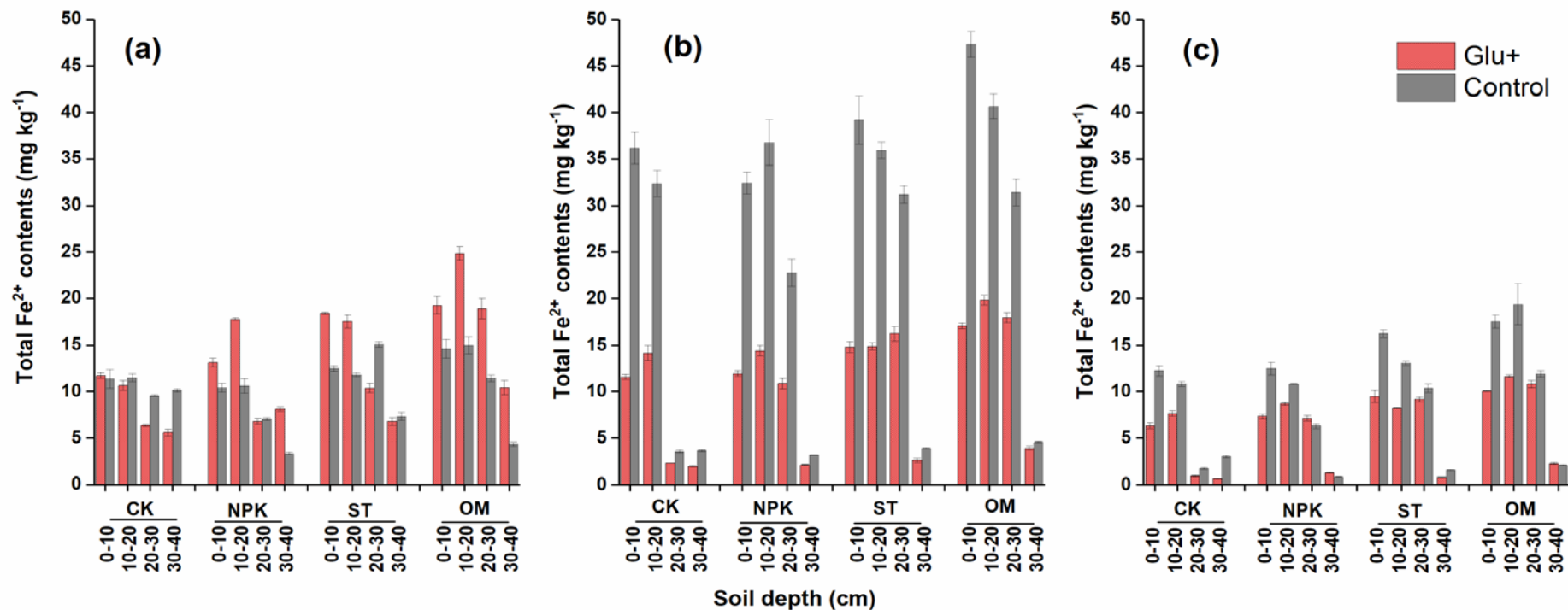


Figure II.4-5 total Fe (II) contents (mg kg⁻¹) at sampling time day 2 (a), day 20 (b), and day 60 (c) in 60-days incubated paddy soil with (Glu+) and without (Control) glucose addition under long-term fertilization regimes at different soil depths (mean ± SE, n=3).

4. Discussion

4.1. Apparent vs. real PE mechanisms shortly after glucose addition

The observed dynamics of the priming effects in paddy soils comprehensively illustrated microbial responses to substrate addition after long-term fertilization. Three microbial process groups may simultaneously occur after glucose addition: 1) Respiration increases with microbial activity causing microbial biomass ^{12}C loss ($^{12}\text{MBC}\downarrow$), 2) The added ^{13}C from glucose is incorporated into microbial biomass and substitutes ^{12}C ($^{13}\text{MBC}\uparrow$ and $^{12}\text{MBC}\downarrow$), 3) More SOM is utilized for biomass formation ($^{12}\text{MBC}\uparrow$). The ^{12}MBC that is lost through respiration could contribute to $^{12}\text{CO}_2$ efflux (positive PE_{CO_2}) indicating apparent priming (Fontaine *et al.*, 2004; Hamer and Marschner, 2005). ^{12}MBC loss (negative PE_{MBC}) was mainly observed at 0-10 cm soil depth at day 2 indicating that the induction of apparent PE was closely related to C input, i.e. rhizodeposition and/or organic fertilizers (Fig. 4a). Soon after adding glucose to the upper soil depths that are not C-deficient, the activated microorganisms renewed their old biomass ^{12}C with added labile ^{13}C resulting in slow microbial biomass growth. By contrast, microorganisms in subsoils directly utilized both SOM-derived and glucose-derived C for their growth and increased the biomass (Figs. 3d & 4b).

4.2. Nutrient mining vs. stoichiometric decomposition

The maximum CO_2 efflux observed on day 1 or day 2 coincided with highest soil PE_{CO_2} (Figs. 1 and 2). This phenomenon was consistent with previous studies as glucose was rapidly mineralized by soil microorganisms (Hamer and Marschner, 2005; Gunina and Kuz'yakov, 2015; Wei *et al.*, 2021). In line with our hypotheses, PE_{CO_2} was weaker at high nutrient conditions (mineral fertilizers), and extra C input through straw and manure amendment increased PE_{CO_2} intensity in the upper 30 cm (Fig. 2). These findings confirmed our hypothesis that microbial activities were higher in low-nutrient soils due to nutrient mining mechanism (Phillips *et al.*, 2011). Moreover, PE_{CO_2} was higher in deeper soil depths (20-40 cm) compared to topsoil (0-20 cm) due to lower nutrient availability and higher abundances of actinomycetes and G+ bacteria which can decompose recalcitrant C (Xu *et al.*, 2015; Fanin *et al.*, 2019; Liu *et al.*, 2022a).

Interestingly, SOM-derived DOC relative to the control, i.e., primed DOC, was much higher in topsoil than in subsoil (Fig 3a & Table S2). However, a higher PE_{CO_2} in subsoil should also have caused a higher release of SOM-derived DOC relative to the control. This discrepancy, i.e., a much higher SOM-derived DOC in topsoil was also reported in other paddy soils (Cui *et al.*, 2020; Li *et al.*, 2020; Wei *et al.*, 2020). Moreover, from day 2 to day 20, a strong decline in SOM-derived DOC was observed (Fig 3a-b). This decline should result in higher SOM-derived MBC and/or CO_2 . However, SOM-derived MBC declined from day 2 to day 20 together with weak PE_{CO_2} (Fig. 3e and Table S5). Overall, nutrient mining well explained the trend of PE_{CO_2} but it cannot explain the SOM-derived DOC change over the incubation time (Fig. 3a).

4.3. Possible mechanisms for organic matter priming

We propose that biotic and/or abiotic desorption of mineral-bound organic C is a key mechanism explaining the SOM-derived DOC increase at day 2. In paddy soils, there are many ways of organic C release as microorganisms utilize glucose. First, microbial Fe reduction under anaerobic condition can release organic C after desorption from Fe

oxides (Rasmussen *et al.*, 2006; Dong *et al.*, 2017; Jeewani *et al.*, 2020; Liu *et al.*, 2022b). Strong correlations between microbial Fe reduction and C release were demonstrated using synthetic ferrihydrite- organic C compounds (Wordofa *et al.*, 2019; Wei *et al.*, 2022). Second, adding organic C to sterilized soil increased extractable Fe and Al (Jilling *et al.*, 2021). Thus, organic C addition can also disrupt mineral-organic associations abiotically (Keiluweit *et al.*, 2015). Also, anionic intermediates such as formate and acetate with higher sorption capacity on Fe oxides may displace the C that was originally absorbed (Adhikari *et al.*, 2019; He *et al.*, 2020). After glucose addition, those SOM-derived organic C appeared to be the direct source for positive PE_{CO_2} rather than C released from SOM decomposition by stimulating microbial activity (Figs. 2 and 3a).

4.4. Negative priming at later incubation stage

In paddy soils at 0–20 cm depth, glucose and acetate induced negative PE_{CO_2} at the later incubation phases (Qiu *et al.*, 2017; Cui *et al.*, 2020; Li *et al.*, 2020; Wei *et al.*, 2020; Wei *et al.*, 2021). This phenomenon could not be explained by preferential substrate utilization as glucose is thoroughly exhausted after first few days (Gunina and Kuzyakov, 2015; Zhang *et al.*, 2015). We propose that organic C resorption accounts for negative PE_{CO_2} commonly observed in paddy soils: organic C may rebind or co-precipitate with iron oxides or other newly formed minerals such as FeS (Ayotade, 1977; Maguffin *et al.*, 2020) thus reducing Fe(II) and SOM-derived DOC contents (Figs. 5b and 5c). The rebound or co-precipitated organic C is inaccessible for microorganisms and result in negative PE_{CO_2} . In a similar study, paddy soil with ferrihydrite and goethite addition showed stronger negative PE_{CO_2} than C addition alone (Li *et al.*, 2020).

5. Conclusions

The present study demonstrated the impact of long-term fertilization on microbial responses to labile glucose addition to paddy soils. In soils that are not C-deficient (with frequent C input through rhizodeposition and organic fertilization), microorganisms renew their C shortly after glucose addition rather than investing in growth (apparent PE). At this early stage, a massive release of SOM-derived C biotically and/or abiotically in topsoil (0-20 cm) serves as a direct source for the low but positive PE_{CO_2} rather than by stimulating microbial activity and producing extracellular enzymes. Topsoil showed negative PEs at later incubation phases because of the resorption of organic C to soil minerals which reduce substrate availability to microorganisms; whereas subsoils (30-40 cm) had net C loss due to higher abundances of actinomycetes and Gram-positive bacteria decomposing SOM to obtain organically bound nutrients.

Acknowledgments

This study was financially supported by the National Natural Science Foundation of China (Nos. 42177334, 41977093 and 42141006), by the K. C. Wong Magna Fund of Ningbo University and the RUDN University Strategic Academic Leadership Program. Financial support to Qiong Liu was granted by the China Scholarship Council (CSC).

References

- Adhikari, D., Dunham-Cheatham, S.M., Wordofa, D.N., Verburg, P., Poulson, S.R., Yang, Y., 2019. Aerobic respiration of mineral-bound organic carbon in a soil. *Science of The Total Environment* 651, 1253-1260.
- Ayotade, K.A., 1977. Kinetics and reactions of hydrogen sulphide in solution of flooded rice soils. *Plant and Soil* 46, 381–389.
- Blagodatskaya, E.V., Blagodatsky, S.A., Anderson, T.H., Kuzyakov, Y., 2007. Priming effects in Chernozem induced by glucose and N in relation to microbial growth strategies. *Applied Soil Ecology* 37, 95-105.
- Blagodatskaya, E., Kuzyakov, Y., 2008. Mechanisms of real and apparent priming effects and their dependence on soil microbial biomass and community structure: critical review. *Biol Fert Soils* 45, 115-131.
- Bonde, T.A., Christensen, B.T., Cerri, C.C., 1992. Dynamics of soil organic matter as reflected by natural ¹³C abundance in particle size fractions of forested and cultivated oxisols. *Soil Biology and Biochemistry* 24, 275-277.
- Chen, R., Senbayram, M., Blagodatsky, S., Myachina, O., Dittert, K., Lin, X., Blagodatskaya, E., Kuzyakov, Y., 2014. Soil C and N availability determine the priming effect: microbial N mining and stoichiometric decomposition theories. *Glob Chang Biol* 20, 2356-2367.
- Chen, X., Xia, Y., Rui, Y., Ning, Z., Hu, Y., Tang, H., He, H., Li, H., Kuzyakov, Y., Ge, T., Wu, J., Su, Y., 2020. Microbial carbon use efficiency, biomass turnover, and necromass accumulation in paddy soil depending on fertilization. *Agriculture, Ecosystems & Environment* 292.
- Cheng, W., 1996. Measurement of rhizosphere respiration and organic matter decomposition using natural ¹³C. *Plant and Soil* 183, 263-268.
- Cui, J., Zhu, Z., Xu, X., Liu, S., Jones, D.L., Kuzyakov, Y., Shibistova, O., Wu, J., Ge, T., 2020. Carbon and nitrogen recycling from microbial necromass to cope with C:N stoichiometric imbalance by priming. *Soil Biology and Biochemistry* 142.
- Daquiado, A.R., Kuppasamy, S., Kim, S.Y., Kim, J.H., Yoon, Y.-E., Kim, P.J., Oh, S.-H., Kwak, Y.-S., Lee, Y.B., 2016. Pyrosequencing analysis of bacterial community diversity in long-term fertilized paddy field soil. *Applied Soil Ecology* 108, 84-91.
- Dong, Y., Sanford, R.A., Chang, Y.J., McInerney, M.J., Fouke, B.W., 2017. Hematite Reduction Buffers Acid Generation and Enhances Nutrient Uptake by a Fermentative Iron Reducing Bacterium, *Orenia metallireducens* Strain Z6. *Environ Sci Technol* 51, 232-242.
- Fadrus, H., Malý, J., 1975. Suppression of iron (III) interference in the determination of iron (II) in water by the 1, 10-phenanthroline method. *Analyst* 100, 549-554.
- Fanin, N., Kardol, P., Farrell, M., Nilsson, M.-C., Gundale, M.J., Wardle, D.A., 2019. The ratio of Gram-positive to Gram-negative bacterial PLFA markers as an indicator of carbon availability in organic soils. *Soil Biology and Biochemistry* 128, 111-114.
- Fontaine, S., Bardoux, G., Abbadie, L., Mariotti, A., 2004. Carbon input to soil may

- decrease soil carbon content. *Ecology Letters* 7, 314-320.
- Fontaine, S., Henault, C., Aamor, A., Bdioui, N., Bloor, J.M.G., Maire, V., Mary, B., Revalliot, S., Maron, P.A., 2011. Fungi mediate long term sequestration of carbon and nitrogen in soil through their priming effect. *Soil Biology and Biochemistry* 43, 86-96.
- Gunina, A., Kuzyakov, Y., 2015. Sugars in soil and sweets for microorganisms: Review of origin, content, composition and fate. *Soil Biology and Biochemistry* 90, 87-100.
- Hamer, U., Marschner, B., 2005. Priming effects in different soil types induced by fructose, alanine, oxalic acid and catechol additions. *Soil Biology and Biochemistry* 37, 445-454.
- He, Y., Cheng, W., Zhou, L., Shao, J., Liu, H., Zhou, H., Zhu, K., Zhou, X., 2020. Soil DOC release and aggregate disruption mediate rhizosphere priming effect on soil C decomposition. *Soil Biology and Biochemistry* 144.
- Jeewani, P.H., Gunina, A., Tao, L., Zhu, Z., Kuzyakov, Y., Van Zwieten, L., Guggenberger, G., Shen, C., Yu, G., Singh, B.P., Pan, S., Luo, Y., Xu, J., 2020. Rusty sink of rhizodeposits and associated keystone microbiomes. *Soil Biology and Biochemistry* 147.
- Jilling, A., Keiluweit, M., Gutknecht, J.L.M., Grandy, A.S., 2021. Priming mechanisms providing plants and microbes access to mineral-associated organic matter. *Soil Biology and Biochemistry* 158.
- Keiluweit, M., Bougoure, J.J., Nico, P.S., Pett-Ridge, J., Weber, P.K., Kleber, M., 2015. Mineral protection of soil carbon counteracted by root exudates. *Nature Climate Change* 5, 588-595.
- Kuzyakov, Y., Friedel, J.K., Stahr, K., 2000. Review of mechanisms and quantification of priming effects. *Soil Biology and Biochemistry* 32, 1485-1498.
- Kuzyakov, Y., Xu, X., 2013. Competition between roots and microorganisms for nitrogen: mechanisms and ecological relevance. *New Phytol* 198, 656-669.
- Li, Y., Shahbaz, M., Zhu, Z., Chen, A., Nannipieri, P., Li, B., Deng, Y., Wu, J., Ge, T., 2020. Contrasting response of organic carbon mineralisation to iron oxide addition under conditions of low and high microbial biomass in anoxic paddy soil. *Biol Fert Soils* 57, 117-129.
- Liu, Q., Atere, C.T., Zhu, Z., Shahbaz, M., Wei, X., Pausch, J., Wu, J., Ge, T., 2022a. Vertical and horizontal shifts in the microbial community structure of paddy soil under long-term fertilization regimes. *Applied Soil Ecology* 169.
- Liu, Q., Li, Y., Liu, S., Gao, W., Shen, J., Zhang, G., Xu, H., Zhu, Z., Ge, T., Wu, J., 2022b. Anaerobic primed CO₂ and CH₄ in paddy soil are driven by Fe reduction and stimulated by biochar. *Sci Total Environ* 808, 151911.
- Maguffin, S.C., Abu-Ali, L., Tappero, R.V., Pena, J., Rohila, J.S., McClung, A.M., Reid, M.C., 2020. Influence of manganese abundances on iron and arsenic solubility in rice paddy soils. *Geochimica et Cosmochimica Acta* 276, 50-69.
- Mi, W., Sun, Y., Xia, S., Zhao, H., Mi, W., Brookes, P.C., Liu, Y., Wu, L., 2018. Effect of inorganic fertilizers with organic amendments on soil chemical properties and rice yield in a low-productivity paddy soil. *Geoderma* 320, 23-29.

- Phillips, R.P., Finzi, A.C., Bernhardt, E.S., 2011. Enhanced root exudation induces microbial feedbacks to N cycling in a pine forest under long-term CO₂ fumigation. *Ecol Lett* 14, 187-194.
- Qiu, H., Zheng, X., Ge, T., Dorodnikov, M., Chen, X., Hu, Y., Kuzyakov, Y., Wu, J., Su, Y., Zhang, Z., 2017. Weaker priming and mineralisation of low molecular weight organic substances in paddy than in upland soil. *European Journal of Soil Biology* 83, 9-17.
- Rasmussen, C., Southard, R.J., Horwath, W.R., 2006. Mineral control of organic carbon mineralization in a range of temperate conifer forest soils. *Global Change Biology* 12, 834-847.
- Wei, L., Zhu, Z., Liu, S., Xiao, M., Wang, J., Deng, Y., Kuzyakov, Y., Wu, J., Ge, T., 2021. Temperature sensitivity (Q) of stable, primed and easily available organic matter pools during decomposition in paddy soil. *Applied Soil Ecology* 157.
- Wei, L., Zhu, Z., Razavi, B.S., Xiao, M., Dorodnikov, M., Fan, L., Yuan, H., Yurtaev, A., Luo, Y., Cheng, W., Kuzyakov, Y., Wu, J., Ge, T., 2022. Visualization and quantification of carbon "rusty sink" by rice root iron plaque: Mechanisms, functions, and global implications. *Glob Chang Biol*.
- Wei, X., Zhu, Z., Liu, Y., Luo, Y., Deng, Y., Xu, X., Liu, S., Richter, A., Shibistova, O., Guggenberger, G., Wu, J., Ge, T., 2020. C:N:P stoichiometry regulates soil organic carbon mineralization and concomitant shifts in microbial community composition in paddy soil. *Biol Fert Soils* 56, 1093-1107.
- Wordofa, D.N., Adhikari, D., Dunham-Cheatham, S.M., Zhao, Q., Poulson, S.R., Tang, Y., Yang, Y., 2019. Biogeochemical fate of ferrihydrite-model organic compound complexes during anaerobic microbial reduction. *Science of The Total Environment* 668, 216-223.
- Wu, J., Joergensen, R., Pommerening, B., Chaussod, R., Brookes, P., 1990. Measurement of soil microbial biomass C by fumigation-extraction-an automated procedure. *Soil biology & biochemistry* 22, 1167-1169.
- Xu, Z., Yu, G., Zhang, X., Ge, J., He, N., Wang, Q., Wang, D., 2015. The variations in soil microbial communities, enzyme activities and their relationships with soil organic matter decomposition along the northern slope of Changbai Mountain. *Applied Soil Ecology* 86, 19-29.
- Zhang, Y., Yao, S., Mao, J., Olk, D.C., Cao, X., Zhang, B., 2015. Chemical composition of organic matter in a deep soil changed with a positive priming effect due to glucose addition as investigated by ¹³C NMR spectroscopy. *Soil Biology and Biochemistry* 85, 137-144.
- Zhu, Z., Zhou, J., Shahbaz, M., Tang, H., Liu, S., Zhang, W., Yuan, H., Zhou, P., Alharbi, H., Wu, J., Kuzyakov, Y., Ge, T., 2021. Microorganisms maintain C:N stoichiometric balance by regulating the priming effect in long-term fertilized soils. *Appl. Soil Ecol.* 167, 104033.

Supplementary materials

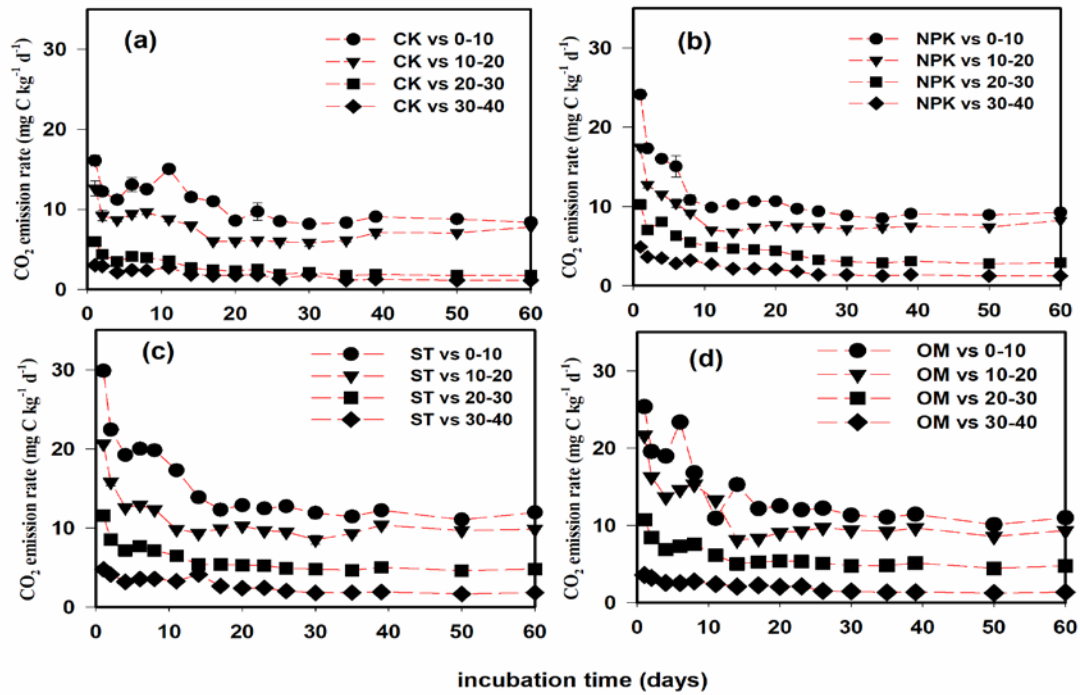


Figure II.4-S1 Absolute amount of CO₂ emission rates (mg C kg⁻¹ dry soil per day, basal respiration rate) in 60-days incubated paddy soil without glucose addition under fertilization regimes at different soil depths (mean ± SE, n=3). CK, no fertilizer; NPK, chemical fertilizers; ST, rice straw combined with chemical fertilizers; OM, 70% NPK + 30% chicken manure.

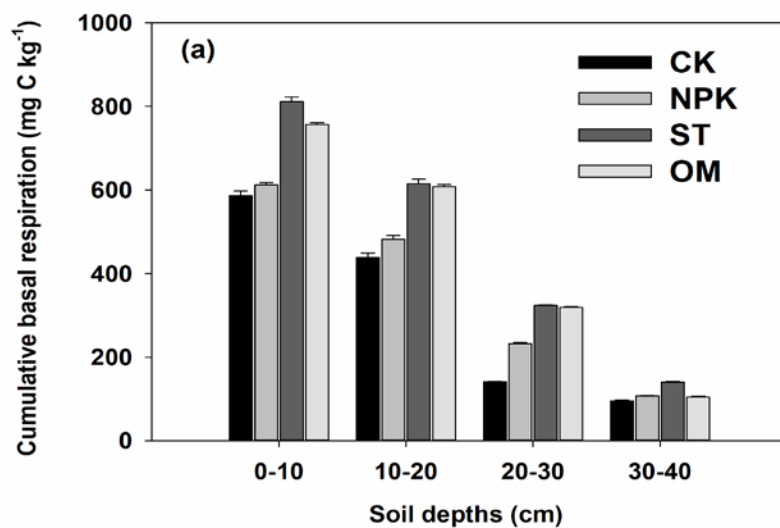


Figure II.4-S2 Absolute amount of cumulative CO₂ emission at day 60 (mg C kg⁻¹ dry soil, basal respiration) in 60-days incubated paddy soil without glucose addition under fertilization regimes at different soil depths (mean ± SE, n=3).

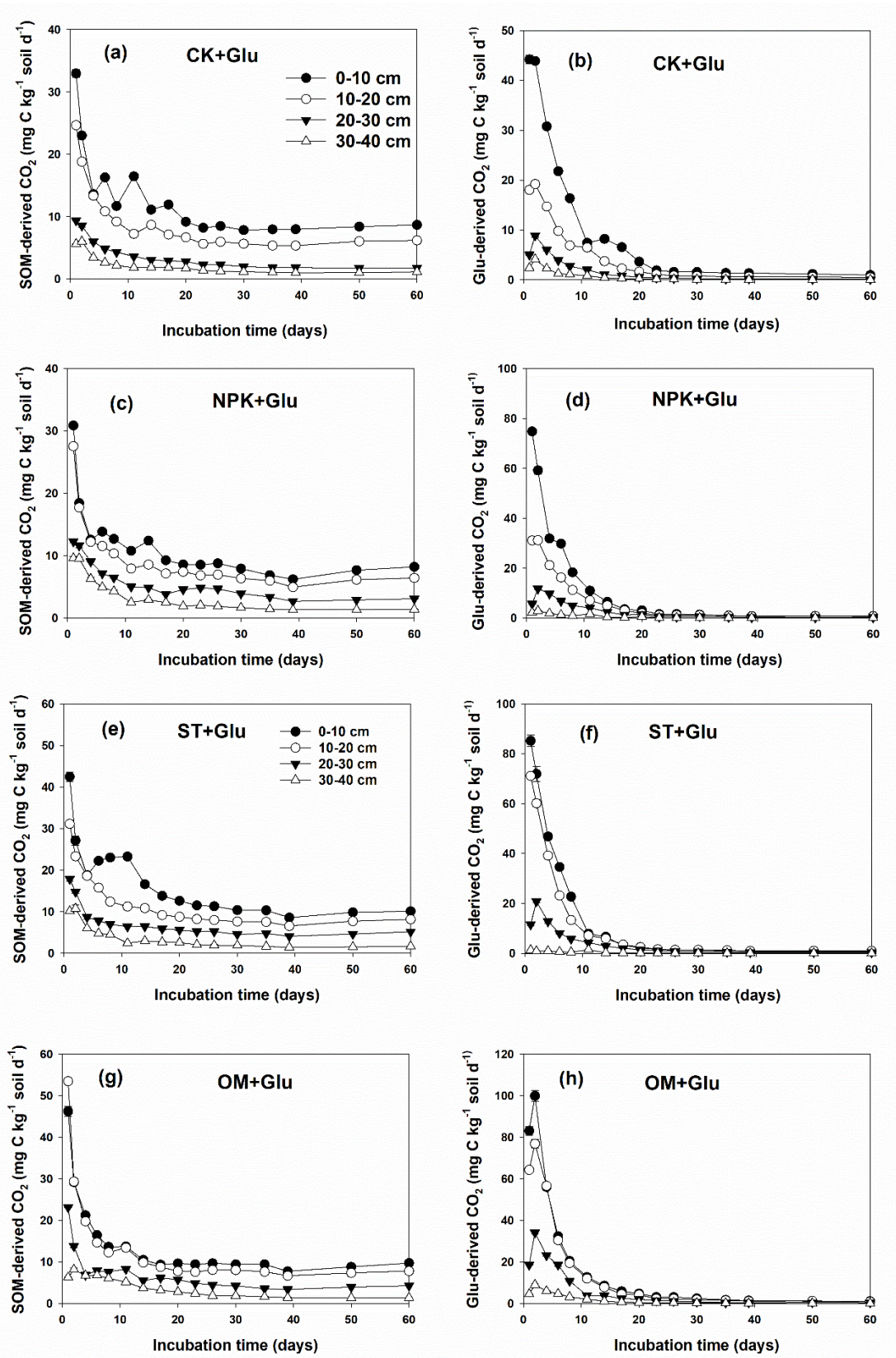


Figure II.4-S3 Absolute amount of CO₂ efflux derived from soil organic matter and glucose (mg C kg⁻¹ dry soil per day) in 60-days incubated paddy soil under fertilization regimes at different soil depths (mean ± SE, n=3).

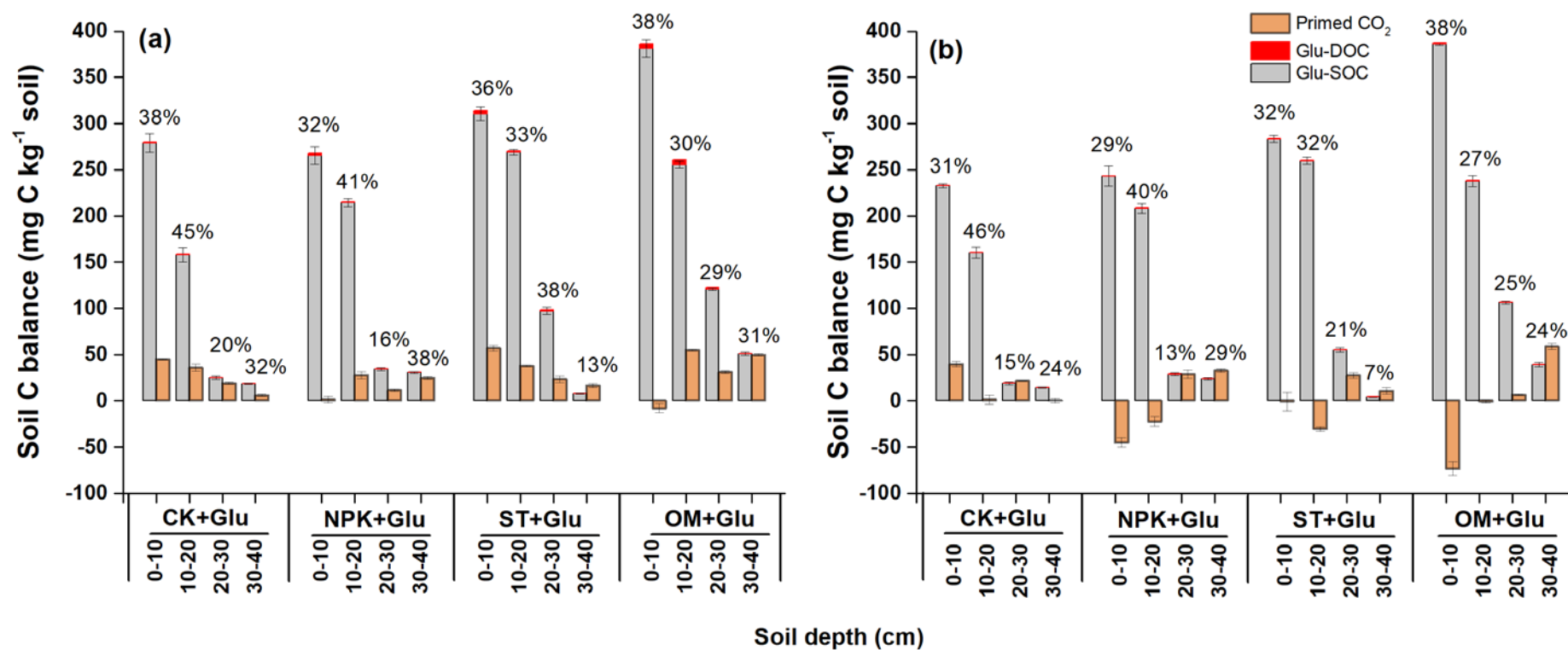


Figure II.4-S4 C retention in soil system (including glucose-derived soil organic C and glucose-derived dissolved organic C in the supernatant) and C loss through cumulative primed CO₂ at day 20 (a) and day 60 (b) in incubated paddy soil under long-term fertilization regimes at different soil depths (mean \pm SE, n=3). SOC: soil organic C; DOC: dissolved organic C. Numbers above the bar represent the total C retention as a percentage of added glucose at the corresponding treatment and depth.

Table II.4-S1 Basic physicochemical properties of paddy soil under fertilization regimes at different soil depths before incubation (mean \pm SE, n=3).

Treatments		pH	SOC (g kg ⁻¹)	MBC (mg kg ⁻¹)	MBN (mg kg ⁻¹)	DOC (mg kg ⁻¹)	Available N (mg kg ⁻¹)
CK	0–10	7.2 \pm 0.01	18.3 \pm 0.1	740 \pm 33	128 \pm 4	43 \pm 2	151 \pm 2
	10–20	7.4 \pm 0.02	15.8 \pm 0.2	351 \pm 19	44 \pm 6	30 \pm 1	108 \pm 1
	20–30	7.5 \pm 0.01	6.5 \pm 0.1	124 \pm 5	16 \pm 3	19 \pm 0	47 \pm 1
	30–40	7.6 \pm 0.02	5.4 \pm 0.1	59 \pm 2	9 \pm 1	18 \pm 1	45 \pm 1
NPK	0–10	6.5 \pm 0.01	17.5 \pm 0.5	830 \pm 9	100 \pm 7	47 \pm 1	182 \pm 5
	10–20	6.8 \pm 0.01	16.1 \pm 0.0	527 \pm 5	67 \pm 2	38 \pm 1	129 \pm 1
	20–30	7.2 \pm 0.02	9.4 \pm 0.1	220 \pm 6	64 \pm 10	33 \pm 1	71 \pm 1
	30–40	7.3 \pm 0.02	6.1 \pm 0.0	82 \pm 7	22 \pm 3	27 \pm 2	43 \pm 1
ST	0–10	6.6 \pm 0.02	22.0 \pm 0.1	881 \pm 27	140 \pm 21	51 \pm 1	210 \pm 2
	10–20	6.8 \pm 0.01	20.1 \pm 0.3	808 \pm 30	100 \pm 8	49 \pm 1	185 \pm 1
	20–30	7.1 \pm 0.01	11.9 \pm 0.1	259 \pm 11	45 \pm 5	40 \pm 1	97 \pm 3
	30–40	7.2 \pm 0.02	6.1 \pm 0.1	63 \pm 4	13 \pm 2	23 \pm 1	50 \pm 1
OM	0–10	6.7 \pm 0.02	25.5 \pm 0.4	1020 \pm 52	155 \pm 10	54 \pm 1	251 \pm 1
	10–20	6.9 \pm 0.01	25.0 \pm 0.7	869 \pm 22	130 \pm 2	49 \pm 1	193 \pm 7
	20–30	7.2 \pm 0.02	12.1 \pm 0.0	421 \pm 2	82 \pm 7	43 \pm 2	98 \pm 4
	30–40	7.3 \pm 0.02	5.9 \pm 0.2	165 \pm 2	28 \pm 7	27 \pm 1	42 \pm 2

Table II.4-S2 Glucose-derived CO₂ emission rates (% of total glucose input per day) at three soil samplings, and the absolute amount of primed MBC, DOC and cumulative primed CO₂ (mg kg⁻¹) at day 2 in 60-days incubated paddy soil under long-term fertilization regimes at different soil depths (mean ± SE, n=3). Lower-case letters represent significant differences between soil depths within the same fertilization regime. Uppercase letters represent significant differences between fertilization regimes within the same soil depth.

Treatments	Soil depth (cm)	Glucose-derived CO ₂ emission rates (%)			Primed MBC	Primed DOC D2 (mg kg ⁻¹)	Cumulative primed CO ₂
		D2	D20	D60			
CK+Glu	0–10	5.93±0.05Db	0.50±0.00Aa	0.13±0.00Ab	-62.1±51.6	352±6.1	27.7±0.6
	10–20	5.47±0.14Cb	0.47±0.00Aab	0.15±0.00Aa	168±9.9	109±7.0	21.6±0.5
	20–30	7.16±0.25Ba	0.49±0.01Ca	0.12±0.00Bc	24.4±12.3	20.3±1.0	7.6±0.3
	30–40	6.96±0.13Aa	0.43±0.03Bb	0.10±0.00Ad	21.4±6.9	6.3±2.0	5.7±0.2
NPK+Glu	0–10	7.14±0.19Ca	0.37±0.01Bb	0.10±0.00Cb	-79.6±30.8	419±7.1	7.9±0.5
	10–20	5.92±0.14Cb	0.36±0.01Bb	0.14±0.00Ba	149±24.0	209±4.0	15.1±0.9
	20–30	5.35±0.15Cc	0.68±0.02Aa	0.09±0.00Cc	92.1±16.0	51.8±3.5	6.6±0.6
	30–40	3.59±0.09Cd	0.71±0.02Aa	0.05±0.00Cd	31.6±8.2	25.1±1.7	10.6±0.4
ST+Glu	0–10	8.17±0.34Ba	0.25±0.01Cc	0.08±0.00Dc	-140±19.9	384±4.2	17.3±2.3
	10–20	7.45±0.18Ba	0.31±0.00Cb	0.12±0.00Cb	-20.6±40.0	358±11.5	18.0±0.6
	20–30	8.03±0.18Aa	0.56±0.01Ba	0.15±0.00Aa	78.5±23.5	46.7±4.8	12.5±0.8
	30–40	1.38±0.10Db	0.18±0.01Dd	0.04±0.00Dd	6.8±5.5	8.9±0.2	12.0±0.6
OM+Glu	0–10	9.80±0.26Aa	0.47±0.01Aa	0.11±0.00Bb	-95.9±51.3	279±66	30.5±2.0
	10–20	8.85±0.23Ab	0.49±0.00Aa	0.11±0.00Db	-36.8±23.6	256±11.8	44.9±0.5
	20–30	8.10±0.19Ab	0.49±0.01Ca	0.12±0.00Ba	-0.7±16.3	147±5.1	17.8±0.3
	30–40	5.47±0.27Bc	0.28±0.00Cb	0.05±0.00Bc	19.7±2.9	57.4±2.2	7.7±0.5

Table II.4-S3 Two-way ANOVA results of the effects of fertilization regimes and soil depths and their interaction on glucose-derived CO₂ emission rates and total Fe (II) contents (permutation=999). Basis of results for Table II.4-S2 and Figure II.4 & 5.

	Fertilization			Depth			Fertilization *Depth		
	<i>F</i>	R ²	<i>P</i>	<i>F</i>	R ²	<i>P</i>	<i>F</i>	R ²	<i>P</i>
Emission rates D2	3.928	0.056	0.04	16.54	0.237	0.001	5.36	0.077	0.021
Emission rates D20	3.168	0.063	0.08	0.96	0.019	0.31	2.32	0.046	0.128
Emission rates D60	3.98	0.058	0.04	19.40	0.283	0.001	1.20	0.017	0.271
Fe (II) D2	1.59	0.019	0.21	31.5	0.387	0.001	4.43	0.054	0.031
Fe (II) Glu+D2	60.2	0.320	0.001	78.9	0.419	0.001	5.40	0.029	0.021
Fe (II) D20	6.86	0.047	0.01	91.6	0.633	0.001	2.11	0.0146	0.16
Fe (II) Glu+ D20	13.5	0.10	0.002	71.6	0.534	0.001	5.11	0.038	0.031
Fe (II) D60	6.9	0.055	0.008	72.9	0.585	0.001	0.851	0.007	0.339
Fe (II) Glu+ D60	12.6	0.099	0.001	63.7	0.502	0.001	6.51	0.051	0.016

Table II.4-S4 Percentage priming effect (% of basal respiration per day) and the absolute amount of SOM-derived CO₂ (mg kg⁻¹) at three sampling times in 60-days incubated paddy soil under long-term fertilization regimes at different soil depths (mean ± SE, n=3). Lower-case letters represent significant differences between soil depths within the same fertilization regime. Uppercase letters represent significant differences between fertilization regimes within the same soil depth.

Soil	Depth (cm)	Percentage priming effect (%)			Cumulative SOM-derived CO ₂ (mg C kg ⁻¹)		
		D2	D20	D60	D2	D20	D60
CK+Glu	0–10	88.2±1.6Ab	7.2±0.2Ab	3.6±0.2Aa	56.0±0.6	285±0.4	626±2.9
	10–20	104±5.2Aab	11.1±0.9Ab	-20.7±0.4Cb	43.5±0.5	200±4.0	439±4.9
	20–30	94.5±6.8Aab	22.0±2.2Aa	2.7±0.4Ba	18.0±0.3	85.5±1.0	163±0.2
	30–40	107±3.9Ba	-3.7±5.7BCc	1.4±2.2Ba	11.7±0.2	49.9±1.2	95.7±2.4
NPK+Glu	0–10	6.5±2.8Dd	-19.4±2.5Cc	-11.3±0.7Bc	49.3±0.5	251±3.6	566±5.3
	10–20	39.2±3.2Cc	-3.4±3.9ABab	-21.9±0.1Dd	45.3±0.9	207±3.9	460±5.2
	20–30	65.2±4.7Bb	3.0±2.7Ba	6.6±1.0Ab	23.9±0.6	124±1.1	262±4.5
	30–40	164±6.6Aa	-8.7±2.2Cb	13.5±0.1Aa	19.1±0.4	79.6±1.5	140±1.8
ST+Glu	0–10	20.8±5.1Cd	-2.2±3.8Bab	-15.6±0.3Cc	69.6±2.3	397±3.0	810±10
	10–20	47.3±3.6Cbc	-14.5±0.9Bb	-17.2±0.5Bd	54.5±0.6	268±0.9	584±2.3
	20–30	73.2±3.9Bb	8.0±2.7Ba	8.2±0.6Aa	32.6±0.8	155±3.5	351±2.9
	30–40	162±18.8Aa	6.4±6.0Ba	-7.8±0.4Bb	20.9±0.6	83.3±2.2	151±3.5
OM+Glu	0–10	49.3±4.0Bc	-23.0±1.5Cd	-11.6±0.2Bb	75.5± 2.0	308±4.8	683±7.6
	10–20	80.1±4.6Bb	-14.0±0.6Bc	-15.9±0.4Ac	82.9±0.5	296±0.8	607±1.4
	20–30	63.7±3.9Bbc	6.7±2.8Bb	-9.9±1.1Cab	37.0±0.3	159±1.5	326±0.8
	30–40	154±12.6Aa	36.5±2.0Aa	5.3±3.4Ba	14.4±0.5	98.3±1.3	163±3.2

Table II.4-S5 C pool changes from day 2 to day 20 (mg kg^{-1}) in 60-days incubated paddy soil under long-term fertilization regimes at different soil depths (mean \pm SE, $n=3$). X_{Glu} and X_{SOM} represented the glucose-derived C and SOM-derived C in X pool, respectively. The data was calculated using the equation: $X_{20}-X_2$. X_{20} and X_2 represented the different C pools at day 20 and day 2, respectively. Positive values indicate a pool increase, whereas negative values indicate a pool decrease. Basis of results for Figure 3 & S3.

Soil	Depth (cm)	Without glucose (basal)			With glucose					
		MBC	DOC	CO ₂	MBC _{Glu}	DOC _{Glu}	CO ₂ Glu	MBC _{SOM}	DOC _{SOM}	CO ₂ SOM
CK	0–10	-116 \pm 50.5	-12.5 \pm 0.2	212 \pm 3.3	-74.5 \pm 1.0	-269 \pm 4.0	216 \pm 2.9	-29.1 \pm 28.2	-357 \pm 6.6	229 \pm 0.5
	10–20	44.5 \pm 25.0	-26.2 \pm 0.2	142 \pm 2.3	-50.3 \pm 3.1	-71.8 \pm 5.4	106 \pm 2.9	12.5 \pm 30.4	-122 \pm 6.7	156 \pm 3.6
	20–30	20.0 \pm 6.2	-16.4 \pm 1.0	56.2 \pm 0.8	-9.5 \pm 0.5	-15.9 \pm 0.7	39.2 \pm 0.9	-84.9 \pm 6.0	-33.7 \pm 1.3	67.5 \pm 1.3
	30–40	-13.8 \pm 2.5	-12.9 \pm 0.6	38.3 \pm 1.3	-10.4 \pm 0.3	-5.7 \pm 0.4	14.6 \pm 0.2	-73.8 \pm 1.1	-12.8 \pm 2.3	38.3 \pm 1.2
NPK	0–10	-82.2 \pm 49.0	-17.8 \pm 1.2	208 \pm 3.2	-66.4 \pm 3.7	-318 \pm 1.7	232 \pm 3.1	110 \pm 24.9	-415 \pm 8.8	201 \pm 3.1
	10–20	-95.9 \pm 5.3	-19.4 \pm 2.5	149 \pm 3.3	-49.0 \pm 3.6	-147 \pm 3.3	149 \pm 2.6	-81.8 \pm 19.1	-215 \pm 0.4	162 \pm 3.0
	20–30	-30.7 \pm 12.5	-21.3 \pm 2.7	95.5 \pm 2.0	-18.2 \pm 0.6	-31.9 \pm 1.7	71.0 \pm 0.6	-11.5 \pm 9.1	-59.6 \pm 1.9	100 \pm 1.0
	30–40	-28.6 \pm 3.1	4.4 \pm 0.9	46.2 \pm 1.0	-10.6 \pm 1.1	-6.3 \pm 0.5	16.4 \pm 0.5	-81.4 \pm 21.4	-14.4 \pm 2.9	60.5 \pm 1.5
ST	0–10	-47.1 \pm 35.2	-26.1 \pm 0.7	287 \pm 2.5	-145 \pm 10.4	-393 \pm 2.8	268 \pm 3.1	20.7 \pm 47.3	-385 \pm 5.9	327 \pm 1.1
	10–20	-125 \pm 19.5	-1.9 \pm 1.6	194 \pm 3.5	-142 \pm 11.3	-241 \pm 7.3	208 \pm 1.8	-334 \pm 52.2	-352 \pm 9.7	214 \pm 0.3
	20–30	-60.8 \pm 9.2	-21.7 \pm 1.9	112 \pm 0.9	-40.5 \pm 3.7	-40.3 \pm 2.4	87.2 \pm 2.5	-52.2 \pm 31.8	-36.7 \pm 2.6	123 \pm 3.0
	30–40	-38.8 \pm 4.2	-12.5 \pm 1.4	58.0 \pm 1.6	-6.8 \pm 0.5	-5.9 \pm 0.2	9.8 \pm 0.2	-40.8 \pm 13.8	-14.1 \pm 0.7	62.3 \pm 1.6
OM	0–10	-36.3 \pm 44.7	-15.8 \pm 0.3	271 \pm 1.5	-181 \pm 11.5	-483 \pm 30.9	314 \pm 3.1	-134 \pm 44.3	-293 \pm 5.7	233 \pm 3.2
	10–20	-23.4 \pm 41.6	-6.3 \pm 0.8	203 \pm 1.9	-209 \pm 9.1	-401 \pm 11.6	299 \pm 1.4	-37.4 \pm 10.7	-242 \pm 12.3	213 \pm 0.8
	20–30	-52.9 \pm 3.8	-19.3 \pm 2.8	109 \pm 1.3	-47.5 \pm 1.0	-173 \pm 0.8	142 \pm 0.6	30.6 \pm 13.6	-160 \pm 0.8	122 \pm 1.2
	30–40	-58.7 \pm 4.5	-20.0 \pm 1.0	42.0 \pm 1.6	-2.1 \pm 0.1	-24.9 \pm 1.1	40.9 \pm 0.5	-72.0 \pm 2.8	-59.8 \pm 1.3	83.8 \pm 1.0

Table II.4-S6 C pool changes from day 20 to day 60 (mg kg^{-1}) in 60-days incubated paddy soil under long-term fertilization regimes at different soil depths (mean \pm SE, $n=3$). X_{Glu} and X_{SOM} represented the glucose-derived C and SOM-derived C in X pool, respectively. The data was calculated using the equation: $X_{60}-X_{20}$. X_{60} and X_{20} represented the different C pools at day 60 and day 20, respectively. Basis of results for Figure 3 & S3.

Soil	Depth (cm)	Without glucose (basal)			With glucose					
		MBC	DOC	CO ₂	MBC _{Glu}	DOC _{Glu}	CO ₂ Glu	MBC _{SOM}	DOC _{SOM}	CO ₂ SOM
CK	0–10	-30.5 \pm 9.7	13.3 \pm 0.4	346 \pm 6.8	-54.7 \pm 1.1	-1.65 \pm 0.04	54.1 \pm 0.5	-94.7 \pm 12.0	0.23 \pm 0.28	341 \pm 2.5
	10–20	10.7 \pm 37.9	7.0 \pm 0.2	275 \pm 7.3	-24.8 \pm 0.5	-0.75 \pm 0.02	27.5 \pm 0.2	-37.2 \pm 12.6	0.68 \pm 0.32	240 \pm 1.2
	20–30	-2.2 \pm 8.5	8.8 \pm 0.7	74.6 \pm 0.8	0.06 \pm 0.02	-0.09 \pm 0.01	9.3 \pm 0.1	7.7 \pm 3.5	0.49 \pm 0.30	77.1 \pm 0.9
	30–40	21.9 \pm 1.3	4.7 \pm 0.8	51.3 \pm 1.0	-0.41 \pm 0.01	-0.07 \pm 0.01	3.3 \pm 0.1	-2.6 \pm 0.8	-0.37 \pm 0.37	45.8 \pm 1.2
NPK	0–10	49.7 \pm 31.8	18.9 \pm 1.1	362 \pm 3.6	-68.1 \pm 2.4	-2.83 \pm 0.10	41.5 \pm 0.3	-65.7 \pm 39.3	-5.87 \pm 2.02	316 \pm 1.7
	10–20	35.3 \pm 8.4	6.2 \pm 2.0	304 \pm 5.0	-30.7 \pm 0.1	-1.08 \pm 0.06	35.8 \pm 0.2	-69.0 \pm 7.1	0.81 \pm 0.30	254 \pm 1.3
	20–30	8.2 \pm 8.5	6.4 \pm 1.4	120 \pm 2.1	-6.8 \pm 0.3	-0.43 \pm 0.03	13.7 \pm 0.4	-8.7 \pm 10.3	2.06 \pm 0.46	138 \pm 3.5
	30–40	7.7 \pm 4.0	-1.9 \pm 0.7	52.7 \pm 1.3	-1.5 \pm 0.2	-0.35 \pm 0.02	1.9 \pm 0.0	4.1 \pm 1.7	-0.34 \pm 0.41	60.7 \pm 0.5
ST	0–10	32.7 \pm 11.1	26.1 \pm 1.8	471 \pm 9.5	-73 \pm 1.6	-4.28 \pm 0.07	38.0 \pm 0.8	-217 \pm 35.0	-4.33 \pm 0.09	414 \pm 7.8
	10–20	107 \pm 44.3	20.5 \pm 2.1	384 \pm 7.3	-40.5 \pm 0.8	-1.50 \pm 0.02	45.7 \pm 0.3	-136 \pm 9.1	0.72 \pm 0.81	316 \pm 1.7
	20–30	-43.8 \pm 5.6	15.0 \pm 2.7	192 \pm 1.1	-18.3 \pm 0.8	-2.20 \pm 0.08	20.5 \pm 0.2	-182 \pm 23.1	1.17 \pm 0.85	196 \pm 0.8
	30–40	-6.8 \pm 1.7	22.3 \pm 0.5	73.8 \pm 0.5	-3.1 \pm 0.4	-0.73 \pm 0.02	1.4 \pm 0.0	-25.4 \pm 11.4	0.50 \pm 0.55	68.1 \pm 1.4
OM	0–10	-136 \pm 43.9	30.1 \pm 1.2	441 \pm 2.5	-84.8 \pm 2.4	-5.33 \pm 0.28	68.5 \pm 0.7	-81.6 \pm 47.5	-0.96 \pm 1.46	375 \pm 2.8
	10–20	11.9 \pm 24.7	38.1 \pm 1.4	366 \pm 2.6	-76.1 \pm 1.0	-6.05 \pm 0.01	57.7 \pm 0.6	-145 \pm 24.8	-2.01 \pm 0.51	311 \pm 2.2
	20–30	-38.0 \pm 12.3	19.2 \pm 3.2	191 \pm 0.7	-22.4 \pm 0.7	-2.75 \pm 0.07	27.6 \pm 0.3	-95.0 \pm 21.2	-0.01 \pm 0.62	167 \pm 2.1
	30–40	42.6 \pm 4.0	24.4 \pm 0.9	55.5 \pm 1.0	-2.9 \pm 0.3	-1.42 \pm 0.10	6.5 \pm 0.3	-0.1 \pm 3.7	2.98 \pm 0.34	64.5 \pm 2.0

(Eidesstattliche) Versicherungen und Erklärungen

(§ 8 Satz 2 Nr. 3 PromO Fakultät)

Hiermit versichere ich eidesstattlich, dass ich die Arbeit selbstständig verfasst und keine anderen als die von mir angegebenen Quellen und Hilfsmittel benutzt habe (vgl. Art. 64 Abs. 1 Satz 6 BayHSchG).

(§ 8 Satz 2 Nr. 3 PromO Fakultät)

Hiermit erkläre ich, dass ich die Dissertation nicht bereits zur Erlangung eines akademischen Grades eingereicht habe und dass ich nicht bereits diese oder eine gleichartige Doktorprüfung endgültig nicht bestanden habe.

(§ 8 Satz 2 Nr. 4 PromO Fakultät)

Hiermit erkläre ich, dass ich Hilfe von gewerblichen Promotionsberatern bzw. –vermittlern oder ähnlichen Dienstleistern weder bisher in Anspruch genommen habe noch künftig in Anspruch nehmen werde.

(§ 8 Satz 2 Nr. 7 PromO Fakultät)

Hiermit erkläre ich mein Einverständnis, dass die elektronische Fassung der Dissertation unter Wahrung meiner Urheberrechte und des Datenschutzes einer gesonderten Überprüfung unterzogen werden kann.

(§ 8 Satz 2 Nr. 8 PromO Fakultät)

Hiermit erkläre ich mein Einverständnis, dass bei Verdacht wissenschaftlichen Fehlverhaltens Ermittlungen durch universitätsinterne Organe der wissenschaftlichen Selbstkontrolle stattfinden können.

.....
Ort, Datum, Unterschrift